Syracuse University
SURFACE at Syracuse University

Dissertations - ALL | SURFACE at Syracuse University

5-12-2024

Geometric-Templated Cardiac Organoids for Drug Developmental Toxicity Screening

Shiyang Sun
Syracuse University

Follow this and additional works at: https://surface.syr.edu/etd

Recommended Citation

Sun, Shiyang, "Geometric-Templated Cardiac Organoids for Drug Developmental Toxicity Screening" (2024). *Dissertations - ALL*. 1887.
https://surface.syr.edu/etd/1887

This Dissertation is brought to you for free and open access by the SURFACE at Syracuse University at SURFACE at Syracuse University. It has been accepted for inclusion in Dissertations - ALL by an authorized administrator of SURFACE at Syracuse University. For more information, please contact surface@syr.edu.

Abstract

Nowadays 9 of every 10 women take at least one medicine during their pregnancy. However, unfortunately, many pregnant women have to face a severe problem that there is not enough evidence to prove the safety of their medication, and an appropriate medication might cause birth defects or even infant death. Researchers need an accurate and reliable drug developmental platform. Compared to the traditional animal and cell models, organoids have the ability to highly mimic the human organ developmental process, which allow researchers investigate the developmental toxicity to human development with organoid platform. The goal of this work is to explore the potential of cardiac organoid models to investigate heart development and cardiac function.

In this work, we have utilized different patterns, including circles, squares and rectangles, and pentagrams, to create the geometrical confinement to cardiac organoids development, which is shown as having different functional properties and morphology due to the geometrical designs. We also tested the developmental toxicity of 14 drugs or chemical compounds with 600-micron circle organoids. Cardiac organoid development was interfered with the high-concentration drug treatment. These new cardiac organoids were utilized as potential advancements in drug screening applications for better predictions of drug-related developmental toxicity.

Geometric-Templated Cardiac Organoids for Drug Developmental Toxicity Screening

By

Shiyang Sun

B.S., Jilin University, 2013

M.S., Syracuse university, 2019

Dissertation

Submitted in partial fulfillment of the requirements for the degree of Doctor of Philosophy in Bioengineering

Syracuse University

May 2024

Copyright © Shiyang Sun 2024

All Rights Reserved

Acknowledgements

I would first like to extend my utmost gratitude to my advisor, Professor Zhen Ma, who e has mentored me from my master project at Syracuse and has taught me how to be a good researcher in future. It was my honor to be his student and participate in his lab. Then, I would like to thank my dissertation committee members, Professors Teng Zhang, James H Henderson, Julie Hasenwinkel, and Jeffrey Amack, for taking the time to review my PhD work and provide valuable feedback on my dissertation. To all the behind-the-scenes personnel, Lynore de la Rosa, Karen Low, Eric Finkelstein, Sabina Redington, Amy Forbes, Jason Markle and Emilia M Stojanovski, thank you for orchestrating everything that keeps our department and labs running. I thank members of the Ma lab that have become not only my coworkers, but also my closest friends who were my motivation to report to work. I would like to acknowledge Plansky Hoang for selflessly assisting the lab whenever in need. Lastly, I wanted to show appreciation to my parents, who have supported me to focus on my academic life, especially my, you save me from unhappiness, upset and pressure each, which is really important for me. Unfortunately, I don’t have a chance to share my joy with you again, but I hope you can enjoy your new life in another world.

Table of Contents

List of Figures

List of tables

1. CHAPTER 1: INTRODUCTION

1.1 Human Stem Cells Technology

Stem cells exist in stages of life with the ability to self-renew and differentiate into multiple other cell types. Those cells are essential in the developmental process of new creatures and the recovery process from injury or disease by proliferation and differentiation into tissue or organ of stem cells[1]. Stem cells emerged and were exploited in many fields by research teams as a valuable tool in the past decades, such as basic research and regenerative medicine. Although embryonic stem cells (ESCs) have comprehensive abilities to differentiate into all cell types and form all tissue types, ESCs were not considered the best cell resource. On the other hand, in mature human bodies, stem cells showed less as the differentiated potency increased, which caused hard gain enough human stem cells with high differentiated potency. Induced stem cells provide an opportunity for stem cell research[2]. In 2006, research showed mouse fibroblasts re-acquire the high differentiated potency, which is similar to ESCs using four transcriptional factors, including Oct4, Sox2, Klf4, and c-Myc, also known as "Yamanaka Factors"[3] (Figure 1). The next year, human induced pluripotent stem cells (hiPSCs) were successfully generated from human fibroblasts in laboratories[45]. HiPSCs were proven to have the ability to differentiate to most cell types and form most types of tissue, allowing researchers to exploit iPSCs in the in vitro modeling of cells and tissues. In addition, hiPSCs also showed excellent self-renewing ability and became a more popular cell source for in vitro modeling of human development.

1.2 Stem Cell Organoid Technology

Although researchers have made a huge breakthrough in understanding organogenesis in recent years, there are many challenges to mimicking all processes of human body development in vitro models. In previous studies, animal models were considered the closest model for human organ research. However, the huge physiological difference between human and animal and the limited similarity between human and animal organs demonstrated that the animal model was not a perfectly accurate and reliable model[6]. Human tissue explants and slices also cannot maintain their phenotype or physiological structure and function for an extended period. In recent years, organoid technology has provided an opportunity to generate human tissue and organs in vitro, which can mimic the generation, development, and mature function in the long term. An organoid was termed as a resembling organ is derived and formed from primary tissue or differentiated from ECSs or PSCs[7], which have the same structure and function as the natural organ and can represent the complex and specific functionalities of the organ, and organoids were considered as a miniaturized and simplified version of an organ. Organoids can be used to study developmental processes, model diseases, and test drugs in vitro.

In the traditional view, the generation and development of the human organ is a highly precisely controlled process and begins with stem cell proliferation, self-organization, and differentiation to specific cell types[8]. Thus, through establishing the artificial cell culture environment by precisely controlling of 3D scaffold and biochemical factors, researchers can induce stem cells to differentiate into specific cell lineages and form the micro-organ, known as organoids, which highly mimic the human organ structure and physiological function[9]. Organoids technology was developed from ECSs as a cell source to form three germ layers in the early stage to induce human pluripotent stem cells using four transcription factors in recent research[10]. Currently, human organoids have successfully mimicked multiple organs, including gut[11], lung[12],

thyroid[13], gastric[14], heart[15], kidney, liver[16], brain[17], and retina[18] (Figure 2). Therefore, these stem cell-based organoid systems can recapitulate events of early organogenesis, and play more important roles in wide fields, such as basic research and regenerative medicine.

Because of their highly physiological similarity and self-renewable abilities, organoids provide us with an excellent model system for disease modeling. Unlike cell lineages, organoids include all cell types in specific, representing all organ components, including cells and interaction. They are suitable for infectious disease research, especially human demands disease. For instance, researchers exploit PSC and ASC to create the stomach organoids and investigate the interaction between Helicobacter pylori and stomach organoids[19] [20]. Researchers also developed brain organoids with the Zika virus and found the virus causes cell death, proliferation reduction, and volume reduction of the brain, which helps the medicine selection and therapy foundation[21]. On the other hand, organoids also played an important role and modeled in organ-specific hereditary diseases. Researchers created gene mutants in stem cells and developed organoids to mimic natural genetic defects in organs, or researchers develop organoids with stem cells derived from patients and correct gene mutants with CRISPR/Cas9 to find genetic therapy for hereditary diseases. Such as, the Verma lab used CRISPR/Cas9 to treat cystic fibrosis by correcting genetic defects[22]. Moreover, organoids also provide an opportunity in cancer research as an excellent model from wild-type stem cells; there are labs proving the feasibilities of organoids development from colon, prostate, and pancreatic cancers[23, 24, 25]. For instance, researchers found several genetic mutants, such as Tp53 and KRAS, that can cause stem cell-formed 3D tissue with s structure and physiological properties similar to pancreatic tumors in vivo[26]. Researchers also used organoid technology in the personalized medicine field. Through organoids derived from patient stem cells, researchers can mimic the personal condition in vitro and find the best therapy for the patient, which has

been applied for cystic fibrosis therapy and personal drug tests[27].

Another popular field of organoids is regenerative medicine. In the current treatment of diseased or defective organs or tissue, transplantation of healthy organs or tissues is the mainstream treatment. However, the lack of replaceable organs and immune rejection are the main challenges of traditional therapy. The recent significant progress in organoid technology provides a potentially new alternative therapy strategy to organ transplantation. Researchers showed the ability to induce the patient cells to transfer stem cells and develop the organoid with the same structure and function[28]. The feasibility of organ replacement has been proven by labs, such as Yui's lab, which showed that mouse colonic organoids can be transplanted into mouse colons and form functional crypt units[29]. Dekkers lab exploited CRISPR/Cas9 gene editing to correct CFTR mutation in patient cells and create colonic organoids, which replace the diseased tissue and restore the function. In addition, more research reported the success of organoids transplantation in organs, including the liver, stomach, pancreas, and kidney[30, 31, 32, 33]. Although the application of organoid technology in organ transplantation and regenerative medicine is exciting, many challenges still exist, including safety, ethical issues, and legal problems, which is needed to be decided by researchers, patients, the government, and society[34].

1.3 Biomaterial Approaches for Organoid Engineering

In past decades, the huge amount of research about stem cells provides further understanding of the fate and behavior of stem cells based on molecule level controlling, which allowed researchers to control stem cell proliferation and differentiation to specific cell lineage. The progress in stem cell technologies and developmental biology allowed researchers to establish micro-human organs, known as organoids, in vitro. The stem cell behavior is highly influenced

by extracellular micro-environmental signal systems, including surrounding cells, extracellular matrices (ECM), mechanical signals, and biochemical conditions[35]. ECM, as an essential component of organoids, supports organoid structure and provides signaling for stem cell behavior. In the early stage, natural ECM or decellularized matrix were used as bio-scaffolds to culture stem cells and create organoids[36.] Researchers exploited single or several components of ECM as materials to fabricate scaffolds for inducing specific cell differentiation, such as hyaluronic acid for neural stem cells and hematopoietic stem cells. In recent research, synthetic polymers, such as polyacrylamide and polyethylene glycol (PEG), were also used to fabricate biomimetic scaffold[37]. For further bio-similarity increase, the ECM component was combined with signaling molecules on synthetic materials by micro-contact printing technology. For instance, Perl lab exploited PDMS stamp to deposit proteins, ECM, or cells on polymerized hydrogel substrate[38]. In addition, researchers used bio-fabrication methods, such as electoral spinning, electron beam, and selective etching, to fabricate a scaffold with a pore size similar to that of natural ECM, which was proven for stem cell proliferation and differentiation.

The environmental mechanical signal was proven to highly influence cell differentiation and organoids' development, growth, and function, and the lack of mechanical signal might cause developmental differences or defects[39]. In recent research, researchers utilized bioengineering tools to manipulate the mechanical properties of substrates or scaffolds to control the fate and development of organoids, such as shear stress, which was proved to improve cell differentiation into specific cell types. North's team found that the shear stress created by blood flow hugely improved the hematopoietic stem cell formation and differentiation[40]. Lee's team found that shear stress can improve the vascularization in the kidney, and they utilized designed chip to mimic the natural shear stress and successfully to establish the kidney organoids on chip[41]. Matsui's team also improved the vascularization of brain organoids on the chip.

Moreover, substrate stiffness was also a crucial mechanical factor in organoid development, affecting cell proliferation, differentiation, and migration. Sorrentino's team developed the liver organoid on the gel with different stiffness. The YAP pathway was highly activated in the stiffer gel, which showed that liver organoids have a higher generation rate in the stiffer gel than in the soft gel[42].

Shkumatov's team found that hydrogel influenced the differentiation and function of the embryoid bodies (EBs) to cardiac organoids, and a hydrogel with an elastic modulus of 6 KPa exhibited the highest percentage of contractile EBs, cardiomyogenic differentiation, and frequency of cardiomyoblast division[43]. Moraes's team developed brain organoids in hydrogel with different stiffness. They found that brain organoids grown in different matrix stiffnesses exhibited differences in growth and development. Stiffer matrices restricted organoid growth and skewed cell populations toward mature neuronal phenotypes, with fewer and smaller neural rosettes[44]. Schneeberger's team also proved that liver organoids showed different differentiation results due to different materials with different stiffness, and the stiffness of 1KPa PIC hydrogel was most compatible with liver organoid development and expansion. Light-sensitive materials were used to fabricate the stiffness of changeable substrates, such as PEG hydrogel, which can become softer with crosslink degradation by light[45], or UV light, which can stiffen the materials through UV light-triggered crosslink increasing[46]. In addition, the photo-degradable materials also allowed researchers to temporally control organoid development by controlling degradation and biochemical signal-releasing speed[39].

Except for the material's properties, the geometry of organoids was also considered to play a significant role in their development and function. The 3D culture environment in which organoids are grown influences their spatial organization, size, and shape, all of which can have

significant effects on the behavior of the cells within the organoids. Lutolf's team used bioengineering techniques to photo-pattern the hydrogel surrounding the organoids, resulting in localized matrix softening and crypt-like structures. They created structures that closely resembled the native architecture of the intestinal epithelium[47] (Figure 3a). Nikolaev's team utilized the soft-lithography method to generate microchannel structure on chips, which induced the formation of tube-shaped epithelia with an accessible lumen and a similar spatial arrangement of crypt- and villus-like domains from intestinal stem cell[48] (Figure 3b). Cheng's team designed three types of geometrical microwell, and they found that embryonic bodies had a higher formation rate in curved devices (LRC and HRC) than flat devices (HRF)[49] (Figure 3c).

As organoid technologies developed, organoids were used in the broader field. The more complex and specific requirement needs a more complex design, which means a single type or simple structure organoids cannot be satisfied by researchers. Researchers combined multiple strategies to establish a more complex design for more complex organoid development, and more bioengineering methods were used to create organoids. For instance, researchers used 3D printing techniques to precisely place cells into specific locations with ECM components by layers [50]. Researchers preliminarily mixed the cells and hydrogel as the bioink, and the bioink was printed on the substrate with the designed pattern multiple times to form the complex 3D structure, allowing the researchers to generate the complicated 3D structured organoid with required cell types. Xu's team utilized 3D printing technology to print the embryonic motoneuron cells into pre-defined patterns and mammalian cells assembled into viable structures[51].

In addition, researchers design and fabricate organ chips to create a similar biochemical

microenvironment through nutrition and chemical signaling control as well as cell-cell interaction[52]. Such as, to support the larger organoid with lung function, Kim's team designed upper and lower two-layer chambers, and cells were seeded in the upper chamber with airflow and the lower chamber as the vascular to transport the nutrients and support the function to mimic the lung structures[53] . In Chrobak's work, blood vessel-like structures were designed to allow fluids to pass through by placing endothelial cells (ECs) within a hollow space created in a collagen gel after the removal of a stainless-steel needle, which showed high permeability after five days[54]. Moreover, Wang's team also designed the independent chamber to allow the media and nutrient flow as the vascular to support their brain organoid growth and development on the chip[55]. Lee's team designed three chamber chips to mimic the stomach's functional environment. The central chamber was utilized for culturing the human gastric organoids, and two in-line chambers were used for restoring media. Three chambers were connected, and micropipettes were inserted on the opposite side of the human gastric organoid and connected to flexible tubing to mimic the stomach environment. In addition, complex designed chips provide researchers with opportunities to combine multiple types of organoids with their interaction. Kim's team established a multi-organ chip of liver, intestinal, and stomach organoids in separate sections, but they were permitted to interact through a media flow between the culture chambers. Combining bioengineering technologies will create more possibilities for researchers in future organoid studies.

1.4 State-of-Art Cardiac Organoids

The heart is the first developmental and one of the most essential organs. Cardiovascular disease is the most severe reason for patient death around the world. The difficulties of research on cardiac behavior and disease mechanisms make researchers urgently need an accurate and

reliable cardiac model, and an excellent cardiac model in vitro also plays an important role in regeneration therapies and drug discoveries[56]. In previous studies, researchers exploited animal models or 2D stem cell-derived cardiomyocyte culture as the platform for basic research and drug testing. However, animal models cannot perfectly represent human cardiac tissue because of the physiological differences between species and also have disadvantages, such as longer experimental time consumption and high cost[57]. Although traditional 2D culture can partly show physiological properties, 2D culture lacks the cell-matrix and cell-cell interaction with lower cardiac maturity[58]. In the current decade, new organoid technology has allowed researchers to establish 3D cardiac organoids, which maintain biological properties and function, The new organoid model provides researchers with a more accurate and reliable platform for further research in many applications[59], such as disease modeling; cardiac organoids can be derived from specific iPSC lines or patient-specific iPSCs, which creates cardiac organoids as disease models. Cardiac organoids can also provide a platform for drug screening and testing the safety and efficacy of potential cardiac medications. In addition, Cardiac organoids hold promise in regenerative medicine. They can be used to study cardiac tissue regeneration and the integration of engineered tissues into damaged hearts to improve cardiac function after injury or disease. Finally, Cardiac organoids provide researchers with a versatile tool to study fundamental questions in cardiac biology and physiology.

Organoids were defined to satisfy several characteristics, including containing the different organ-specific cell types, including CMs, endothelial cells (ECs), and cardiac fibroblasts (CFBs), abilities about the specific function of organs, and cells group together and organized like real organ[60]. Thus, a mature and functional cardiac organoid is three-dimensional (3D) structure that closely mimics the architecture and functionality of human heart tissue in a laboratory setting. These organoids are generated from hPSCs through a process called cardiac

differentiation. The differentiation process involves exposing the hPSCs to specific signaling molecules and growth factors that transform them into cardiac cells. As the cells continue to grow and self-organize, they form intricate cardiac tissue-like structures, resembling early stages of heart development. From the early 2010s, researchers successfully induced stem cell differentiation into cardiomyocytes and formed 3D clusters or aggregates resembling early heart tissue. The mainstream method to generate cardiac organoids has always been divided into two categories. On the one hand, researchers induced stem cells differentiated into all required cell types, and all cell types were mixed and placed in specific locations with the bioengineering technologies. In the early stage, cardiomyocytes were aggregated to cell spheroids, and CM spheroids showed function with mechanical and electrical stimulation[61] (Figure 4a).

As the techniques developed, endothelial cells, cardiac fibroblasts, and other cells were added and mix into cell sources for organoid generation, which showed a better mimic of the real heart[62]. In addition, Hudson's team utilized PDMS to generation the mold to generate the elastic pillars in 96 well-plates, allowing the cells to attach the pillar and form the cardiac organoids later[63] (Figure 4b). Khademhosseini's team seeded cardiomyocytes on the hyaluronic acid (HA) pattern, and 2d structure cardiac organoids detached and formed synchronously contractile in 3 days[64]. Nugraha's team set up cardiac organoids from hiPSC-derived cardiomyocytes mixed with fibroblasts and microvascular endothelial cells to form the compact ball-like structure[65] (Figure 4c). Forsythe's team utilized the hESCs derived 7 day-differentiated cardiomyocytes mixing with Matrigel to establish the cardiac organoids as a platform for environmental toxin screening[66]. In addition, Guerrero's team induced hiPSCs to differentiate into cardiomyocytes, and CMs were seeded into agarose microwell and aggregated to ball-structure cardiac organoids.

Nowadays, modern bioengineering techniques, such as 3D printing technology or biomaterial-based micro-mold[67], were used to fabricate cardiac organoids. This method can precisely control each organoid cell population, but it is hard to mimic the natural cell-cell interaction and developmental process of cardiac tissue. The other standard cardiac organoid generation method is inducing stem cell to differentiate and self-organize cardiac tissue. Hofbauer lab has generated hPSC-derived self-organizing cardiac organoids, and organoids formed chamber-like structures with cavities and beating function[68] (Figure 4d). Lewis-Israeli lab generated cardiac organoids using the Wnt pathway signaling modulation strategy to mimic human cardiac development, similar to embryonic heart development in cell and structure level[69] (Figure 4e). Wu's lab got embryoid bodies formed by suspended ESCs in the media, and EBs were transferred to dishes to differentiate them further to cardiomyocytes. Ma lab established a new cardiac organoids technology by seeding iPSCs with long-period PEG film confinement and creating the cardiac organoids with the Wnt signaling pathway protocol. The stem cell derived cardiac organoids were highly similar to natural developmental processes but could not show a population of each cell component of cardiac organoids. Kim's team also used the same method to generate the cardiac organoids in 6 well plates, which induced the hiPSCs to self-organize to mature function units[70]. In the future, larger-size organoids will be generated with better vascularization, and researchers might create more complex cardiac organoids on chips that combine other types of organoids to mimic more complex and comprehensive physiological behavior and environment[71, 72, 73].

Yin's team incorporated liver and cardiac organoids into a device with multiple layers. The liver organoids were injected into the top layer, while the cardiac organoids were grown in the bottom section. The functional analysis of the organoids together demonstrated a rise in urea

production and an increased display of liver-specific indicators, suggesting the organoids effectively mimicked liver metabolic functions[55]. Zhang's team also generated the cardiac-liver organoid co-system for drug screening, allowing the media to flow with drugs respectively through the cardiac and liver organoids. Their cardiac-liver organoids showed severe toxicity of acetaminophen to liver organoids but a slight impact on cardiac organoids, and they also proved severe toxicity of Doxorubicin on both cardiac and liver organoids[74] (Figure 4f).

The groundbreaking achievement of bioengineering the world's first 3D heart was realized by creating a complex structure comprising blood vessels, ventricles, and chambers. The researchers mixed the hiPSC-derived cardiomyocytes with hydrogel as bioink and decellularized human heart or pig heart as the omenta. Cardiomyocytes with hydrogel were printed into omenta with a pre-designed pattern layer by layer to recurrence the human anatomy structure of the heart. This remarkable feat involved bio-printing the heart using hiPSCs specifically differentiated into cardiovascular cells. However, because of the lack of a heart conduction system, 3D hearts did not show the contractile function[67] (Figure 4g). Though cardiac organoids represent an exciting advancement in cardiovascular research, they are still in their early stages of development. Improving their maturity and complexity remains a focus for researchers to mimic the adult human heart better. Nevertheless, cardiac organoids have the potential to revolutionize our understanding of heart development, disease, and regenerative therapies, moving us closer to more effective treatments for cardiac conditions.

1.5 Drug Embryotoxicity and Developmental Toxicity

Drug embryotoxicity and developmental toxicity are critical aspects of drug safety assessment, particularly in the context of potential risks to the developing fetus during pregnancy. When

medications or pharmaceutical compounds are administered to pregnant individuals, they have the potential to affect the developing embryo or fetus, leading to adverse outcomes and congenital abnormalities. Nowadays, thousands of women are exposed to the risk of drug misuse during pregnancy, and data showed that over 50% pregnant women in the U.S. take prescription or nonprescription drugs at some time during pregnancy. In contrast, about 280,000 pregnant women needed to take category D or X drugs, which were clearly proven to be fatal risks. About one-ninth of women had to face the risk of medicine caused by taking medicine. Drug embryotoxicity caused at least 2% of birth defects, and it also caused but not limited to pregnancy loss, prematurity, developmental disabilities, and even infant death[75].

Embryotoxicity refers to the ability of a substance to cause harm to the developing embryo, interfering with its normal development and resulting in structural abnormalities or functional impairments. On the other hand, developmental toxicity encompasses a broader range of adverse effects on the developing organism, including the fetus and its organs, as well as postnatal development and growth. However, unfortunately, less than 10% of drugs showed enough information to determine the fetal risk, and the drugs might show different reactions in embryos. FDA stopped using former pregnancy risk letter categories because of insufficient information. Researchers have tried to use the urine and hair of newborn babies to estimate the impact on embryonic development, but they cannot provide enough information about the influence on development. Understanding the potential embryotoxic and developmental toxic effects of drugs is crucial for ensuring safe medication use during pregnancy and for protecting fetal health. Regulatory agencies, such as the U.S. Food and Drug Administration (FDA) and the European Medicines Agency (EMA), mandate thorough assessments of drug embryotoxicity and developmental toxicity during preclinical testing and clinical trials before a drug is approved for use in pregnant individuals.

Testing for embryotoxicity and developmental toxicity is a crucial part of the drug development process. The embryotoxicity and developmental toxicity assessment typically involves a tiered approach, utilizing a combination of in vitro and in vivo models. These models aim to evaluate the potential effects of drugs or other substances on embryonic and fetal development. In consecutive studies, researchers utilized vertebrate animal models to test the embryotoxicity of drugs, including rodents[6], frogs[76] and zebrafishes[77]. Zebrafish are frequently employed as models for in vitro experiments and developmental toxicity studies, focusing on embryonic and larval stages. Their short life cycle, high fertility, and genetic similarity to humans make them well-suited for early screening assays.

Zebrafish provide a valuable tool for toxicity screening, which can be instrumental in the assessing potential drug compounds[78]. Ali's team utilized a zebrafish embryo as a predictive model to accomplish the large-scale testing. In their work, they exposed over 20,000 zebrafish embryos to 60 water-soluble compounds representing a range of chemical classes and toxicological mechanisms, and they found that the zebrafish embryo LC50 and rodent LD50 were strongly correlated[79]. Woudenberg's team respectively test zebrafish embryotoxicity of valproic acid (VPA), carbamazepine (CBZ), ethosuximide (ETH), and levetiracetam (LEV) for developmental (neuro)toxicity screening, including morphology, motor activity (MA), histopathology and kinetics. They found that different drugs showed different responses to developmental toxicity. For example, carbamazepine was more sensitive to morphology and motor activity. Valproic acid was more sensitive in histopathology[77] (Figure 5a). Chen's team found the high concentration (1 %) of both ethanol and dimethylsulfoxide increased the deformity rates than lower concentration. Zebrafish showed abnormal motion behavior and hyperactivity in all concentrations of both ethanol and dimethylsulfoxide[80]. Hallare's team also

tested the multiple organic solvent developmental toxicity on the zebrafish model. The result showed that ethanol is the most embryotoxic solvent, which showed a lower survival rate from lower concentrations. Although dimethyl sulfoxide and acetone showed less impact on embryo development, with the higher concentration, zebrafish embryos still showed developmental defects, including weak pigmentation, edema, crooked bodies, eye defect, tail defect, reduced heartbeat, and abnormal hatching[81] (Figure 5b). McPeak's team developed an automated high-content screening assay model with zebrafish embryos, which quantified the teratogenic/embryotoxic potential by measuring the length of zebrafish embryo. The test result of compounds is highly in accord with the known effect of drug developmental toxicity on zebrafish development, such as ethanol retard the zebrafish embryo growth, and nicotine significantly reduces the length and fiber length of zebrafish[81].

Another popular model animal is rodents, which is widely utilized in the field of toxicology to assess embryotoxicity and developmental toxicity of various substances, including pharmaceutical drugs, environmental chemicals, and other compounds, because of their high similarity to humans, large sample size, and short reproductive cycle, and typically involve pregnant rodents exposed to the test substances during critical periods of embryonic and fetal development[82] (Figure 5c). For instance, Bowen's team utilized the pregnancy rate to study the effects of prenatal exposure to toluene. They exposed the pregnant rats to repeated 15-minute high-concentrations of toluene twice a day from gestational day 8 through gestational day 20, and they found high-concentration prenatal toluene exposure patterns significantly increased the rate of adverse postnatal outcomes, including decreased body weight and strength, altered negative geotaxis behavior, and increased numbers of minor malformations[83]. In Chan's work, they investigated the teratogenic effects of diclofenac on rat embryos during organogenesis. They cultured the whole rat embryo and exposed it to different concentrations of diclofenac.

They found that diclofenac significantly reduced the development of the caudal neural tube, flexion, and hindlimb, but yolk sac diameter, crown-rump length, and several somites[84] (Figure 5d).

In addition, the frog model, specifically the African clawed frog (Xenopus laevis) and Xenopus tropicalis, is a widely used system for testing embryotoxicity and developmental toxicity. Xenopus laevis embryos in embryotoxicity testing is that they are susceptible to the effects of environmental chemicals. Moreover, Xenopus laevis embryos have a relatively short development time, making them a convenient and efficient model for studying the effects of chemicals on embryonic development[85].

Due to the physiological differences between the human and animal species, researchers need a more human-relevant and accurate platform for drug developmental toxicity tests with better control and lower cost. At the same time, the push to decrease, improve, and substitute the use of animals for toxicity tests (3Rs) greatly fuels the demand for new approach methods (NAMs) to effectively determine developmental dangers and assess their impact on healthy human pregnancy results[86]. In recent studies, cell models for drug developmental toxicity tests have become more popular. For example, Seiler's team utilized ESCs and 3T3 cells as cell models to test drug developmental toxicity. By assessing cardiac differentiation and MTT test, researchers established the influence of drug developmental toxicity on cardiac development[87]. In West's work, hESCs were utilized as a teratogenicity of drug test platforms. Researchers culture the hESCs with teratogens to establish the database with cell viability assay to create the predictive platform for future teratogenicity tests of drugs[88]. In Pal's work, hESCs were used as a model to evaluate the developmental toxicity of drugs. The researchers treated hESC with penicillin-G, caffeine, and hydroxyurea and observed changes in cell adhesion,

morphology, viability, and gene expression. The result showed that drugs induce downregulation in the expression of a subset of undifferentiated stem cell-, lineage-, and tissue-specific markers and loss of cell adhesion of hESCs with morphological changes and penicillin-G and hydroxyurea significantly interfere with the neuronal differentiation and maturation[89] (figure 5e). Nash's team utilized hESCs to investigate the effects of low-dose ethanol exposure on early development. They grew the undifferentiated hESCs in the 20 mmol ethanol for a week. Researchers assessed the gene expression level, differentiated the hESCs into neuro-progenitors, and assessed their proliferation and differentiation after ethanol exposure. Interestingly, the result showed that low-dose ethanol can increase the proliferation and apoptosis rate of undifferentiated hESCs and neuro-progenitors[89].

Aikawa utilized human iPSCs as the cell model to test the developmental toxicity of multiple drugs. Researchers co-culture the iPSCs with fibroblasts to form the embryo body to represent the embryo and pregnant women, respectively. In this model, the drug whose 50% inhibition concentration of drugs for proliferation/survival of fibroblasts is larger than iPSCs is considered a deadly drug with high embryotoxicity. In contrast, the drug whose 50% inhibition concentration of drugs for proliferation/survival of fibroblasts is larger than cardiac differentiation of iPSCs is considered as deadly drug with high teratogenicity[90]. Adler's team investigated the effects and developmental toxicity of solvents, specifically dimethyl sulfoxide (DMSO) and ethanol, on the differentiation of ESCs and embryonic teratocarcinoma cells (ECCs). Researchers culture the ESCs and ECCs in the media with different solvent concentrations. Researchers assessed the differentiation rate of the cells to represent the developmental toxicity influence, and they found that DMSO induced differentiation in both ESCs and ECCs, while ethanol had a more significant effect on ECCs, and solvents had minimal toxicological effects at non-cytotoxic concentrations[91] (Figure 5f). Johnson's team

investigated the potential developmental toxicity of the antiretroviral drug dolutegravir (DTG) using pluripotent stem cell-based in vitro morphogenesis models. DTG was found to alter the growth and gene expression of hESCs-based morphogenesis models at concentrations of 1 μM and above, and DTG impairs both morphological and molecular aspects of stem cell-based morphogenesis models in a manner dependent on the dose and timing of exposure[92] (Figure 5g).

Lauren's team investigated the developmental toxicity of remdesivir by using in vitro assays with mPSCs and hPSCs. The researchers created morphogenetic EBs (MEBs) using mPSCs and hPSCs, which were exposed to different concentrations of remdesivir. The researchers found RDV exposure led to significant alterations in the morphology of both mouse and human MEBs, and the expression of developmental regulator genes involved in embryonic patterning was also dysregulated[93]. In Yuan's work, the researchers assessed the developmental toxicity of common excipients using a stem cell-based in vitro morphogenesis model. They determined the lowest adverse effect level for three coloring agents (allura red, brilliant blue, and tartrazine) and three preservatives (butylated hydroxyanisole, metabisulphite, and methylparaben). The researchers created three-dimensional cell EBs, from the pluripotent stem cells, which exposed the EBs to different concentrations of excipients, including coloring agents and preservatives, and the lowest concentration that caused adverse effects on EB morphogenesis was defined as the lowest observed adverse effect level (LOAEL)[93] (Figure 5h).

Except for the animal and cell model, the silicon predictive model is another new highly selective choice of embryo toxicity testing platform, such as, Hu's team set up the quantitative structure-toxicity relationship (QSTR) models with zebrafish embryotoxicity testing data. t\These models performed well in predicting acute toxicity and identified the beta-lactam ring,

thiazolidine/dihydrothiazine rings, side chains, and spatial configuration as the main factors responsible for toxicity. Silico models for toxicity testing have several advantages. Firstly, it is a cost-effective approach as it eliminates the need for expensive and time-consuming experimental testing on live embryos. Secondly, it allows for the screening of a large number of compounds in a relatively short period. Additionally, in silico models can provide insights into the structure-toxicity relationships of compounds, helping researchers understand the underlying mechanisms of toxicity[94].

1.6 Organoid Technology for Embryotoxicity and Developmental Toxicity Testing

The physiological difference between human and animal species determines that the animal model is unsuitable for drug embryotoxicity research. Later research utilized some new technologies for drug tests, such as cellular models using permanent cell lines[95]. The advent of stem cell technology provides researchers with a new and better platform for drug testing.

Organoid technology has been a promising tool for toxicity testing, particularly concerning embryotoxicity and developmental toxicity. Traditional toxicity testing methods often involve animal models, which have significant ethical considerations and may not always accurately predict human responses. Human stem cell derived organoids could be used to study the impact of various substances on organ development and function in a controlled environment. Organoids, 3D cell cultures derived from pluripotent stem cells, can replicate the early stages of organ development and mimic the structure and function of human tissues and organs. Current efforts are focused on generating genetically modified differentiated cells, such as neurons, cardiomyocytes, endothelial cells, and hepatocytes, which can be utilized for large-scale toxicology screenings[96], therefore offering a unique opportunity to study the impact of

potentially toxic substances during these critical periods.

Cerebral organoids derived from hPSCs offer considerable potential for gaining insights into the mechanisms of various neurodevelopmental disorders. These hPSC-derived neural constructs serve as valuable tools for rapid compound safety testing due to growing demands[97] (Figure 6a). For example, neural tissue derived from iPSCs containing neuronal and glial organization, endothelial cells, and microglia have been utilized to predict the neural toxicity of 60 compounds[98] (Figure 6d). Nzou's team employed a human neural spheroid, consisting of a functional blood-brain barrier interacting with other cell types like neurons, microglia, and oligodendrocytes, to assess neurotoxicity[99] (Figure 6c). Maternal alcohol exposure during pregnancy can lead to neurodevelopmental disabilities and behavioral and cognitive dysfunctions, collectively referred to as fetal alcohol spectrum disorders (FASDs)[100]. Recently developed human cerebral organoids serve as relevant in vivo systems for identifying the adverse effects of alcohol on neurons[101] (Figure 6b). Ao's team developed a comprehensive microfluidic-based hPSC-derived brain organoid platform[102]. Neurodevelopmental exposure to delta 9-tetrahydrocannabinol (THC), the primary psychoactive component in cannabis, was found to impair neurite outgrowth, reduce neuronal maturation, and decrease spontaneous firing in the brain organoids[102]. Nicotine exposure has also been linked to neuronal disabilities in the fetal brain during pregnancy. To further understand early fetal development under nicotine exposure, a brain organoid combined with a chip device was developed[103] (Figure 6e). Additionally, engineered brain organoids on a chip with octagon-shaped micropillars were utilized to investigate cadmium (Cd)-induced neural dysfunctions. Cd exposure was found to elicit increased neural apoptosis and aberrant differentiation and organization in the brain organoids, indicating impaired neurogenesis during fetal brain development[104].

Drug-induced cardiotoxicity, which can result in cardiac dysfunction and myocardial injuries, represents a significant clinical challenge. The Embryonic Stem Cell Test (EST) comprises in vitro test systems (cytotoxicity test and cardiac differentiation test) and has demonstrated equal or superior accuracy (78%) compared to other in vitro embryotoxicity tests[105, 106] (Figure 6f). Consequently, the inhibition of ESC differentiation into cardiomyocytes has been recognized as a primary indicator of embryotoxicity[107, 108]. The development of spontaneously contracting cardiomyocytes (CMs) from iPSCs has emerged as a novel and highly physiologically relevant tool for testing cardiotoxicity in human cell models[109]. An iPSC embryotoxicity test revealed a reduction in cardiac differentiation efficiency after thalidomide treatment[110], with this test system showing significantly improved predictive capabilities compared to the EST. Assessing the risk of cardiotoxicity involves two main elements: proarrhythmic effects and cardiac cellular contractility. For example, doxorubicin, an effective anticancer agent, can induce cardiotoxicity by upregulating iPSC-derived cardiomyocytes' (iPSC-CMs) apoptosis and reducing the beating rate and amplitude of [111]. Human iPSC-derived cardiac organoids have been developed to overcome the aforementioned obstacles and better mimic in vivo organ functions. This advanced system can be employed to predict the potential toxicity of drugs. Mills et al. utilized this mini-heart model to screen pro-proliferative compounds for heart muscle cells and assess potential side effects on heart contractility[112] (Figure 6g).

The advantage of using organoid technology for embryotoxicity and developmental toxicity testing is that it allows for more accurate replication of human development, potentially providing a better understanding of how substances might impact human embryos. In addition, organoids can be developed from iPSCs reprogrammed from adult cells, which means that they can be patient-specific, potentially allowing for the testing of individual susceptibility to embryotoxicity and developmental toxicity. However, there are still many challenges and

limitations. These include the technical difficulties in creating and maintaining organoids, the complexity of accurately modeling organ development and interactions, and the need for more standardized and validated protocols for in toxicity testing. Overall, while the use of organoids in toxicity testing holds great promise, this is an active area of research, and many improvements and advancements are likely to occur in the future.

1.7 The Goal and Structure of the Dissertation

This dissertation will chiefly focus on the characterization, optimization, and utilization of cardiac organoids with the capability to mimic early heart development. Moreover, a chapter is dedicated to analytical instruments for evaluating cardiac contraction, particularly drug-induced cardiac toxicity. Overall, this dissertation integrates techniques and tools for progressive drug testing related to cardiac functions. The primary objectives of this dissertation include: 1) initiating preliminary research to deepen the understanding of how geometric confinement affects the development of cardiac organoids; 2) employing the cardiac organoids for embryotoxicity assessment; and 3) utilizing advanced computational techniques to investigate cardiac reactions to drugs further. Chapter 2 will focus on the procedures used to create cardiac organoids for the ensuing chapters. Chapter 3 elaborates on how the structure and function of cardiac organoids are directed by examining diverse geometric designs. Chapter 4 explores the potential of this system for embryotoxic drug evaluation, given that the organoids are theorized to replicate an early-stage heart. A consistent shape and size were selected to produce organoids extensively for drug testing during differentiation, resembling continuous drug intake or medication use throughout pregnancy. Finally, Chapter 5 will summarize the dissertation and reflect on the forward-looking implications of this research.

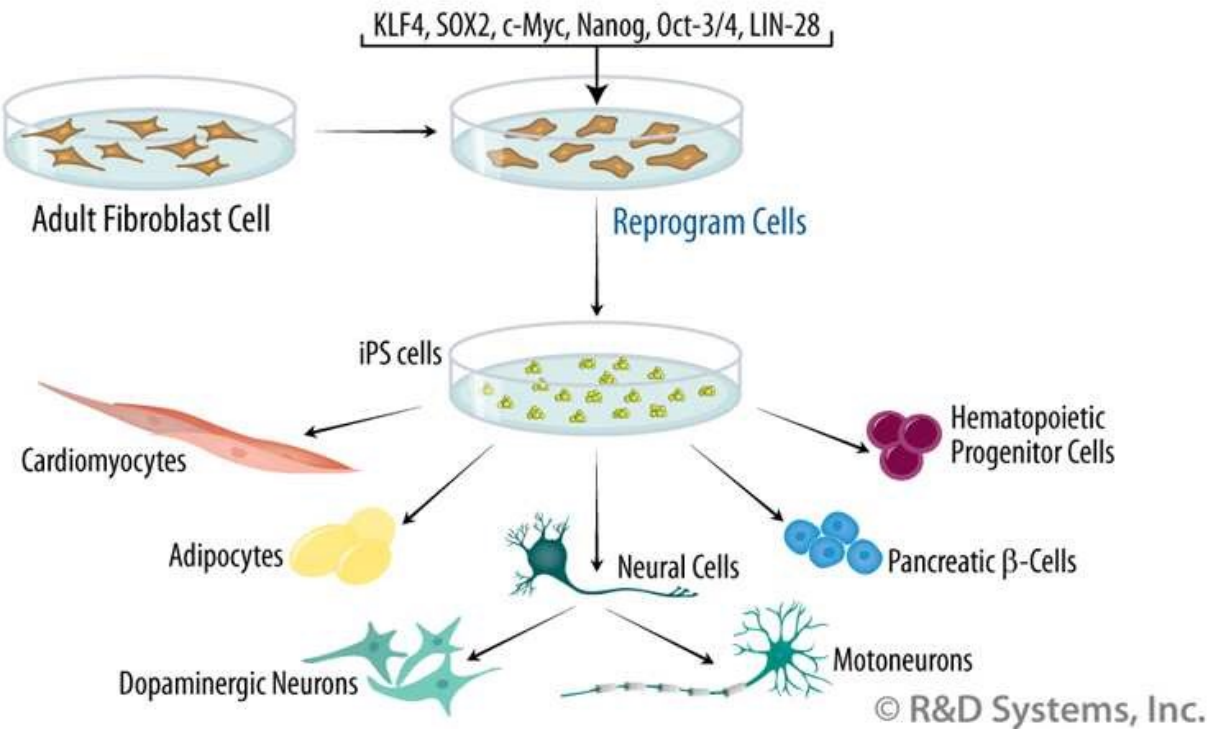

Figure 1. Stem cell biology and human development. Potentials of using *in vitro* induced pluripotent stem cell biology to model *in vivo* human cell and tissue development[113].

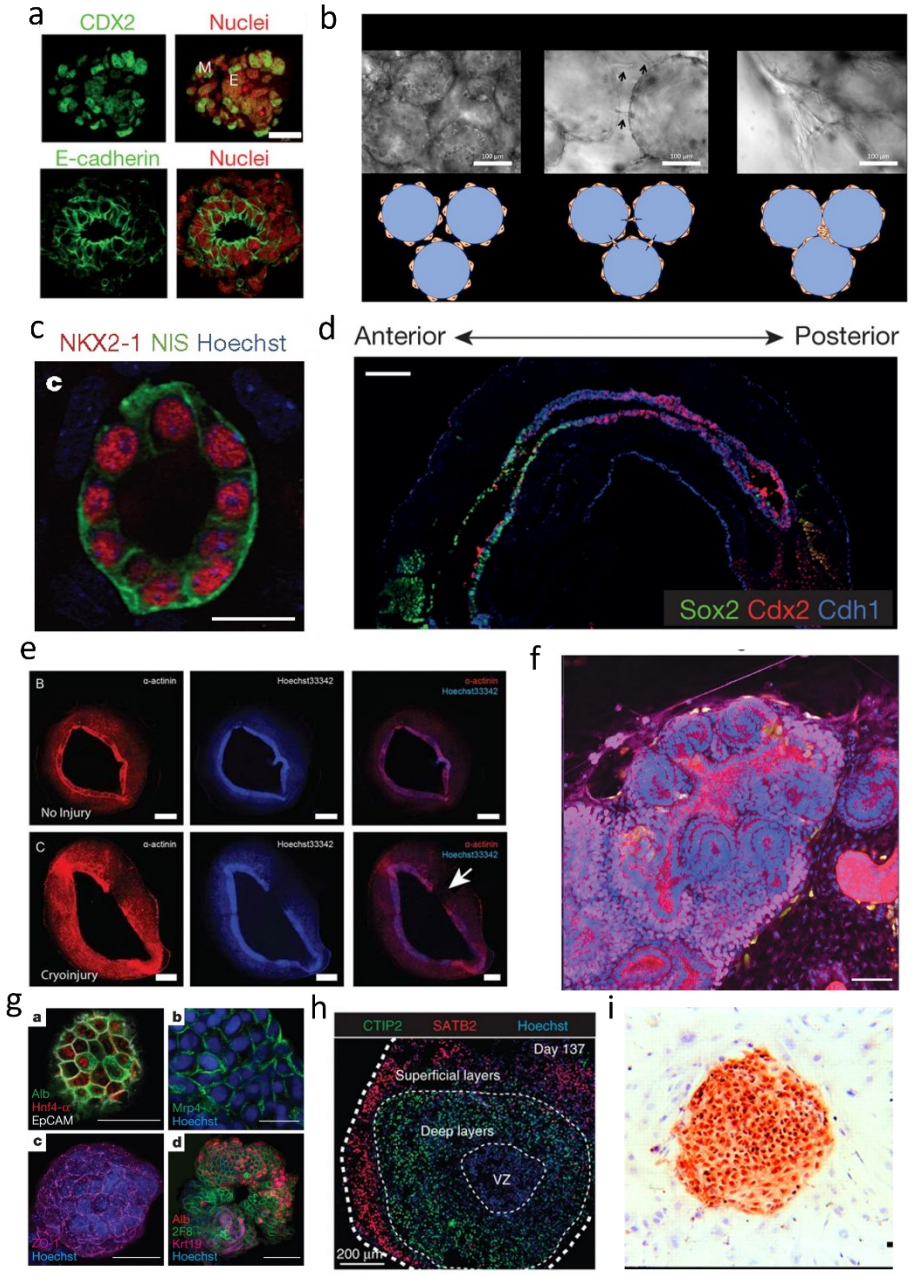

Figure 2. Stem cell organoids exhibit spatial organization and features that resemble native *in vivo* organs. Stem cell organoids with spatial organization and patterning have been engineered to model numerous organs, including **(a)** gut[20], **(b)** lung[12], **(c)** thyroid[114], **(d)** gastric[20], **(e)** heart[15], **(f)** kidney, **(g)** liver[16], **(h)** brain[63], and **(i)** retina[10]. All figures are reproduced with copyright permission.

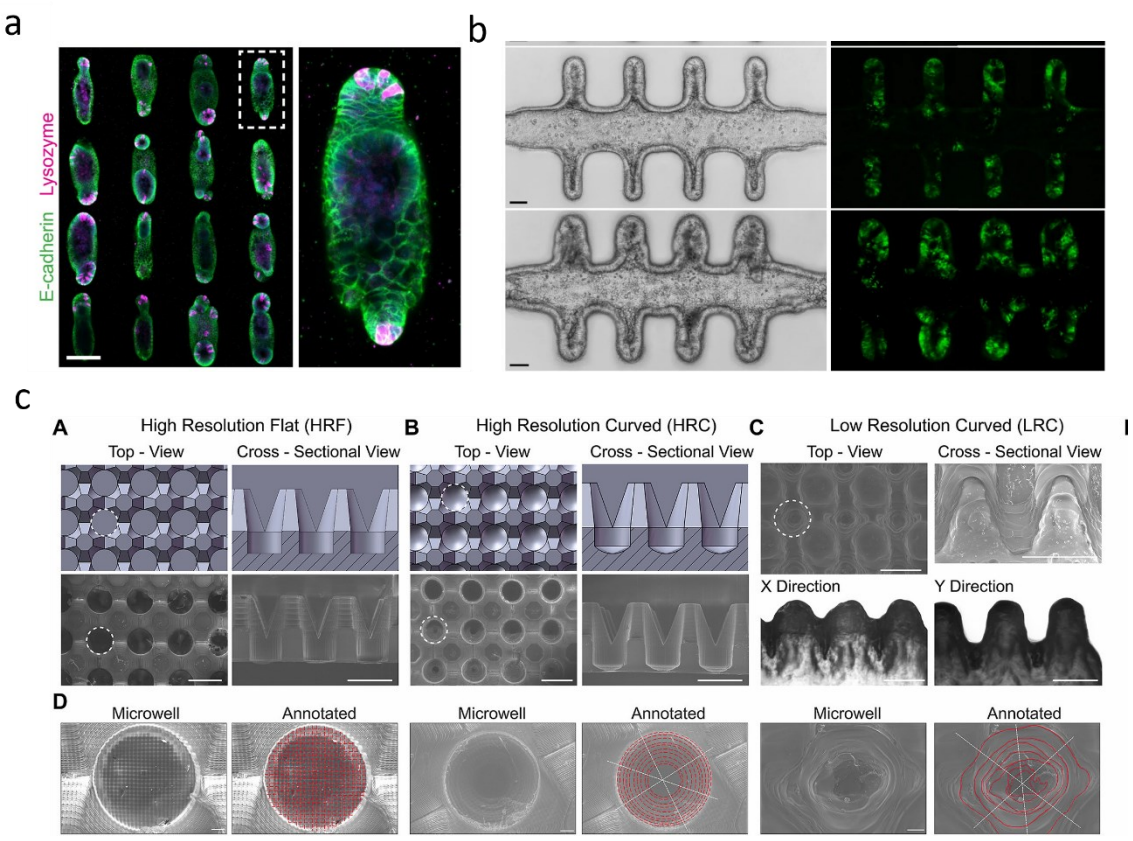

Figure 3. Organoid development influenced by the geometry of the pattern: (a) Photopattern area softening allows the crypt-like structure formation[47]. **(b)** the soft-lithography method was used to generate microchannel, which induced the formation tube-shaped epithelia[48]. **(c)** curved devices (LRC and HRC) and flat devices (HRF) had different influences on embryonic body formation. All figures are reproduced with copyright permission.

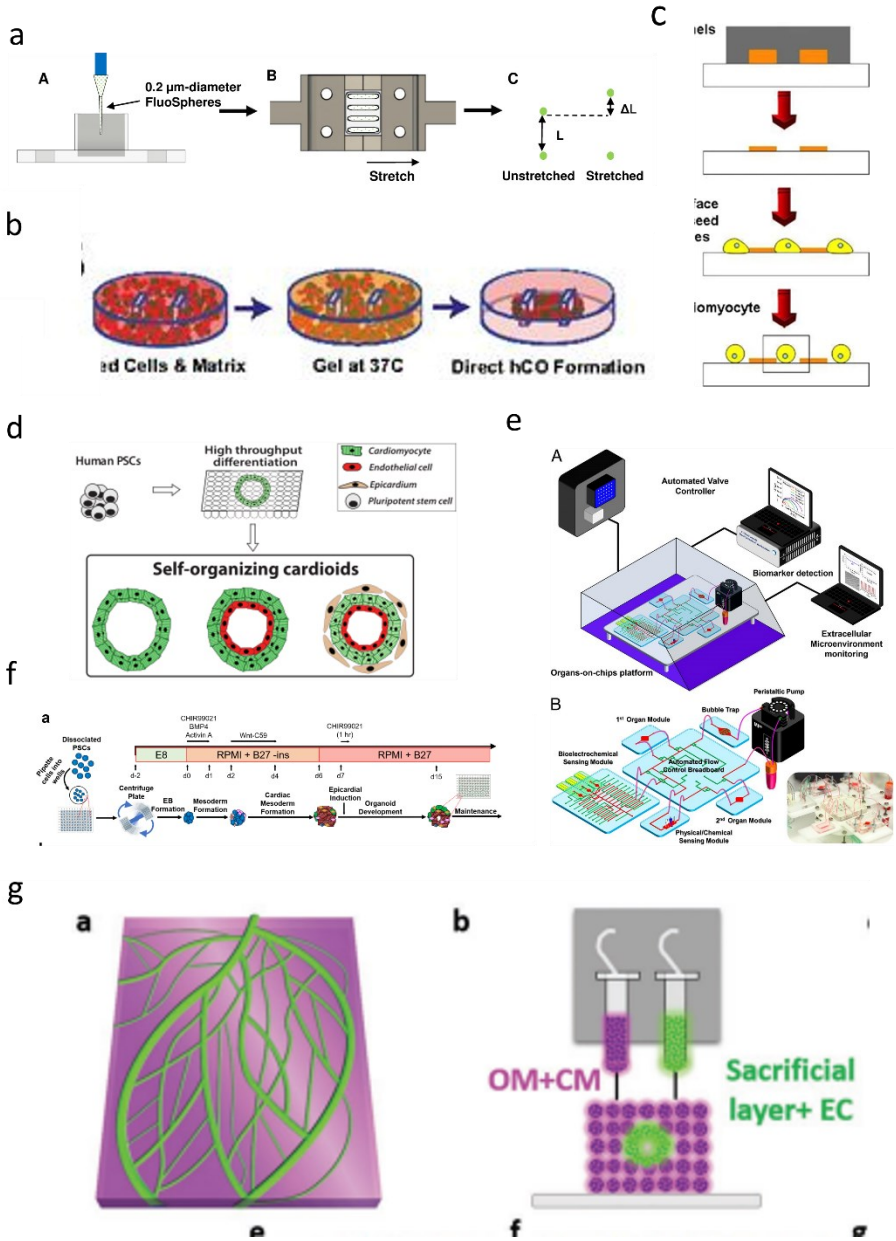

Figure 4. Generation of cardiac organoids with different bioengineering methods. (a) Early-stage cardiac organoid formation with mechanical and electrical stimulation[61]. (b) Cardiomyocytes are seeded on hyaluronic and form the functional organoid after detachment[115]. (c) cardiomyocytes mix with other cell types to form a compact ball-like structure c4. (d) Human stem cells form cardiac organoids by their self-organization[68]. (e) Stem cells form embryonic bodies and then form cardiac organoids[69]. (f) Cardiac organoids combine with liver organoids for drug screening f3. (g) The first 3D heart has a complex structure, including blood vessels, ventricles, and chambers, by 3D printing technology[67]. All figures are reproduced with copyright permission.

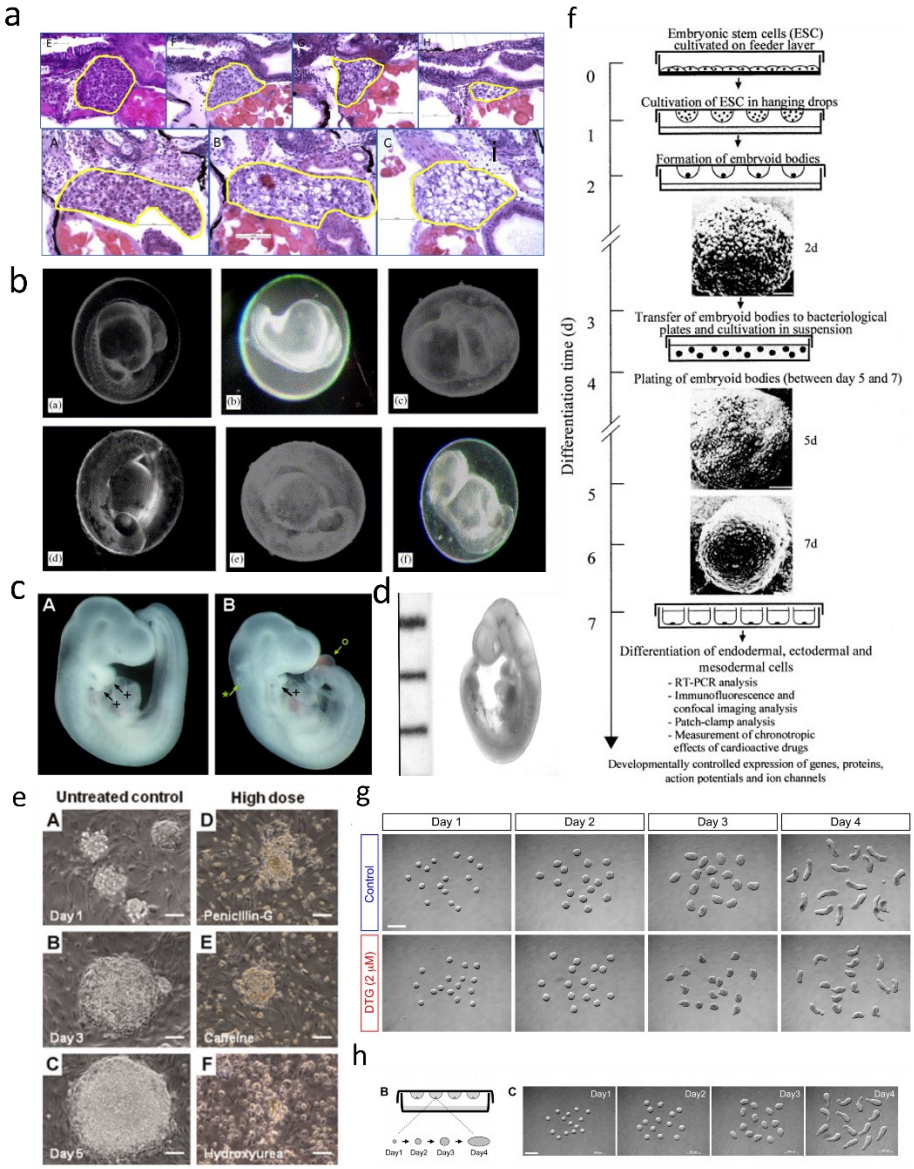

Figure 5. The traditional model for drug developmental toxicity testing. (a) Zebrafish model for embryotoxicity testing of valproic acid (VPA), carbamazepine (CBZ), ethosuximide (ETH), and levetiracetam[77]. **(b)** Solvent developmental toxicity test on zebrafish embryo model[81]. **(c)** Rodent model for drug developmental toxicity testing[82]. **(d)** Teratogenic effects of diclofenac on rat embryos, shown as abnormal morphology of rodent embryo[84]. **(e)** hESCs were used to test the developmental toxicity of penicillin-G, caffeine, and hydroxyurea[116]. **(f)** dimethyl sulfoxide (DMSO) and ethanol both increased ES cell differentiation[91]. **(g)** dolutegravir impairs the stem cell morphology[92]. **(h)** EBs were used to determine the lowest observed adverse effect level[93]. All figures are reproduced with copyright permission.

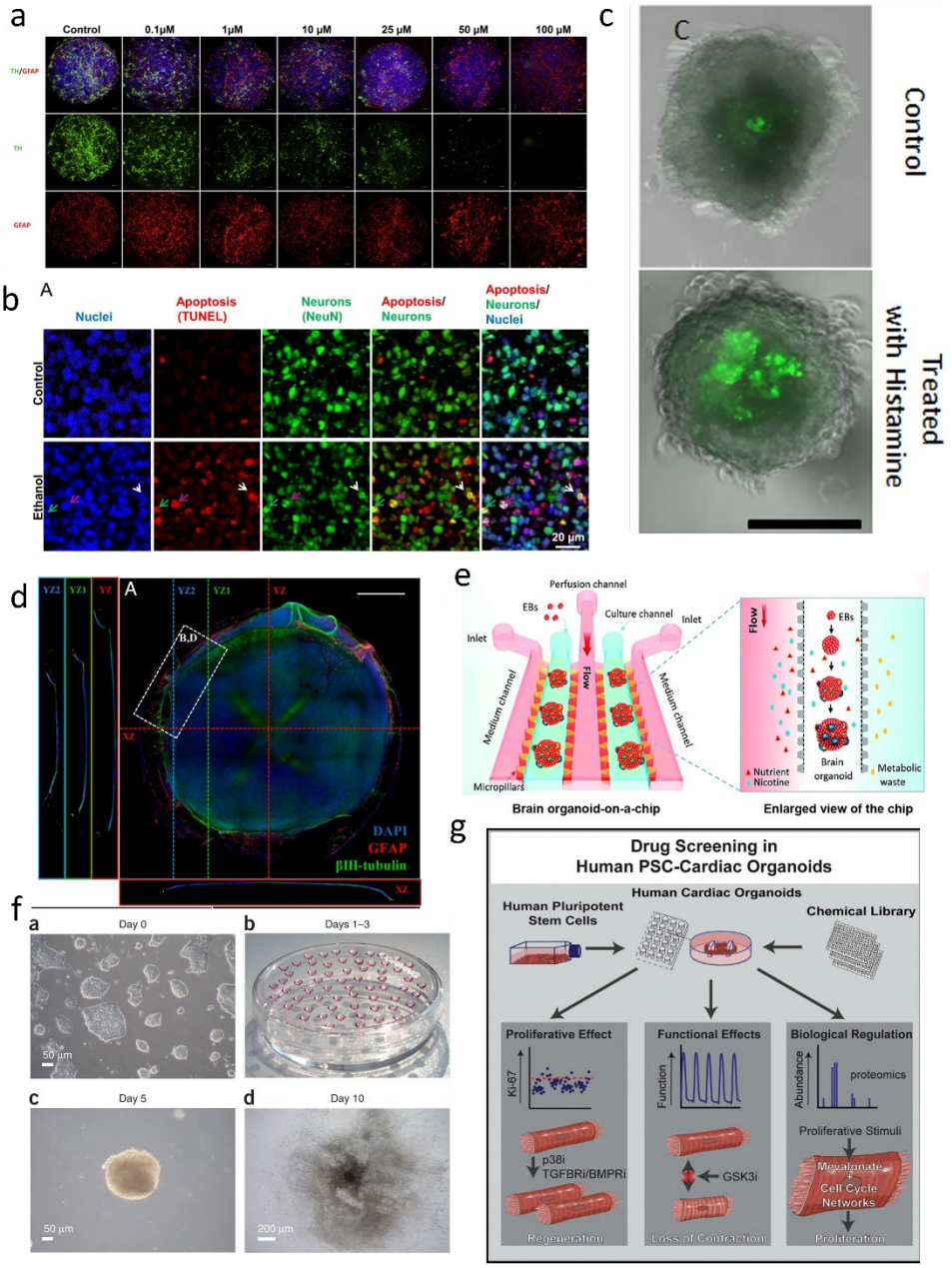

Figure 6. Organoids for drug developmental toxicity testing. (a) hPSC-derived neural organoids were testing the growing demands[97]. **(b)** human cerebral organoids were used to identify the adverse effects of ethanol[101]. **(c)** human neural spheroids were used to assess neurotoxicity[99]. **(d)** Brain organoids were used to test 60 compound neuronal toxicity[98]. **(e)** brain organoid combined with a chip device was developed nicotine exposure impact[103]. **(f)** Embryonic Stem Cell Test (EST) comprises in vitro test systems with higher accuracy than other tests[106]. **(g)** mini hearts were used to screen pro-proliferative compound potential effect[112]. All figures are reproduced with copyright permission.

2. CHAPTER 2. METHODS: CARDIAC ORGANOID GENERATION AND CHARACTERIZATION

2.1 Micropatterning Techniques to Create Organoids

Geometrical and mechanical properties of cell culture microenvironments were proven to influence cell morphogenesis and function significantly. Especially, stem cells can be induced into different cell fates and differentiate into different cell types because of the different environmental mechanical impacts. Han's team proved that material stiffness, ECM ligand density, surface topography, and ECM micropattern can all impact stem cell fate and differentiation into adipogenesis, myogenesis, and osteogenesis[117]. Micropatterning techniques can be generated on surfaces such as silicon wafers, polymers, metals, or glass, and they can consist of features such as lines, dots, circles, or more complex shapes. Micropatterning techniques enable researchers and engineers to manipulate the arrangement and organization of materials or structures at a microscopic level. This level of control is vital for a wide range of applications, including microelectronics, microfluidics, tissue engineering, biosensors, and microfabrication.

In previous studies, many researchers have successfully generated functional organoids with micropatterning, and the common micropatterning technologies include photolithography, soft lithography, microcontact printing, and many others. Photolithography is one of the most common technologies are widely used to fabricate the designed surface topography. Xu's team utilized micropatterning technology to induce the generation of liver organoids. They fabricated the SU-8 positive mold using the photolithography technology and generated PDMS stencils with SU-8 mold, which interfere with the oxygen plasma treatment to remove the PEG

monomer and allow cell attachment on the removal area where the hiPSCs develop to liver organoids[118] (Figure 7a). Soft lithography is another commonly used micropatterning technology. In Seo's work, they generated polarized spinal cord-like organoids with dorsoventral organization using human pluripotent stem cells (hPSCs) and micropatterning techniques. Soft lithography technique is used to fabricate stamps, and the stamp is created onto a wafer with UV light treatment with a photomask. Matrigel was printed by stamps and transferred the pattern on the coverslips, where hPSCs were induced to differentiate and form the sprouting-like protrusion morphogenesis[119]. Karzbrun's team also used standard soft-lithography technologies to fabricate stamps, which were used to print laminin-521 to the glass surface. The result of the work showed hPSCS seeded on the micropattern developed to the neural tube, and lumen formation and folding were observed in the organoids[83] (Figure 7c). Microcontact printing technology transfers the designed pattern with stamps onto the substrate to control or limit the cell culture microenvironment. Abilez's team utilized microprinting technology to create cardiac vascular organoids. The researchers used geometric micropatterning to create spatially organized cardiomyocytes. They used a plasma-treated stencil with a central hole to create circular micropatterns on a multi-well plate, which allowed the formation of cardiac organoids in wells[120] (Figure 7b). Deglincerti's team used commercial microfabricated slides to print human laminin with different size micropatterns on chips, and hESCs were seeded on the micropattern and differentiated into structured and radially balanced circles that are reminiscent of embryonic organization. The differentiation fate is influenced by the colony's size, with larger-sized colonies exhibiting the creation of mesoderm, endoderm, and extra-embryonic trophoblast, respectively[121]. Metzger's team printed and transferred the laminin with micropattern on the dishes, whereas the hESCs were seeded on the pattern. They developed the hESCs to neural organoids for drug screening. To conduct a pharmaceutical investigation aimed at identifying potential therapeutic targets that could rectify developmental

anomalies in organoids, these organoids were sourced from stem cells bearing mutations associated with Huntington's disease[122].

2.2 Photolithography Technique

The earliest micropatterning technology can be traced back to the mid-20th century; photolithography was considered one the first micropatterning technologies and was widely used in semiconductor manufacturing, microelectronics, and microfabrication. Photolithography enables the precise control of feature size and shape, allowing for the fabrication of intricate microscale structures. It involves a series of steps to create precise patterns on a substrate using light-sensitive materials known as photoresists. The process of photolithography typically involves the following steps. The first step is substrate preparation, and the most common substrate materials were often chosen as clean glass or silicon. Next, a thin photoresist layer was coated on the substrate by technologies, such as spin coating or vapor deposition, which is sensitive to ultraviolet (UV) or deep ultraviolet (DUV) light. After coating, the coated substrate was treated with a gentle heating process, known as soft baking, which removes the solvent and improves photoresist adhesion on substrate. Then, the mask with pattern designs was placed and covered on the substrate, which allowed the light to pass through and transfer pattern to the substrate. The masked substrate is exposed to UV or DUV light. After exposure, the substrate undergoes a development step using a developer solution. Etching or deposition processes are then performed to remove or add materials to the exposed regions, creating the desired pattern on the substrate. Finally, the remaining photoresist is typically removed from the substrate using solvents or plasma-based techniques, leaving behind the patterned structure.

In this project, we produced patterned wafers using SU8 photolithography technologies. Initially, various pattern shapes and sizes were designed using AutoCAD software and professionally printed by CAD/Art Services Inc. The pattern designs were separated into 3 categories, including circle, square and rectangle, and pentagram. Circle patterns were designed with different diameters from 200 microns to 1000 microns to investigate the influence of size on cardiac differentiation, and square and rectangle patterns were designed with the same area but different aspect ratios from 1 to 1 to 1 to 4 for the investigation of shape influence on cardiac development. The pentagram patterns with different central and peripheral area ratios from 1 to 4 were designed for central and peripheral impact. The desired characteristics were subsequently transferred onto SU8 Master wafers through conventional photolithography procedures, adhering to the guidelines provided by the photoresist manufacturer (Figure 8a).

In summary, a negative photoresist named SU8-50 (MicroChem) was applied to the wafers using a specified spin-coating speed, resulting in features with a height of 100 μm. SU8 is a negative photoresist that solidifies upon exposure to UV light, rendering it resistant to removal by a developer solution. The coated wafers were swiftly exposed to intense UV light with the corresponding photomasks positioned on top, allowing UV penetration in the desired shapes and sizes through the transparent regions of the masks. Following that, the wafers underwent a post-UV exposure baking process and were immersed in a developer solution to eliminate the uncured photoresist. This standard procedure yielded a mold with raised features, forming the foundation for the fabrication of PDMS stencils. Additionally, a silane solution (1H,1H,2H,2H-Perfluorooctyltriethoxysilane; Sigma Aldrich) was vacuum-deposited onto the wafers to enhance their hydrophobicity, facilitating the effortless removal of the stencils.

2.3 Soft Lithography Technique

Another common micropatterning technique is soft lithography, which researchers used more because of its broad adoption and diverse application. Soft lithography is a versatile and widely used micro- and nano-patterning technique that involves using elastomeric stamps or molds to transfer patterns onto substrates. The whole process of soft lithography always includes these several steps. First, soft lithography begins with fabricating a master mold, known as a template or a stamp, fabricated with other technologies. Next, the replica molding, usually PDMS mold, is fabricated by liquid PDMS poured and cured on the master mold. The PDMS replica mold is then coated with ink, functional materials, and contact substrate with gentle pressure to transfer the pattern to the substrate.

This work generated using the standard procedure of soft lithography. The PDMS pre-polymer (Sylgard 184) was mixed at a weight-to-weight ratio 10:1 between the elastomer base and the curing agent. The mixture was then subjected to vacuum degassing for at least one hour. A small volume (approximately 1 mL) of the PDMS pre-polymer solution was poured onto each wafer with the target pattern created in the last step (Figure 8b), followed by the placement of a square piece of transparent plastic, cut to match the wafer's size. The transparency was further pressed down by positioning glass slides on top (Figure 8c). Subsequently, the wafer-PDMS-transparency-glass assembly was secured using two large binder clips on both sides. This ensured the uniform spreading of PDMS across the pattern array, forming holes that corresponded to the features on the wafer. The wafer assemblies with transparency and glass were placed in a 60 ºC oven overnight, allowing the PDMS to be cured. The resulting cured stencils were then peeled off and trimmed to fit into a 35 mm tissue culture well, and cured stencils were cut into small pieces to match the 6-well plates and 12-well plates (Figure 8d).

2.4 PEG Hydrogel Preparation

To create patterns on tissue culture polystyrene, a thin layer of PEG is grafted and selectively removed using PDMS stencils and oxygen plasma treatment. The PEG solution is prepared by combining and mixing 150 mg of PEG 1000 (Polysciences), 1.8 mL of PEG (400) diacrylate (PEGDA) (Polysciences), 15.55 mL of isopropanol, and 0.45 mL of MilliQ water, and total volume of PEG solution is 16.8 mL. Then, 760 µL of the solution is grafted onto individual wells of a 6-well plate, or 350 µL of the solution is grafted onto individual wells of a 12-well plate that has been pretreated with oxygen plasma for three minutes. The grafted plates are exposed to high-intensity UV light to polymerize the PEG on the surface (approximately 45 seconds with Oxygen plasma treatment system, PlasmaEtch PE50XL), leaving behind residual polymer. The residual polymer is subsequently rinsed away with MilliQ water to achieve a clear surface.

2.5 Plasma Etching, Surface Cleaning and Geltrex Coating

Next, the PDMS stencil made by soft lithography is placed over the PEG-grafted surfaces (Figure 8e), exposing selective patterned regions of the PEG. These exposed regions are then subjected to oxygen plasma treatment (about 3 minutes). The plasma etching process removes the PEG from these stencil-exposed regions, creating patterns that discourage biofouling and promote cell attachment in patterned areas.

The well-plate surfaces with the stencils in place were sterilized and coated with hESC-qualified Geltrex Matrix (ThermoFisher) to facilitate the attachment of hiPSCs. For sterilization, the whole plate was sprayed with 70% ethanol, and each well and plate lid was filled with 70% ethanol and left under UV light for 1 hour within a biosafety cabinet. Afterward,

the ethanol was aspirated, and the wells were washed with phosphate-buffered saline (PBS) three times. Subsequently, a thin layer of hESC-qualified basement membrane matrix (Geltrex) was added to each well, finalizing the surface patterning and preparing the wells for cell seeding.

2.6 GCaMP6f hiPSC Culture and Seeding

GCaMP6f human iPSCs (hiPSCs) derived from healthy adult donors were cultured and expanded using standard pluripotent stem cell maintenance techniques. Our laboratory protocol involved culturing hiPSCs on Geltrex-coated plates in Essential 8 (E8) medium and passaging them using Accutase dissociation reagent. The E8 medium was changed daily to ensure optimal cell health and viability. When the cells reached approximately 80% confluence, they were considered ready for passaging and seeding. Prior to cell seeding, the patterned and coated plates were incubated at 37ºC for 1 hour to activate the proteins within the Geltrex matrix. The confluent hiPSCs were washed with PBS and treated with Accutase dissociation reagent for 4 minutes until the cells were visibly detached. Following centrifugation, the cells were resuspended in E8 medium supplemented with 10 μM Y27632 and seeded onto the patterned tissue culture plates at a seeding density ranging from 0.4E6 to 0.7E6 cells. This range accounts for the different sizes to be explored in this study and considers the variable growth kinetics of each cell line. After 24 hours, the stencils inside the wells were carefully removed using sterilized tweezers, leaving only the cells that had attached within the patterned regions. Additionally, the E8 medium was changed to remove the Y27632 supplement. With daily feeding, the hiPSC colonies were typically able to proliferate and fill the patterns to confluency around 72 hours after seeding, thus initiating the differentiation process.

2.7 Organoid Differentiation

Cardiac differentiation was initiated approximately three days after the initial seeding, when the cells reached confluency within the patterned regions. The differentiation process was induced by the modulation of the Wnt/Beta-catenin pathway using small molecules. The small molecule stocks were dissolved in sterile DMSO and then diluted to their final concentrations in RPMI 1640 medium supplemented with B27 minus insulin (RPMI1640/B27-I). To initiate differentiation, the culture medium was replaced with 10 μM GSK3 inhibitor CHIR99021 on Day 0, and this medium was maintained for 24 hours. On Day 1, the medium was exchanged with fresh RPMI1640/B27-I. Subsequently, on Day 2, the medium was replaced with 5 μM WNT pathway inhibitor IWP4, and this medium was maintained for 48 hours. On Day 4, the IWP4 was removed and replaced with fresh RPMI1640/B27-I. From Day 6 onward, the medium was changed to RPMI1640 supplemented with B27 complete supplement (RPMI1640/B27+C) every two days until the termination of the differentiation process around Day 20 (Figure 9). Around Day 12 of the differentiation timeline, the differentiated cells started displaying spontaneous contractions, indicative of the development of functional cardiac-like tissue.

2.8 Bright-field Video Recording and Motion Tracking Analysis

The functional contraction of cardiac organoids was evaluated around Day 20 of the differentiation process. Prior to termination, videos capturing the contractions were recorded or subsequent analysis of contraction behavior. The organoids were imaged within an onstage microscope incubator (OkoLab Stage Top Incubator, UNO-T-H-CO2) maintained at 37˚C and 5% CO2 to preserve physiological activities (Figure 10a). Imaging was performed using a Nikon Ti-E inverted microscope equipped with an Andor Zyla 4.2+ digital CMOS camera. The

recorded videos were exported as sequences of individual images and subsequently analyzed using an open-source Motion Tracking Matlab script developed by Huesch et al. This software utilized block matching algorithms to calculate motion vectors representing the velocities of tissue contraction and relaxation (Figure 10b). Furthermore, the motion vectors were utilized to reconstruct contraction motion waveforms, representing of the muscle's contraction and relaxation cycles within the tissues. Notable parameters extracted from the analysis included contraction and relaxation velocities, beat rate, and beat duration, which quantitatively measure the organoids' contraction behavior (Figure 10c).

2.9 Fluorescent Video Recording and Calcium Transient Analysis

The functional contraction of cardiac organoids was evaluated with calcium signal change, since the cardiac beating begins with inner cell calcium ion concentration increase and ends with calcium ion concentration recovery. Video capturing the concentration changes were recorded or subsequent analysis of contraction behavior. The organoids were imaged within an onstage microscope incubator (OkoLab Stage Top Incubator, UNO-T-H-CO2) maintained at 37˚C and 5% CO2 to preserve physiological activities (Figure 10d). Imaging was performed using a Nikon Ti-E inverted microscope equipped with an Andor Zyla 4.2+ digital CMOS camera under the GFP channel. Videos were exported as an nd2 file type and analyzed by calcium signal analysis the Matlab script was developed by Schuftan et al. The software traced the fluorescence signal change in videos to represent the function of cardiac organoids. Furthermore, the motion vectors were reconstructed to calcium signal waveform and represented beating function (Figure 10e), which provides the parameters, such as T0, T50, T75, max signal, F/F0, and beat duration. In addition, the calcium signal change area was considered a functional cardiac tissue area (Figure 10f), and The *Area Ratio* was measured to

approximate the area of fluorescence of tissue and normalize this area relative to the area of the entire pattern (Figure 10d).

2.10 Statistics

All box plots in the figures display the minimum, maximum, median, and 25th and 75th percentiles. Unless explicitly mentioned, statistical analysis was conducted using analysis of variance (ANOVA) with Tukey's multiple comparison test as the post-hoc analysis. Data were considered with significant differences, when the p-value is less than 0.05, and data were labeled with *, **, ***, and **** to respectively represent p-value < 0.05, 0.01, 0.001, and 0.0001.

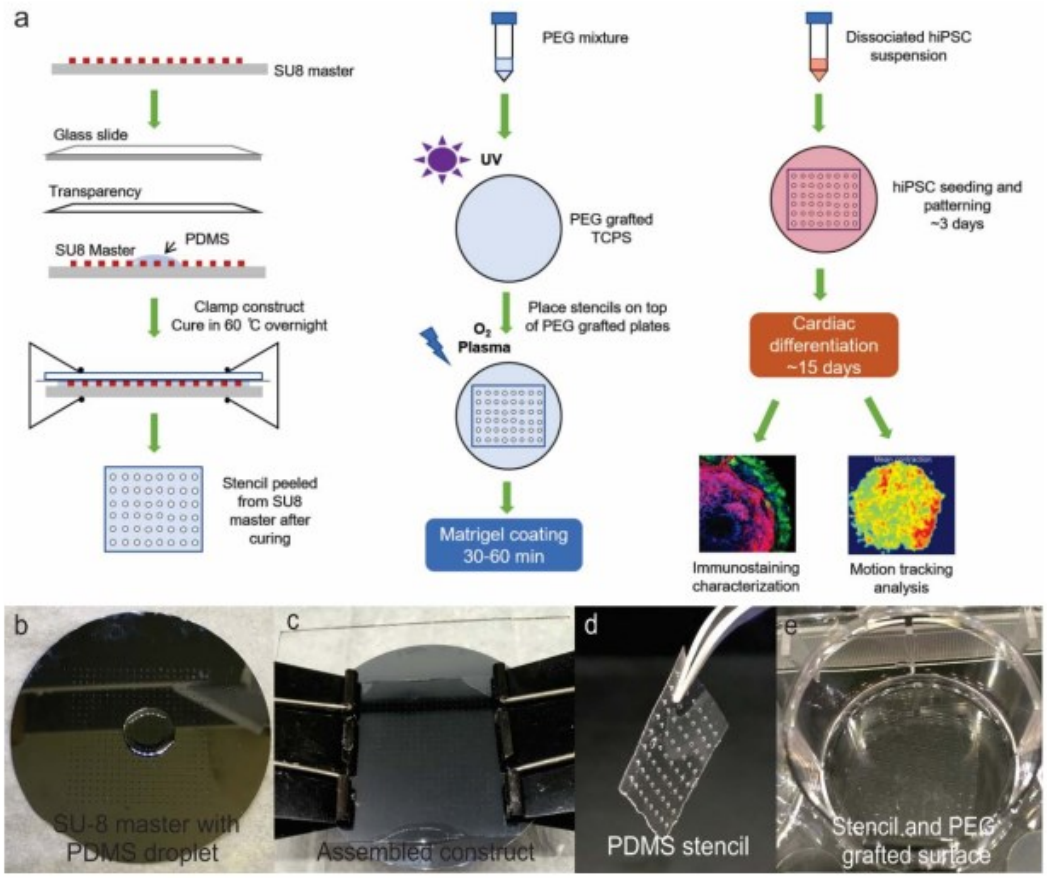

Figure 7. Procedure and process of PDMS stencil fabrication. (a) critical steps of the entire procedure. (b) PDMS prepolymer was pure on the SU-8 wafer. (c) The entire structure of PDMS stencil fabrication, including patterned SU8 wafer, liquid PDMS, transparency, and glass slide. (d) Stencils were cut into suitable sizes after a thin layer of PDMS film formed on the wafer. (e) PDMS stencil was placed into PEG-covered wells for oxygen plasma treatment[123]. All figures are reproduced with copyright permission.

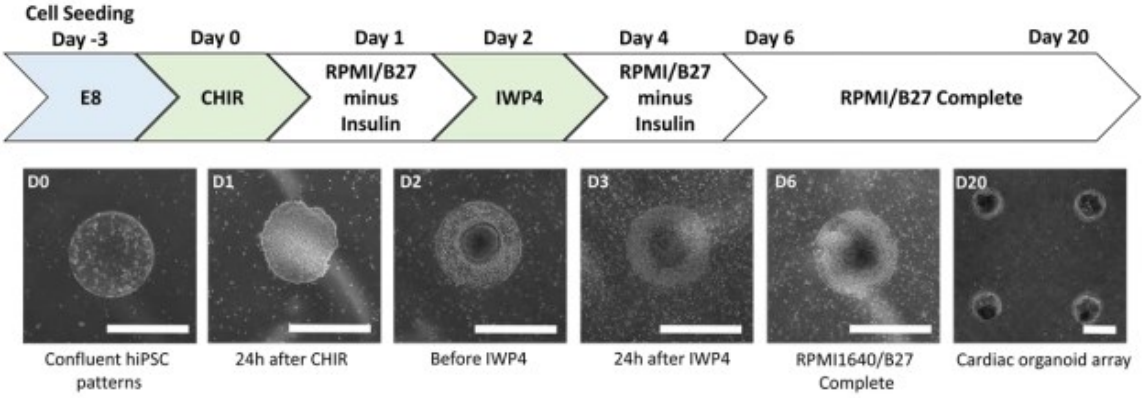

Figure 8. Cardiac differentiation timeline to generate cardiac organoids. IPSCs were seeded in the patterned well at day -3. On day 0 and Day 2, small molecules CHIR and IWP4 were added to the media. From day 6, the differentiation media of cardiac organoids was every two days until day 20, cardiac organoid formation. All scale bars are 600 μm.

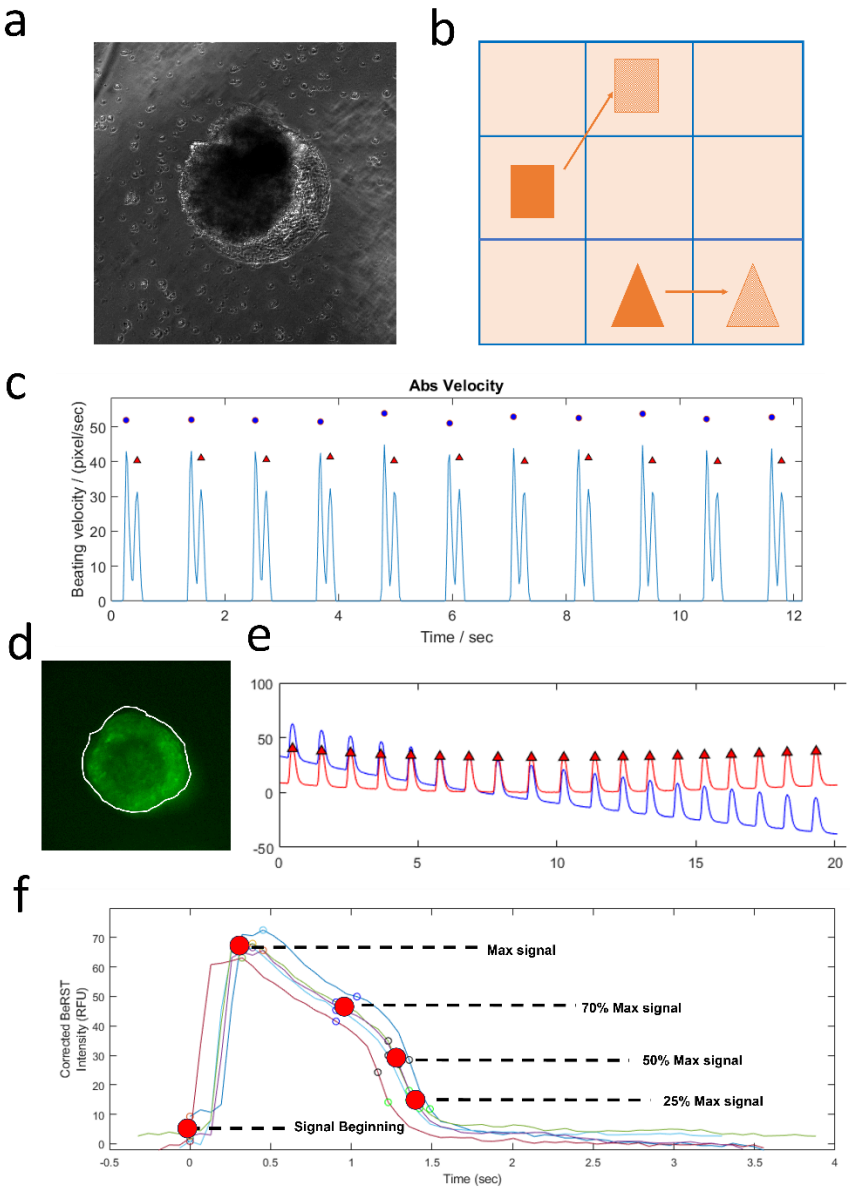

Figure 9. Cardiac organoid function analysis. (a) On day 20, the organoids were imaged to record brightfield video for function analysis. **(b)** Matlab software traces the pixel movement to analyze the cardiac organoid function. **(c)** The brightfield videos were reconstructed to contraction motion waveforms to extract parameters, including contraction and relaxation velocities, beat rate, and beat duration. **(d)** Calcium concentration change was recorded with green fluorescent video, and fluorescent areas were considered to function tissue. **(e)** The software traced the fluorescence signal change and reconstructed the calcium signal waveform. Calcium signal waveforms were detrended to remove the photo bleach influence. **(f)** Waveforms were separated into single peaks to analyze the function of cardiac organoids.

3. CHAPTER 3. GEOMETRIC INFLUENCE ON CARDIAC ORGANOID STRUCTURE AND FUNCTION

3.1 Overview

Organoid methodology presents a unique avenue to simulate the biological progression of organ development into spatially structured tissue formations that emulate the design and function of specific tissues[54, 124]. The 3D organoid approach, grounded in the core principles of developmental biology, leverages dynamic multi-cellular self-organization to generate functional biological tissues under the guidance of the extracellular environment. Traditional monolayer human-induced pluripotent stem cell (hiPSC) differentiation and 2D organoids fall short in accurately depicting the complexity of morphogenetic occurrences during organ development[74], which are dictated by the synergistic interplay of biochemical and biophysical elements. There exists a pressing requirement to comprehend the impact of biophysical constraints on crucial aspects of organ growth, including expansion, differentiation, and cellular and tissue functionality.

Cell design techniques have been widely utilized to examine the biological actions and functions of stem cells by establishing precise geometric limitations. The patterned surfaces provide control over cell-surface interactions and establish biophysical gradients influencing cell size, shape, and differentiation. Initial investigations on micropatterning mesenchymal stem cells indicated that stem cell differentiation could be directed by the geometric limitations that modify cytoskeletal tension[118]. These early two-dimensional experiments emphasized the essential role of geometric cues in steering stem cell differentiation via pathways dependent on mechanotransduction.

In addition, two-dimensional surface design has been utilized to study early embryogenesis using pluripotent stem cells. With the administration of developmental growth factors, the hESCs subjected to patterned geometric constraints developed self-organized differentiation with specific radial domains[122, 120]. In terms of organoid engineering, kidney organoids produced by micropatterning techniques were utilized to simulate the process of tubulogenesis in vitro[119], showcasing a physiological formation of a vascular lumen encircled by renal epithelium. These instances highlight the crucial necessity for spatiotemporal guidance via cellular microenvironments to direct the structure and function of stem cell organoids of particular biological tissues.

In this Chapter, we manipulated the intricacy of two-dimensional geometric models, maintaining consistent geometric areas but altering between quadrilateral and pentagram forms. This resulted in changes to the biophysical constraint gradients inherent to each shape. Our observations indicated that specific attributes, such as the aspect ratio in quadrilaterals and the central area of pentagrams, can steer organoid self-assembly and cardiac functions due to modifications in cellular arrangement and cell-edge interaction. The selected geometries in our research underscored the impact of biomechanical cues on heart differentiation and tissue formation. Each geometry displayed variations in cellular positioning within patterned cell colonies, emphasizing on cell-edge interaction at pattern boundaries in the pentagram designs. Besides the variations in biomechanics, the rectangular forms exhibited potential biological significance as they could serve as models for the linear formation of the heart tube during early embryonic development.

3.2 Pattern Shape and Size Design

As previously mentioned, the fates of stem cell differentiation were highly influenced by the shape and size of the geometrical pattern, which is likely because the different types of the pattern produce mechanical stress differently. Therefore, we hypothesize the sharper corner of the patterns, and the more elongated patterns will generate more stress pulling along the axial direction and stress compressing perpendicularly to the axis of cell growth and tissue formation. On the other hand, due to the spontaneous expansion of cells, cells receive pulling force from the edge of the patterns, while cells are also squeezed by the surrounding cells due to the increasing cell density near the pattern center. Thus, in this work, we design different patterns to investigate mechanical stimulation's influence on cardiac organoid development. Circles have the same mechanical stress in all directions. However, as the circle diameter increase, the stress generated by the pattern edge decreases according to the distance to the center. Therefore, circular patterns were used to investigate the size effect on cardiac organoid development. Compared to square patterns, rectangular patterns with a larger aspect ratio will produce more pulling force to the entire cardiac organoids, so they were used to investigate the shape influence on cardiac organoid development. Finally, pentagram patterns have both sharp periphery corners and a symmetric pentagonal central area, allowing us to compare the peripheric and central influences on cardiac organoid development.

Geometric designs of circle, quadrilateral, and pentagram shapes were created using computer-aided design software and transferred onto photomasks for photolithography and soft lithography processing. Quadrilateral designs varied based on the rectangle's aspect ratio from 1:1, 1:2, 1:3, and 1:4 (Figure 12a), while ensuring all patterns had the same area. The pentagram templates were designed by altering the central pentagon area and adjusting the triangular vertex area so that the area across all four pentagram designs remained constant. Pentagram 1

was designed to have the smallest central pentagon area with the longest and most acute triangular vertices, while pentagram 4 had the largest central pentagon area with the shortest and most obtuse vertices (Figure 12b).

3.3 Immunofluorescence Staining and Morphological Characterization

Organoids were evaluated based on immunofluorescence staining of cardiac tissue with cardiac troponin T and total organoid structure with actin (Phalloidin). Samples were treated with a 4% (vol/vol) solution of paraformaldehyde for 10 minutes, permeabilized with 0.2% (vol/vol) Triton X-100 for 5 minutes and blocked with 2% (wt/vol) bovine serum albumin for 30 minutes. Samples were exposed to the primary antibody against cardiac troponin T (dilution 1:200) for 1 hour and then treated with the secondary antibody and Phalloidin for 1 hour at room temperature. A Leica Thunder upright fluorescent microscope with a ×40 water immersion lens was used to acquire z-stack images of the organoids for height estimations and Z-projection in ImageJ. The Area ratio was determined using the circular or elliptical tool to estimate the fluorescence area of GCaMP flux for cardiac tissue and normalize this area against the entire pattern's area. The height was measured by identifying the organoid's top and bottom points.

3.4 Quadrilateral and Pentagram Ratios Influence Cardiac Organoid Structure

Cardiac organoids were successfully developed in all geometrical patterns (Figure 12c, d). For organoids with quadrilateral shapes, there was a noteworthy reduction in tissue thickness as the rectangle's length-width ratio increased (Figure 12e). This indicated that rectangular patterns with larger aspect ratios are less conducive to the cell's self-organization into 3D tissues during differentiation. Initially, the cell distribution in a 1:4 template showed less uniform radial

distribution than in a 1:1 square template, limiting the regions where cells can congregate to form a larger organoid. Organoids grown on five-sided star-shaped geometries also exhibited the influence of template shape on organoid formation. P1 organoids, with the smallest central five-sided area, had the most negligible thickness and 3D structure. Compared to the P1 template, an increase in the central pentagon area enhanced in tissue thickness with P2-4 templates (Figure 12f). However, the increase in thickness was significantly noticeable only for heart tissue organoids formed from the P2 templates, indicating that this shape promoted optimal tissue assembly. The five-sided star with steeper and more acute-angled shapes, like the P1 template, restricted uniform radial cell distribution, thus diminishing tissue formation. This indicates that by altering the 2D geometric templates, the structure of the organoid can be fine-tuned to precisely guide tissue development.

3.5 Cardiac Functional Outputs Are Dependent on the Template Geometries

To assess the contractile physiology, we comprehensively evaluated of the GCaMP6f calcium flux and heart tissue movement (Figure 12a). As the length-width ratio of the rectangle was increased, the beating frequency was significantly reduced in R3 and R4 templates (Figure 12b), correlating with a substantial increase in the area ratio between contracting tissues and the area of the template (Figure 12c). We also observed that larger length-width ratio rectangular templates resulted in a peak calcium flux (Figure 12d), which required less time to reach maximum fluorescence, as evidenced by a reduced $\tau 0$ for the R3 and R4 templates (Figure 12e). This demonstrated that a higher aspect ratio enhanced the calcium release properties of the muscle. However, across various four-sided shaped template heart organoids, the calcium decay properties, $\tau 50$ (Figure 12f) and $\tau 75$ (Figure 12g) showed no significant changes, indicating a negligible effect of the length-width ratio on calcium reabsorption. Moreover, we

discovered that organoids from square templates had considerably lower contraction (Figure 12h) and relaxation (Figure 12i) speeds than those from rectangular templates. We propose that rectangular templates facilitate a degree of alignment of heart tissues, which is known to enhance contractile functions in a laboratory setting.

Pentagram templates could create contractile heart tissue, primarily located in the center (Figure 12a). The beat rate slightly decreased as the central area increased (Figure 12b), but it was only significantly lower in P3 templates. We discovered that P1 templates generated heart organoids with a larger area ratio but the least thickness (Figure 12c), indicating that this design only produced a shallow layer of heart muscle that had a wider distribution across the template, as opposed to a dome-like tissue structure at the template center, similar to other template organoids. This further suggested that pronounced architecture organoid self-assembly necessitates a 2D template with a sufficiently large central portion to facilitate 3D tissue formation. Regarding to calcium management properties, calcium transient remained relatively stable, with only P3 templates showing significant deviations (Figure 12d, e, f, g). We observed decreased contractile motion as the central area increased, especially when comparing P1 and P2 with P3 and P4 templates (Figure 12h, i). However, we noticed a peak in contraction and relaxation speed values at the P2 template, which coincided with the trend of morphological measurements of thickness and area ratio for P2. This implies that P2, a perfect star polygon, was the best shape to achieve the broadest range of contractile motion and the most robust heart tissue distribution and structure.

3.6 Summary

In this work, we created cardiac organoids in different sizes and shapes. We discovered that the shape affects how these organoids look and function. Unlike other methods that directly create

3D aggregation, we started with a 2D patterned layer of cells, which then naturally formed and self-organized into 3D structures. This method gives us precise control over the number of cells and their arrangement. By experimenting with different shapes like quadrilaterals and pentagrams, we saw how the different shapes could influence the development and function of these cardiac organoids. Especially with pentagram shapes, one particular design, P2, showed the best structure and performance. From past experiments, we noticed similar patterns with circles of around 600 μm in diameter. In essence, the shape or design we use significantly affect on how well the organoid functions. This discovery is critical for designing organoids with predictable outcomes. With the techniques we have developed, we can create cardiac organoids that look the way we want and function efficiently. This is beneficial for the future of organoid engineering.

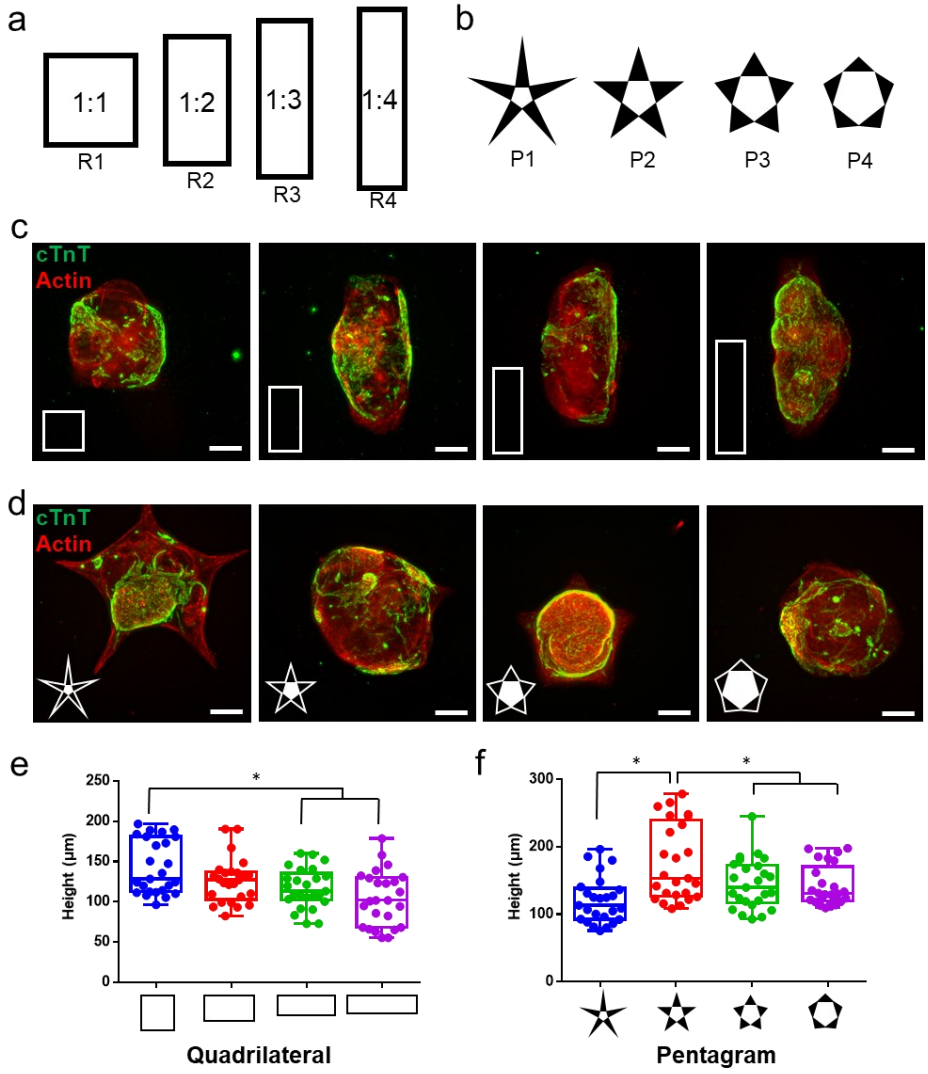

Figure 10. Pattern designs for geometrical confinement to cardiac organoids. (a) rectangular and (b) pentagram designs of the pattern. Cardiac organoids were successfully produced in all (c) rectangular and (d) pentagram patterns. Organoids were stained with troponin T (green) and actin (red). (e) The square pattern organoids and (f) pentagram pattern (p2) organoids have the largest height. All scale bars are 200 µm.

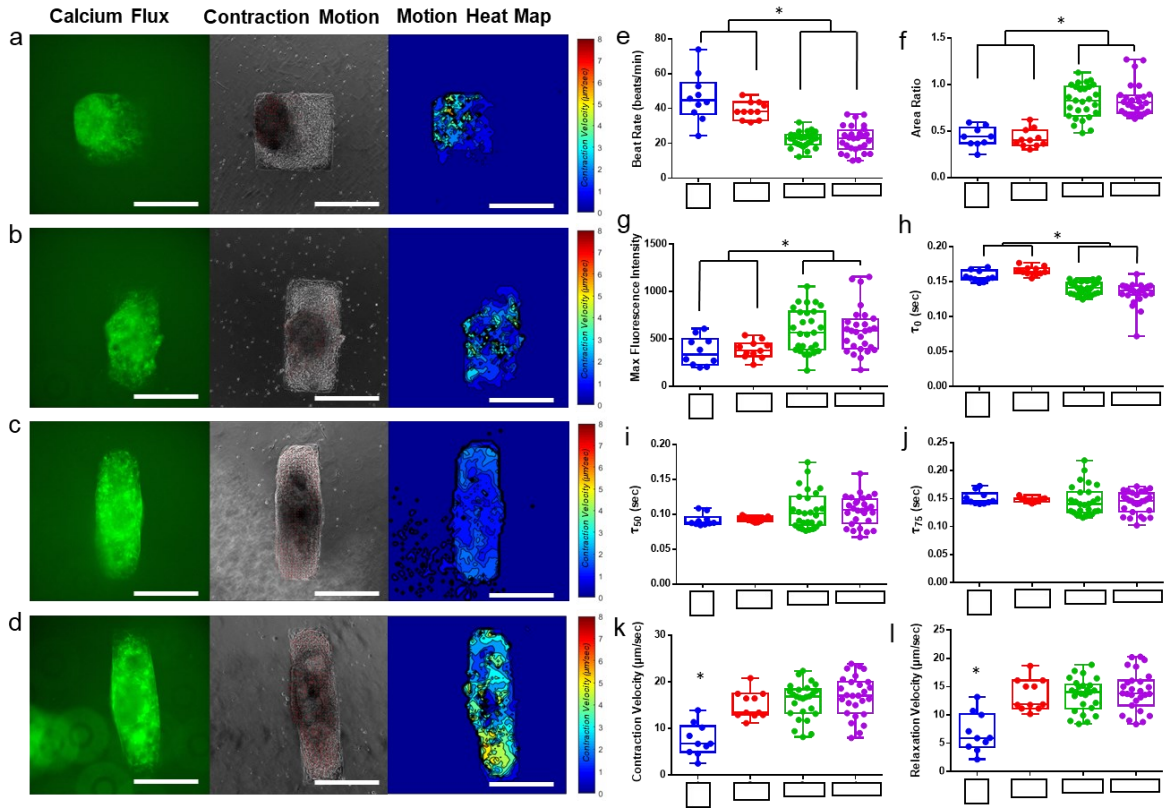

Figure 11. Rectangular geometry influenced cardiac contractile functions. (a) Fluorescent calcium flux and cardiac contraction motion video were recorded for function analysis. (b) the beat rate decreased, (c) while the area ratio increased. With the increasing aspect ratio, (d) the maximum calcium flux was increased at a faster upstroke rate as indicated by (e) a τ0. Calcium decay rates (f) τ50 and (g) τ75 did show much difference. Except for square patterns, the cardiac organoids in other patterns have a stronger function and showed significantly higher (h) contraction and (i) relaxation velocities. Scale bars 500 μm.

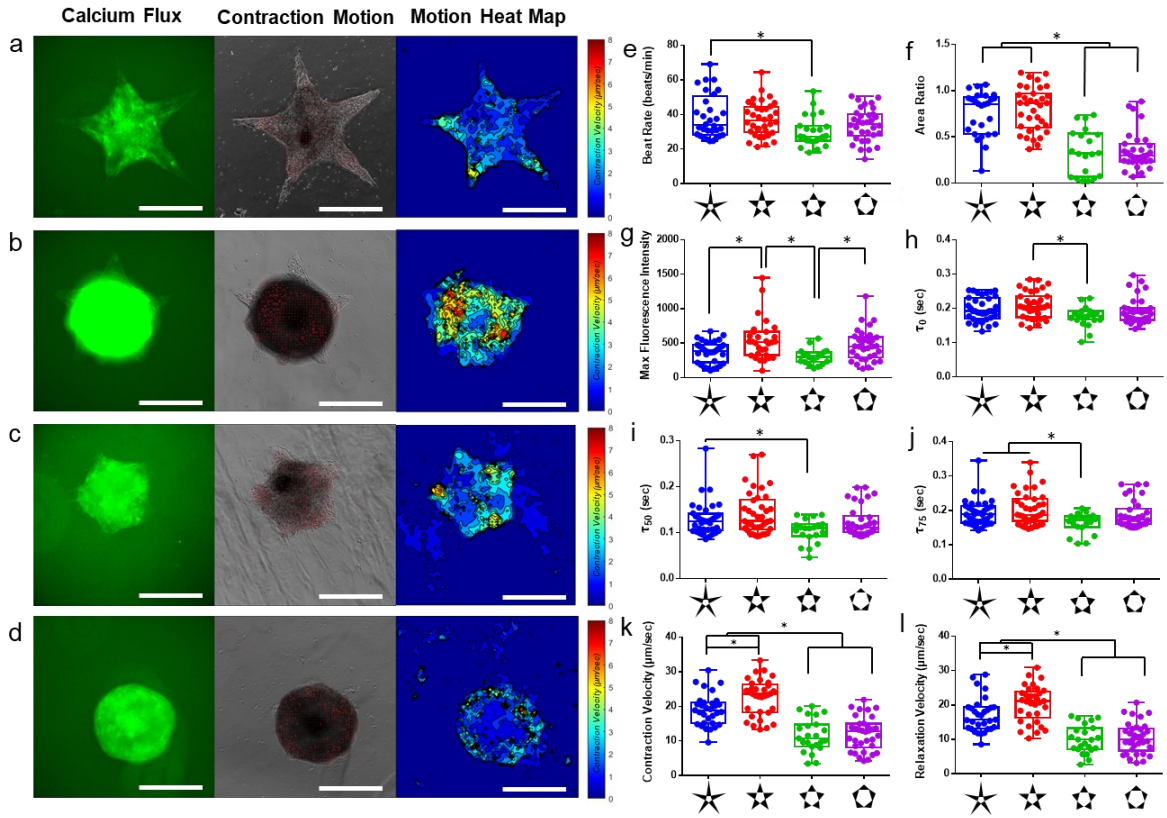

Figure 12. Cardiac contractile functions were influenced by pentagram geometry. (a) Fluorescent calcium flux and cardiac contraction motion video were recorded for function analysis. Cardiac organoids did not show much difference in beat rate (b) but decreased area ratio (c) with increasing center pentagon area. In general, the cardiac organoids from P2 templates showed higher (d) max calcium flux, longer calcium upstroke rate (e) τ0, and longer calcium decay rate (f) τ50 and (g) τ75. Cardiac organoids in pentagram patterns with a smaller center pentagon area showed significantly greater contraction motion, higher contraction velocities (h) and relaxation velocities (i), and the peak contraction occurred in the P2 pattern organoids. Scale bars 500 μm.

4. CHAPTER 4: CARDIAC ORGANOIDS AS AN EMBRYOTOXICITY SCREENING PLATFORM

4.1 Overview

As we mentioned earlier, a considerable number of pregnant women have to face the risk caused by inappropriate medication during pregnancy with their unborn baby, and the issue has become more serious. During the embryonic phase, the heart is the first developmental organ to emerge, demonstrating contractile activity and blood circulation as early as the 22nd day of human growth. Due to this naturally occurring event, it is reasonable to speculate that disturbances in cardiac development carry the potential to lead to severe fetal abnormalities, giving us the ability to gauge overall embryonic well-being. Hence, there is a requirement to establish a model that mimics human heart tissue development for a compelling reenactment of cardiac growth. Tissues derived from hiPSCs showed characteristics of nascent developmental lineage. Due to this singular property, hiPSC-sourced tissues have the capacity to function as a flexible instrument for the examining and reenacting of tissue development processes.

This chapter explores the application of cardiac organoids for drug evaluation platforms, particularly concerning drug hazards in fetal growth stages. Given that these organ-like structures originate from a pluripotent state and involve self-assembling cells during maturation, they are believed to simulate immature heart tissues with early developmental characteristics more accurately. Utilizing this model, a panel of 14 common drugs or products was examined, including categories from A to X, and their adverse effects were evaluated through the analysis

of impact on contractile functions and tissue structure using standard and calcium signaling video imaging. This chapter comprehensively compares of all medication outcomes and establishes a system for assessing drug embryotoxicity and developmental toxicity.

4.2 Experimental Procedure

In previous studies, cardiac organoids of 600um circle shape displayed stable and robust contraction characteristics, along with the largest 3D structure. Therefore, they were considered the most dependable for broader drug screening studies. The cardiac differentiation procedure was adapted to incorporate the ongoing addition of the drugs starting on the first day, a full day following the application of GSK3 inhibitor CHIR99021 in media, within the differentiation timeline (Figure 13a). This supplement spanned the entire differentiation process until the point of termination for study. Medication addition during this process is relevant to all unique events related to heart differentiation and it simulates continuous drug exposure throughout pregnancy. Depending on their solubility, concentrated drug solutions were prepared in either DMSO or MilliQ water. These stock solutions were then diluted to the working concentration in their respective growth mediums. In summary, 14 drug substances were examined and analyzed at 7 distinct dosage levels, from 1nM to 1mM, in addition to a control agent (Figure 13b). The medications employed are cataloged in Table 1 and vary in safety, ranging from Categories A to X, based on the previously instituted FDA classification for pregnancy risk. Concentration levels were amplified tenfold for each successive dosage tier to scrutinize the possible toxic impact on the cardiac organoid development.

IC50 is the concentration of agonist that gives a response halfway between function inhibition at zero dose and highest dose. The IC50 calculation for different drugs was performed with GraphPad Prism 6.0 software via nonlinear regression. First, results of all functional parameters

were normalized data based on the means of control groups. The mean values at each concentration were fitted into the dose-response curve based on the logarithm-transformed drug concentrations. The nonlinear regression was set up by fitting the logistic function formula with four parameters, including (a) the normalized y values at minimum drug concentration, (d) the normalized y values at maximum drug concentration, (c) logarithm transformed IC50 concentration at the inflection point halfway on the S-shaped curve, and (b) Hill's slope of the curve related to the steepness of the curve at inflection point:

$$y = d + \frac{a - d}{1 + \left(\frac{x}{c}\right)^{b}}$$

4.3 Results

4.3.1 Category A

4.3.1.1 Folic acid

Folic acid is a form of the water-soluble B vitamin, also known as vitamin B9. It plays a crucial role in various bodily functions, including synthesizing DNA and RNA, forming red blood cells, and the metabolizing amino acids. Folic acid is essential during rapid cell growth, such as pregnancy and infancy. Folic acid is generally considered safe when prescribed or consumed in fortified foods. However, excessive intake can mask symptoms of vitamin B12 deficiency and could potentially lead to complications. Therefore, it is essential to adhere to recommended dosages and consult healthcare providers for personalized medical advice. In the body, folic acid is converted to its active form, tetrahydrofolate (THF), which serves as a coenzyme in several metabolic reactions. A deficiency in folic acid can lead to a form of anemia, where the body does not have enough healthy red blood cells to carry adequate oxygen to its tissues. In pregnant women, a lack of folic acid can cause neural tube defects in the developing fetus, such

as spina bifida. Because of its importance in preventing birth defects, folic acid is often added to processed foods like cereals and bread, known as "fortification." It is also available in supplement form and frequently included in prenatal vitamins.

Cardiac organoids were successfully developed in all 8 concentrations (Figure 14a, b), but organoids in different concentrations showed different function properties. As we increased the concentration of folic acid, the beating rate showed a significant decrease with the 100nM concentration group but recovered to the same level in higher concentration groups (Figure 14c), and the time interval did not show much difference between the different groups (Figure 14d). Both contraction and relaxation velocity were significantly increasing with concentrations, but highest concentration was back to same level as the control group (Figure 14e, f). GCaMP signal of organoids showed similar results. In higher concentration groups, T30, T50, and T75 did not show much difference among different groups, but the 1 mM group showed a significant decrease compared to other groups (Figure 14h, i, j). Except for the 1 mM group, other groups remained relatively consistent, but only 1 mM group had significantly higher than other groups (Figure 14k). For peak time, the highest concentration group still showed the lowest result (Figure 14l). Moreover, cardiac organoids showed signal changes in the highest concentration group but also showed a peak in value of signal change in the middle concentration groups, as the 100 nM concentration group (Figure 14m). At last, 1 mM concentration showed the smallest functional area (Figure 14g), which might represent the development of cardiac organoids that were interfered with in the highest concentration group.

4.3.1.2 Ascorbic acid

Ascorbic acid, commonly known as vitamin C, is a water-soluble vitamin essential for various

physiological functions in the human body. Vitamin C is an antioxidant, helping neutralize free radicals in the body that can cause cellular damage. It is also a cofactor in numerous enzymatic reactions, aiding in the synthesis of collagen, a protein necessary for healthy skin, cartilage, tendons, ligaments, and blood vessels. Additionally, ascorbic acid is involved in the synthesis of neurotransmitters like serotonin, the metabolism of cholesterol, and the absorption of iron from plant-based foods. Vitamin C supplements are widely available and are often used to support the immune system, particularly during cold and flu season. However, scientific evidence on the efficacy of such supplementation for preventing or treating colds is mixed. The vitamin is generally considered safe, but excessive intake can lead to symptoms like gastrointestinal discomfort, diarrhea, and, in extreme cases, kidney stones.

Cardiac organoids were developed in 7 lower concentrations, except for the highest concentration (1 mM) (Figure 15a, b), and organoids in different concentrations showed different function properties. As we increased the concentration of ascorbic acid, the beating rate showed a significant decrease in lower concentration groups but recovered to the same level in the concentration groups higher than 100 nM (Figure 15c), but the time interval showed a significant difference with lower concentration ascorbic acid, including 1nM and 10nM (Figure 15d). Both contraction and relaxation velocity significantly increased with drugs, but the 100 μM group was back to the same level as the control group (Figure 15e, f). GCaMP signal of organoids showed similar results. In higher concentration groups, T30, T50, and T75 only showed significant high in 10uM concentration groups (Figure 15h, i), and as the concentration increased, the result slowly decreased. We did not see much difference between the UPD of different groups (Figure 15k). However, as the concentration of ascorbic acid increased, peak time slowly decreased, and the 100 μM group showed a significant difference from the control group (Figure 15l). Moreover, although there is no significant difference in

calcium amplitude between drug-treated groups to control group, 1 μM and 10 μM groups are slightly higher than other groups (Figure 15m). Only 1μM showed a significantly higher area ratio than control group (Figure 15g).

4.3.1.3 Doxylamine

Doxylamine is an antihistamine commonly used as a sedative and sleep aid and for treating various allergic symptoms like runny nose and sneezing. It belongs to the ethanolamine class of antihistamines. It is often found in over-the-counter (OTC) medications, either as a standalone product or in combination with other drugs like acetaminophen or decongestants. Doxylamine works by blocking the action of histamine, a neurotransmitter involved in allergic reactions and wakefulness. By inhibiting the effects of histamine, doxylamine can relieve allergy symptoms and help induce sleep. The medication is generally considered safe for short-term use. However, it should be used cautiously and under medical supervision in specific populations, such as the elderly or those with respiratory conditions, due to potential side effects like dizziness, dry mouth, and respiratory depression. It is also not generally recommended for long-term treatment of insomnia or allergies without a healthcare provider's guidance. Although doxylamine is considered to be safe for most people, pregnant or breastfeeding women, as well as those with chronic medical conditions, should consult a healthcare provider before starting any new medication, including doxylamine.

Like organoids with ascorbic acid treatment, cardiac organoids were developed in 7 lower concentrations, except for the highest concentration (1 mM) (Figure 16a, b), and organoids in different concentrations showed different function properties. For beating rate, it showed a significantly high beating rate in the 1μM concentration group but a significantly low beating

rate in the 10 nM group. In contrast, there is no significant difference in other groups (Figure 16c), but the time interval showed a significantly shorter time interval in the control group than 1nM and 100 μM (Figure 16d). For contraction and relaxation velocity, higher concentration groups showed lower velocity, showing a significant difference in 100 nM, 1μM, and 100μM groups compared to the control group (Figure 16e, f). The calcium transient result of organoids did not show too much difference. It only showed a significant difference of T30, T50, and T75 in 1nM concentration groups, whereas the 100μM group also showed a significant difference to the control group (Figure 16h, i, j). For the UPD results of different groups, the 1nM and 100nM groups showed differences from the control group (Figure 16k). For peak time, it showed that 1nM and 100nM groups have significant difference to the control group (Figure 16l). Moreover, the control group showed significantly higher calcium transient signal change than all other groups (Figure 16m). At last, control groups showed significantly larger functional areas than all other groups, except for the 1nM group (Figure 16g). From the result, doxylamine impacts on cardiac organoid development, but the impact is not severe.

4.3.2 Category B

4.3.2.1 Amoxicillin

Amoxicillin is a widely used antibiotic medication that belongs to the penicillin group of antibiotics. It is prescribed to treat various bacterial infections in humans. This antibiotic is effective against a broad spectrum of bacteria and is commonly used to treat respiratory tract infections, urinary tract infections, skin infections, ear infections, and other bacterial infections. Amoxicillin works by interfering with the ability of bacteria to build their cell walls, which ultimately leads to the weakening and destruction of the bacterial cell. This action helps the body's immune system better fight the infection.

Cardiac organoids were successfully developed in all 8 concentrations (Figure 17a, b), and organoids in different concentrations showed different function properties. For beating rate, it only showed a significantly higher beating rate in the 1nM concentration group to the control group, whereas there is no significant difference in the other groups (Figure 17c), but time intervals showed significantly longer time interval in 1μM and 10μM to the control group (Figure 17d). For contraction velocity and relaxation velocity, only 10μM showed much higher contraction velocity than the control group. However, we did not see any significant difference in relaxation velocity results among all groups (Figure 17e, f). The calcium transient result of organoids showed a significant difference between the control and drug-treated groups. The control group showed a significant difference of T30, T50, and T75 to drug-treated groups, except for 1μM and 1mM groups (Figure 17h, i, j). For UPD, only 100nM groups showed a significant difference from the control group (Figure 17k). The peak time of control group is much longer than 100nM and 10μM, which is shown as a significant difference (Figure 17l). Moreover, the control group showed significantly lower calcium transient signal change than the 10μM groups (Figure 17m). Finally, all groups have no significant difference in functional area (Figure 17g). From the result, amoxicillin showed a significant impact on the development of cardiac organoids, but the function of 10μM concentration groups was slightly improved by amoxicillin, which is shown as higher contraction velocity and higher calcium transient signal change.

4.3.2.2 Buspirone

Buspirone is a medication primarily prescribed for the treatment of anxiety disorders and is classified as an anxiolytic or non-benzodiazepine anxiolytic. Buspirone is used to manage

symptoms of generalized anxiety disorder (GAD), a common anxiety disorder characterized by excessive worry, restlessness, and physical symptoms such as muscle tension and irritability. Buspirone's exact mechanism of action is not fully understood, but it is believed to work by affecting certain neurotransmitters in the brain, particularly serotonin and dopamine. By modulating these neurotransmitters, buspirone helps reduce excessive anxiety and create a sense of calm.

Unlike amoxicillin-treated groups, cardiac organoids were only successfully developed in lower 7 concentrations, except for the 1mM group (Figure 18a, b), and organoids in different concentrations showed results. For beating rate, it only showed a significantly higher beating rate in the 1μM concentration group to the control group, whereas there is no significant difference in other groups (Figure 18c), but time interval showed a significantly longer time interval in the control to 1mM group (Figure 18d). For contraction velocity and relaxation velocity, only 100nM showed significantly lower relaxation velocity than the control group. However, we did not see any significant difference in contraction velocity among all groups (Figure 18e, f). For calcium transient results of organoids, the control group showed significantly shorter T30, T50, and T75 to 100nM and 10μM groups, and the control group also showed shorter T75 to 100μM groups (Figure 18h, i, j). For UPD and peak time, there is no significant difference in results (Figure 18k and l). We found no significant difference in calcium transient signal change results. Finally, control groups had significantly larger functional area than 100μM (Figure 18g). Although it did not show intense and dramatic change in all concentrations, the results showed buspirone in high concentrations mpactedcardiac organoid development.

4.3.3 Category C

4.3.3.1 Aspirin

Aspirin, chemically known as acetylsalicylic acid, is a widely used medication with analgesic, anti-inflammatory, and antipyretic properties, meaning it can relieve pain, reduce inflammation, and lower fever. Aspirin exerts its effects by inhibiting the enzyme cyclooxygenase (COX), which is involved in the production of substances like prostaglandins that mediate inflammation and pain. By blocking the action of COX, aspirin effectively reduces these symptoms. Additionally, aspirin has antiplatelet effects; it inhibits platelets aggregation making it helpful in preventing blood clots. Because of its antiplatelet activity, aspirin is often recommended in low doses for individuals at high risk of cardiovascular events, such as heart attack or stroke.

With Aspirin treatment, cardiac organoids were developed in all 8 concentrations (Figure 19a, b). There is not much difference in beating rate between different groups (figure c), but control groups showed significantly shorter time intervals than 100μM (Figure 19d). For contraction velocity and relaxation velocity, only 10μM groups showed significant differences in contraction and relaxation velocity to the control group (Figure 19e, f). Calcium transient results of organoids did not show much difference of T30, but a significant difference of T50 and T75 in the 10μM concentration group in the control group (Figure 19h, i, j). For UPD, there is not much difference between different groups (Figure 19k). Only the 100μM group showed a significant difference in peak time, significantly higher than the control group (Figure 19l). For calcium signal amplitude, all groups did not significantly show calcium transient signal change to the control group (Figure 19m). Lastly, there is also no significant difference in area ratio (Figure 19g), so aspirin did not show much influence on cardiac organoid development.

4.3.3.2 Caffeine

Caffeine is a central nervous system stimulant and the most widely consumed psychoactive substance in the world. The primary mechanism of action for caffeine involves blocking the action of a neurotransmitter called adenosine, which promotes sleep and relaxation. By inhibiting adenosine receptors, caffeine effectively increases the release of neurotransmitters like dopamine and norepinephrine, leading to increased alertness, improved mood, and enhanced cognitive function. While generally considered safe for most people when consumed in moderate amounts, excessive caffeine intake can lead to a range of adverse effects, including insomnia, jitters, increased heart rate, and digestive issues. People with certain medical conditions, such as heart arrhythmias, anxiety disorders, or certain gastrointestinal conditions, should consult a healthcare provider before consuming caffeine. Pregnant and breastfeeding women are also advised to limit caffeine intake due to potential risks to the fetus and newborn.

Cardiac organoids were developed in all 8 concentrations with caffeine treatment (Figure 20a, b). Caffeine showed improvement in cardiac beating rate; the group with 10nM, 100nM, and 100μM caffeine treatment showed a significantly higher beating rate compared to the control group (Figure 20c), but it did not show a significant difference in the time interval between different groups (figure d). For contraction velocity and relaxation velocity, the 10nM groups showed significantly lower contraction velocity, and the 1μM group showed lower relaxation velocity than the control group (Figure 20e, f). In the calcium transient result of organoids, the control group showed much shorter T30, T50, and T75 than groups with higher concentrations (Figure 20 h, i, j). For UPD, only the 100μM group showed a significantly higher value than the control group (Figure 20k). For peak time, the 10nM and 100μM groups both showed

longer peak time than the control group (Figure 20l). Moreover, the calcium transient signal change of the control group was much higher than the caffeine-treated groups (Figure 20m). For area ratio, only 10nM has a significant difference to the control group, which is much smaller than the control group (Figure 20g).

4.3.3.3 Rifampicin

Rifampicin, also known as rifampin in the United States, is an antibiotic medication primarily used to treat of tuberculosis (TB). It belongs to the rifamycin class of antibiotics and is effective against a broad range of bacteria, including Mycobacterium tuberculosis, the bacterium responsible for TB. Rifampicin works by inhibiting the DNA-dependent RNA polymerase of bacteria, thereby preventing the transcription of bacterial DNA into RNA, which is a crucial step in bacterial replication. Rifampicin is also used in the treatment of other bacterial infections, including certain types of leprosy, and as prophylaxis in contact with patients with invasive meningococcal disease.

Cardiac organoids were only developed in all 6 concentrations with rifampicin treatment (Figure 21a, b). For cardiac beating rate, the control group showed a significantly lower beating rate than the 1nM and 1μM groups (Figure 21c), but it did not show a significant difference in the time interval between different groups (Figure 21d). For contraction velocity and relaxation velocity, we still did not see any significant difference between the different groups (Figure 21e, f). In the calcium transient result of organoids, there is no significant difference in cardiac beating duration in T30, T50, T75, UPD, and peak time (Figure 21h, i, j, k, l). However, the calcium transient signal change of the 10μM group was much higher than that of the control groups (Figure 21m). Finally, rifampicin highly impacted cardiac tissue formation, showing

the control group having the largest functional cardiac tissue. As the concentration of rifampicin increases, the functional cardiac tissue becomes smaller (Figure 21g). From the result, rifampicin highly interfered with the cardiac development and can be considered to have severe cardiac developmental toxicity.

4.3.3.4 Retinoic acid

Retinoic acid is a metabolite of vitamin A (retinol) that plays critical roles in cell growth, differentiation, and regulation of gene expression. It is a potent bioactive form of vitamin A primarily known for its applications in dermatology and oncology. In dermatology, retinoic acid promotes skin cell turnover, unclogs pores, and helps regulate sebum production. In oncology, retinoic acid has been studied for its potential role in treating certain types of leukemia, specifically acute promyelocytic leukemia. Retinoic acid modulates various of physiological processes, from cellular differentiation to immune response. Due to its teratogenicity (the ability to disturb the development of an embryo or fetus), women who are pregnant or planning to become pregnant should avoid retinoic acid due to the high risk of birth defects.

Organoids with retinoic acid treatment, cardiac organoids were only developed in 5 concentrations, ranging from 1nM to 1μM and the control group (Figure 22a, b). For beating rate, the 1μM group had a much higher beating rate than control group (Figure 22c), but the control group showed significantly shorter time intervals than all other groups (Figure 22d). For contraction and relaxation velocity, the control group showed significantly higher velocity than all other groups (Figure 22e, f). The calcium transient result of organoids did not show much difference in T30. It only showed a significant difference of T50 and T75 in the 100nM

concentration group to the control group (Figure 22h, i, j). For UPD, there is not much difference between different groups (Figure 22k). The peak time of the control group was much longer than the 100nM group but shorter than the 1μM group (Figure 22l). Moreover, no groups show any significant change in calcium transient signal changes compared to the control group (Figure 22m). For area ratio, the control group only showed a significant difference from the 1nM group, which is much smaller than 1nM group (Figure 22g). Due to the low developmental rate of cardiac organoids in concentration and low contraction and relaxation velocity as the concentration increases, retinoic acid was considered a drug with high developmental and cardiac toxicity.

4.3.4 Category D

4.3.4.1 5-Fluorouracil

5-Fluorouracil (5-FU) is an antineoplastic medication, which means it is used to treat various types of cancer. It is primarily used in the treatment of solid tumors, such as those found in colorectal, breast, stomach, pancreatic, and skin cancers, among others. The mechanism of action of 5-FU involves its incorporation into the RNA and DNA of rapidly dividing cancer cells, which leads to cell damage and, eventually, cell death. Specifically, 5-FU is converted into active metabolites that inhibit the enzyme thymidylate synthase, disrupting DNA synthesis and repair. Because 5-FU is a potent drug with significant side effects, it should only be administered under the close supervision of healthcare providers specialized in cancer treatment. Pregnant or breastfeeding women, or those planning to become pregnant, should avoid this medication due to its teratogenic and toxic effects on the fetus or newborn.

For 5-Fluorouracil treatment, cardiac organoids were only developed in 5 concentrations, from

1nM to 1μM and the control group (Figure 23a, b). For beating rate, the 1μM group has a much higher beating rate than the control group (Figure 23c), but there is no significant difference in the time interval between different groups (Figure 23d). We did not see any significant difference among different groups for contraction velocity and relaxation velocity, (figure e, f). For calcium transient results, the control group showed a larger T30, T50, and T75 than 10nM group but only a larger T30 and T75 than the 100nM group (Figure 23h, i, j). For UPD, the 1nM group has a larger UPD time than the control group (Figure 23k). For peak time, there is not much difference between the control and other groups (Figure 23l). Moreover, the control group showed a much larger calcium transient signal change than 5-fluorouracil-treated groups (Figure 23m). At last, we did not see any significant difference in functional area between the control group and the groups with the drug (Figure 23g). Similar to retinoic acid, 5-fluorouracil showed substantial interference with cardiac organoid development and function, which was also considered a drug with high embryotoxicity.

4.3.4.2 Lithium Chloride

Lithium chloride is a chemical compound with the formula LiCl. It is a salt that consists of lithium cations (Li+) and chloride anions (Cl-). Lithium chloride is an essential compound with various industrial, scientific, and medical applications. Lithium chloride does not have direct medical applications in the form of medication or treatment. However, lithium compounds, including lithium carbonate and lithium citrate, are used medically to treat certain mental health conditions, particularly bipolar disorder, by stabilizing mood and preventing or reducing the severity of manic and depressive episodes in individuals with bipolar disorder. Lithium carbonate and lithium citrate are the forms typically prescribed for medical use.

Cardiac organoids were successfully developed in all 8 concentrations (Figure 24a, b), and organoids in different concentrations did not show significant differences in beating rate, time interval, contraction, and relaxation velocity (Figure 24c, d, e, f). For calcium transient results of organoids, the control group showed significantly shorter T30, T50, and T75 to 100nM and 100μM groups, and control group also showed shorter T75 to 1μM groups (Figure 24h, i, j). There is no significant difference of results in the UPD result of different groups, (Figure 24k). The control group showed a significantly shorter peak time than the 100nM and 100μM groups (Figure 24l). We also found that the control group had more considerable calcium transient signal change than 1μM groups (Figure 24m). Finally, control groups significantly differed in area ratio to 1nM and 1μM groups, with smaller functional areas than 1nM and 1μM groups (Figure 24g). Although there is no significant difference in motion tracking results, the calcium signal results showed that cardiac organoid development was impacted by lithium chloride in high concentrations.

4.3.4.3 Amiodarone

Amiodarone is a medication used primarily to treat various heart rhythm disorders, particularly those that are life-threatening or difficult to manage with other medications, and it is known for its effectiveness in regulating irregular heartbeats. Amiodarone is prescribed to manage a range of heart rhythm abnormalities, including atrial fibrillation, atrial flutter, ventricular tachycardia, and ventricular fibrillation. These conditions can lead to dangerously fast or irregular heartbeats, increasing the risk of stroke, heart attack, or sudden cardiac death. Amiodarone is classified as a Class III antiarrhythmic drug and works by influencing ion channels in the heart's cells, slowing down the electrical impulses responsible for irregular rhythms. It can also affect the autonomic nervous system and has anti-adrenergic properties.

Cardiac organoids were only developed in lower 4 concentrations, from the control group to the100nM group (Figure 25a, b). For the beating rate, we only observed that the 10nM group had a much lower beating rate than the control group (Figure 25c), and there was no significant difference in time interval among all groups (Figure 25d). For contraction velocity and relaxation velocity, we saw a significant difference of contraction velocity between the 100nM group and the control group, and the control group had much higher relaxation velocity than the other groups (Figure 25e, f). We observed no significant difference in T30 among groups for the calcium transient results of organoids. However, the control group showed shorter T50 than 100nM groups and shorter T75 than 1nM and 100nM groups (Figure 25h, i, j). There is no significant difference in UPD, peak time, and calcium transient signal change among all groups (Figure 25k, l, and m). However, the control group had a larger functional area than the 10nM group (Figure 25g). Although amiodarone did not strongly impact on cardiac organoids, amiodarone still interfered with the function of cardiac organoids, showing lower contraction and relaxation velocity, shorter peak time, and less calcium transient signal change in high concentrations.

4.3.5 Category X

4.3.5.1 Thalidomide

Thalidomide is a medication that was initially introduced as a sedative and antiemetic to combat insomnia and morning sickness, particularly in pregnant women. However, it was soon found to be teratogenic and could cause severe birth defects. Thousands of children were born with limb deformities and other severe malformations because of thalidomide use during pregnancy. It is currently used in the treatment of multiple myeloma, a type of blood cancer, as

well as for certain complications of leprosy. It has also been studied for its potential anti-inflammatory and immunomodulatory effects. Thalidomide involves multiple pathways, including inhibition of angiogenesis and modulation of immune responses. Because of its known teratogenic effects, the drug is subject to strict prescribing guidelines.

We successfully developed cardiac organoids in all 8 concentrations (Figure 26a, b). We only observed that the 100μM group had a much higher beating rate than control group (Figure 26c), and 100nM group had a much larger time interval than the control group (Figure 26d). For contraction velocity and relaxation velocity, we saw a significant difference in contraction velocity and relaxation velocity between the 100μM group and the control group (Figure 26e, f). For the calcium transient result of organoids, there is no significant difference of T30, T50, and T75 among groups (Figure 26h, i, j). Only the 1mM group has a larger UPD time than the control group (Figure k). However, the control group had a larger peak time than the 1mM group (Figure 26l). Moreover, the control group showed much larger calcium transient signal change than high concentration groups, including 10μM and 1mM groups (Figure 26m). At last, it only showed a significant difference in functional area between 10μM and the control group (Figure 26g). Although thalidomide did not show a strong impact on cardiac organoids, thalidomide still interfered with the function of cardiac organoids, showing lower contraction and relaxation velocity, shorter peak time, and less calcium transient signal change in high concentrations.

4.3.6 Category Unknown

4.3.6.1 Acrylamide

Acrylamide is a chemical compound with the formula C3H5NO. It is commonly used in

industrial processes to produce polyacrylamide and in various applications. acrylamide was also found in some cooked foods, particularly those rich in carbohydrates and cooked at high temperatures. Acrylamide was considered a human carcinogen due to its high level of acrylamide, which can cause cancer in animal studies, but the evidence regarding its carcinogenicity in humans is inconclusive. Regulatory agencies like the U.S. Food and Drug Administration (FDA) and the European Food Safety Authority (EFSA) have suggested avoiding food with high levels acrylamide.

We developed cardiac organoids in all 8 concentrations (Figure 27a, b). For the beating rate, we observed a peak value in the middle concentration group, which also showed a significant difference to the control group (Figure 27c), and the 1mM group had a much longer time interval than the control group (Figure 27d). We saw a significant difference between high-concentration and control groups for contraction velocity and relaxation velocity (Figure 27e, f). For the calcium transient result of organoids, we observed that control groups had much longer T30 than other groups but only T50 longer than the 1μM group, However, T75 of the 1mM group is much longer than the control group (Figure 27h, i, j). There is a peak value of UPD in 100nM and 1μM groups, and the control group has a shorter UPD time than the 100nM and 1μM groups (Figure 27k). However, there is no significant difference in peak time among different groups (Figure 27l). Moreover, the control group showed a much larger calcium transient signal change than all other groups (Figure 27m). We did not see any significant difference in functional area in all groups (Figure 27g). The result proved that the influence of acrylamide on cardiac organoid function was minimal.

4.4 Conclusions and Discussion

In this study, our cardiac organoid platform has the ability to mimic cardiac development and allows us to evaluate human-specific drug-induced developmental toxicity based on the disruption of forming correct 3D organoid structures and developing normal cardiac contractile functions. With our cardiac organoids, we respectively tested the multiple drugs in different concentrations, which included different pregnant risk categories from A to X. We found an overall increase of teratogenic severity on cardiac organoid formation, corresponding to the increase of test concentrations, as well as the increase of risk category from A to X. Although the high concentrations of drugs were proven to impact the development of cardiac organoids, different drugs showed diverse effects on development toxicity. Such as, three categories D drugs were all proven to interfere with the function of cardiac organoids. However, only amiodarone and 5-fluorouacil highly interfere with formation of the cardiac organoids in high concentrations, whereas cardiac organoids were successfully developed in all concentrations of lithium chloride. Retinoic acid, though, it is a category C drug, also strongly impacted on cardiac organoid formation.

Cardiac organoids were successfully developed with thalidomide and lithium chloride in all 8 concentrations, and high concentrations of thalidomide and lithium chloride showed interference with cardiac organoids' function. Motion activities of cardiac organoids with high concentration thalidomide were restrained, showing lower contraction and relaxation velocity, However, cardiac organoids did not show contraction and relaxation velocity decrease with high concentration lithium chloride. Calcium transient signals from high concentration lithium chloride were decayed at a much lower speed. In contrast, there is not much difference in calcium transient signal duration with different concentrations of thalidomide. This difference in interference might show that the drugs influence the cardiac organoid function with different

mechanisms, such as disturbing the structure assembling or calcium handling, which provide us a new train of thought and a more accurate understanding of the toxicity of drugs on cardiac development.

Moreover, results showed the robust improvement of cardiac development and function by essential nutrition, such as ascorbic acid and folic acid. Both ascorbic acid and folic acid showed improvement in the function of cardiac organoids in the middle range of concentrations, and interestingly, cardiac organoids showed high contraction and relaxation velocity with a higher speed of calcium transient signal decay. Compared to the drugs with higher pregnancy risk levels, cardiac organoids showed higher stability in function and more excellent resistance even in high concentrations of essential nutrition, which proves their positive effect on cardiac development.

The IC50, or half maximal inhibitory concentration, is a measure used in pharmacology to assess the efficacy of a substance in inhibiting a specific biological or biochemical function. It represents the concentration of a substance required to inhibit a given biological process by half. Here, we have calculated the IC50 values for all functional parameters, including beating rate, time interval, contraction velocity, relaxation velocity, T30, T50, T75, UPD, peak time, signal change, and area ratio. We found that not all parameters have a IC50 value. This might be because the data did not show a clear difference across different concentrations, or that specific parameter was improved by drug treatment in the middle concentrations. For example, ascorbic acid improved cardiac organoid functions with 1 - 10μM concentrations, which makes it difficult to fit the dose-response curve for IC50 calculation. Some parameters showed extraordinarily low IC50 values because cardiac function showed significant changes in low concentrations. In addition, if there was a consistent increase or decrease trend in the drug

response results, the minimum and maximum values are difficult to be located for a precise calculation. Thus, we calculated the means of available functional IC50 as the integral IC50 of drugs on cardiac organoid development.

The IC50 results of all functional parameters were averaged for each drug (Table 2). Compared to other parameters, the IC50 of time intervals and T75s showed more NA. When the calcium transient signal decay to only 25% of its maximal value, the background noise is high and often causes extended decay time, which interfers the calculation of the IC50s. In addition, not all the drugs have a definitive IC50 values, for example amiodarone. This is because the cardiac organoids were only successfully developed in a few low amiodarone concentrations, which is insufficient for IC50 calculations (minimal requirement is at least four concentrations). Moreover, different functional parameters from the cardiac organoids treated with the same drug might show significant variations in IC50 results, because each function might be influenced by the drug differently. For example, calcium rising time duration and calcium decay time duration have significantly different IC50 values, because the calcium ion inflow and outflow were controlled by different ion gates and biological processes, which might be impacted by the drug differently.

Based on the comparison between the half maximal inhibitory concentration (IC50) of the different parameters of drugs with the highest plasma concentration of a drug (Cmax), we better understand of the safety of drugs in practical application. Higher IC50 does not represent safe application of a drug, but higher IC50 than Cmax means safer practical application. A drug can be considered to be safe even with a low IC50, if the Cmax of the drug is lower. Such as, although thalidomide and buspirone have lower IC50 values than most other drugs, both much lower Cmax values than their IC50. Based on the comparison (Table 2), the drugs include

amoxicillin, aspirin, folic acid, ascorbic acid, retinoic acid, buspirone, and lithium chloride. Among these drugs, all three nutrients, including folic acid, ascorbic acid, and retinoic acid, were safe for cardiac organoid development. Overall, these results verified that our cardiac organoid platform was sensitive to drug-induced developmental toxicity, thus offering an accurate assessment of drug developmental toxicity based on the 3D tissue formation and function, which is often not available from other stem cell-based in vitro assays.

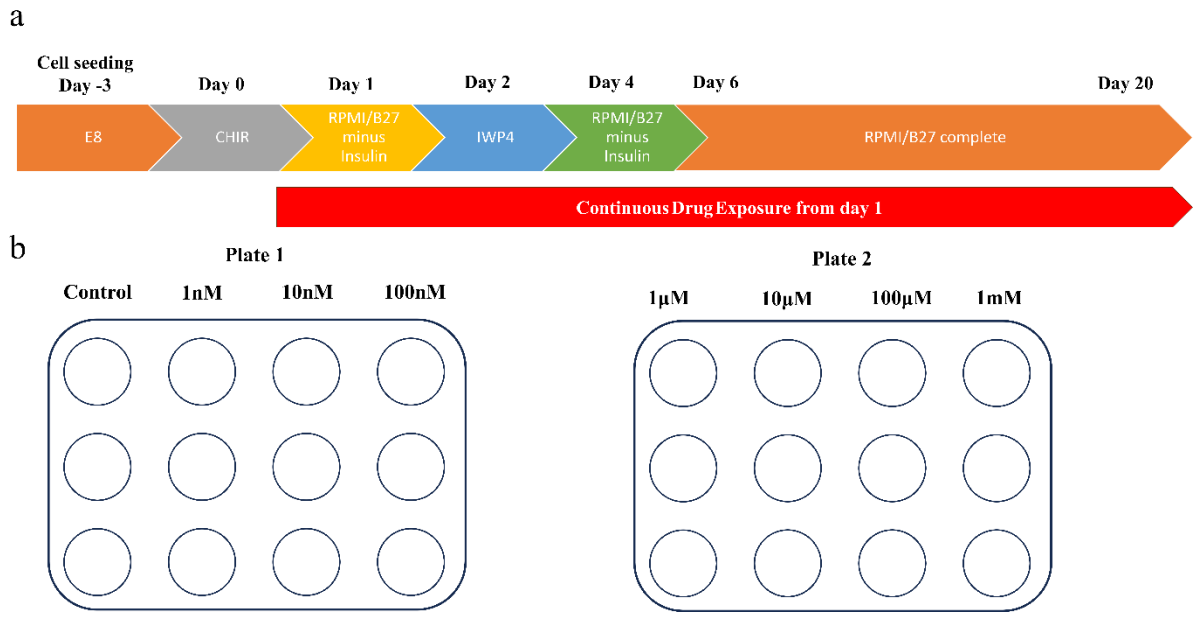

Figure 13. The drug screening design. (a) The procedure of cardiac organoid development with drugs. From day 1, drugs were added to the media. (b) Drug dosing design. Drugs were set up as 8 concentrations, including control group, and concentration levels were amplified tenfold to next level. All groups were placed in two plates with 3 replicates.

Table 3. Drugs used in the developmental toxicity testing.

Drug	Category	Function	Cmax (nM)	mEST IC50 (nM)	hPSC IC50 (nM)
Folic acid	A	Vitamin B9	551200 [125]	14850[126]	2000000000[127]
Ascorbic acid	A	Vitamin C, antioxidant	50000[128]	783500[110]	3736000[110]
Doxylamine	A	Sedative and sleep aid, treatment of various allergic symptoms	366200[129]	317500[130]	NA
Amoxicillin	B	Antibiotic medication	200mg/393000 875mg/1121000[131]	236800[131]	38340000[132]
Buspirone	B	Treatment of anxiety disorders	6485[133]	NA	>1000000000[134]
Aspirin	C	Analgesic, anti-inflammatory, and antipyretic medication	301124.5684[135]	122100000[110]	1376000[110]
Caffeine	C	Central nervous system stimulant	9501 [136]	710600[137]	224700[137]
Rifampicin	C	Antibiotic medication	99640[138]	NA	NA
Retinoic acid	C	Vitamin A	3428 [139]	5.6 [140]	13700[127]
Amiodarone	D	Antiarrhythmic drug	774.8[141]	9977[142]	22600[143]
5-fluorouracil	D	Antineoplastic medication	168360 [144]	720[126]	500[127]
Lithium chloride	D	Bipolar Disorder Treatment	1470000[145]	16980000[146]	100000000[147]
Thalidomide	X	Sedative and antiemetic	200mg/4647 400mg/13550 800mg/3230[110]	2711000[140]	801600[110]
Acrylamide	unknown	Found in brunt food, carcinogen	868000000[148]	963700[149]	19980000[150]

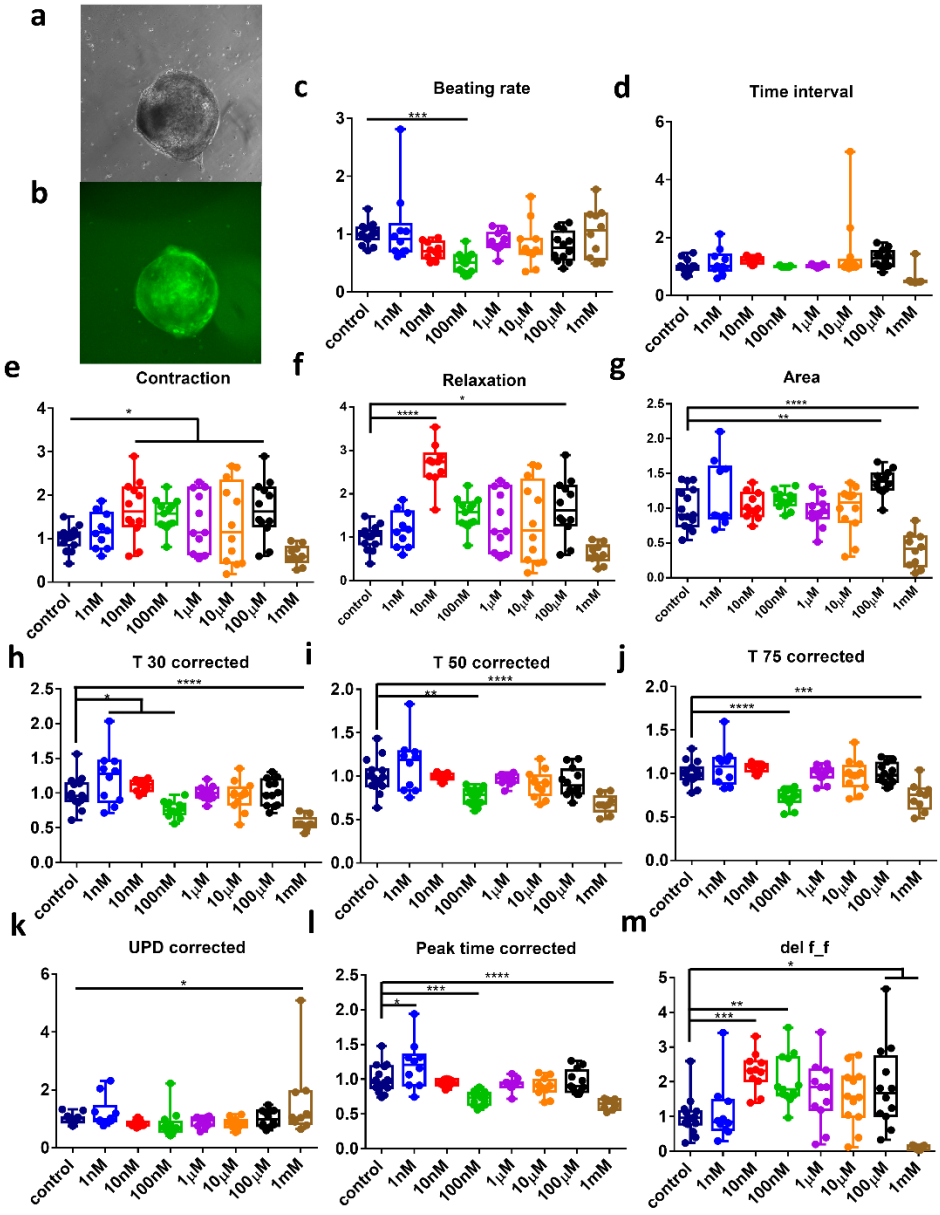

Figure 14. Cardiac organoids' function with folic acid treatment. (a, b) brightfield and GFP image of cardiac organoids at the end of differentiation. (c-f) Contraction motion result of cardiac organoids, higher concentrations showed higher functional activities but decreased in 1mM concentration. (g) Area of functional tissue among different groups, 1 mM group showed the smallest area. (h-m) Calcium transient result of different groups. 1mM showed the lowest functional activities.

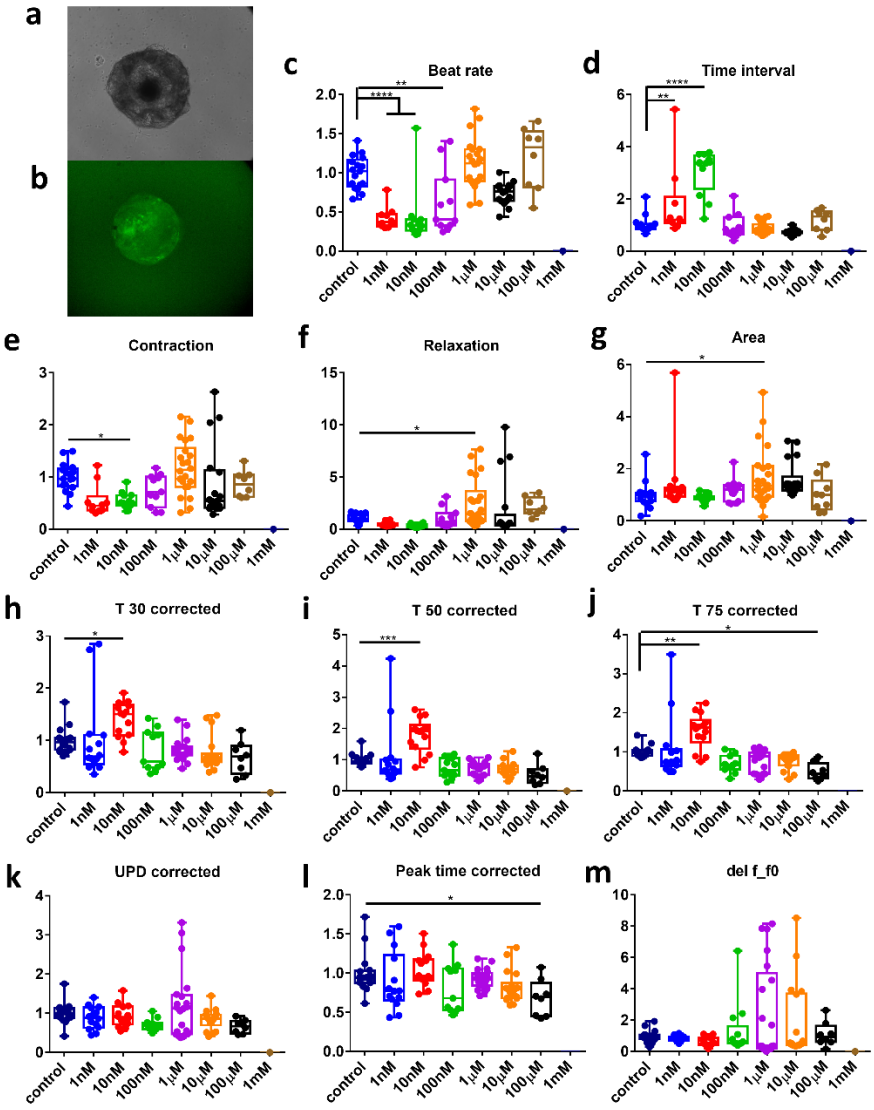

Figure 15. Cardiac organoids' function with ascorbic acid treatment. (a, b) brightfield and GFP image of cardiac organoids at the end of differentiation. (c-f) Contraction motion result of cardiac organoids, higher concentrations showed higher functional activities but decreased in the highest concentration. (g) Area of functional tissue among different groups, 1 mM group showed the smallest area. (h-m) Calcium transient result of different groups.

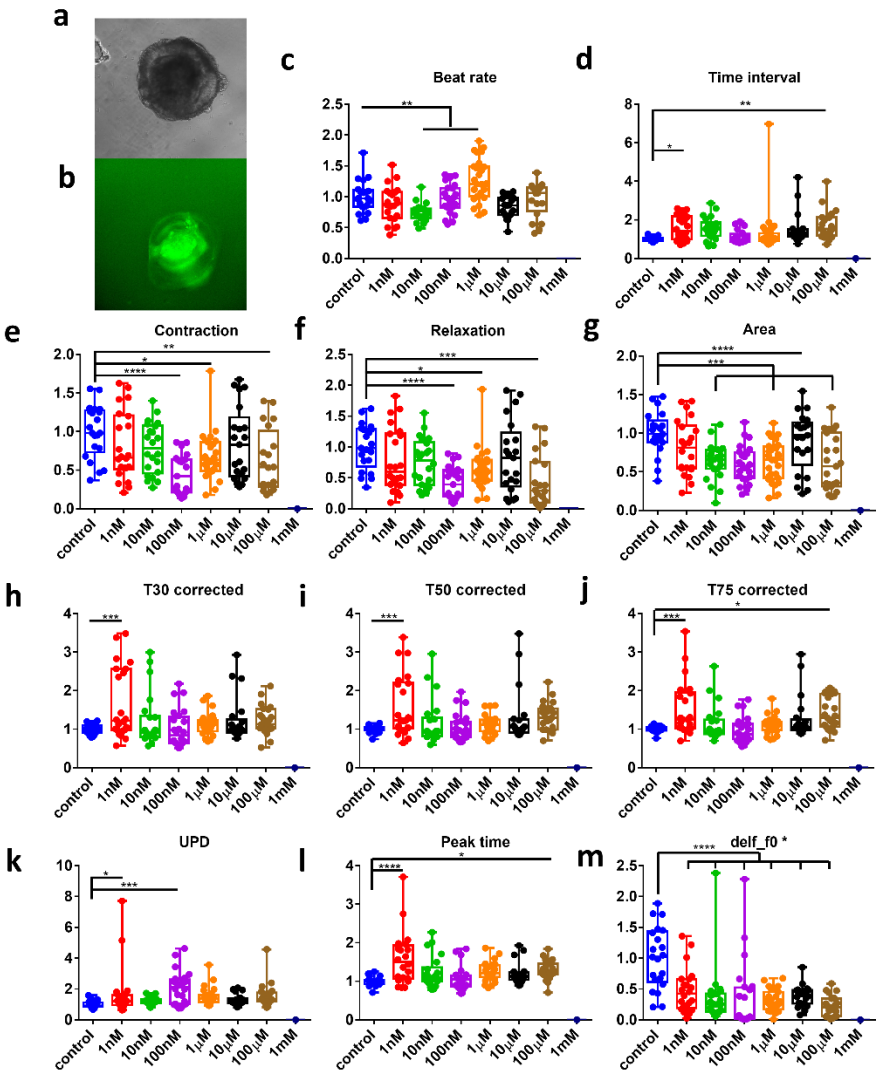

Figure 16. Cardiac organoids' function with doxylamine treatment. (a, b) brightfield and GFP image of cardiac organoids at the end of differentiation. (c-f) Contraction motion result of cardiac organoids, the control group showed higher contraction and relaxation velocity but lower beating rate and time interval. (g) Area of functional tissue among different groups, the control group showed the largest area. (h-m) Calcium transient result of different groups.

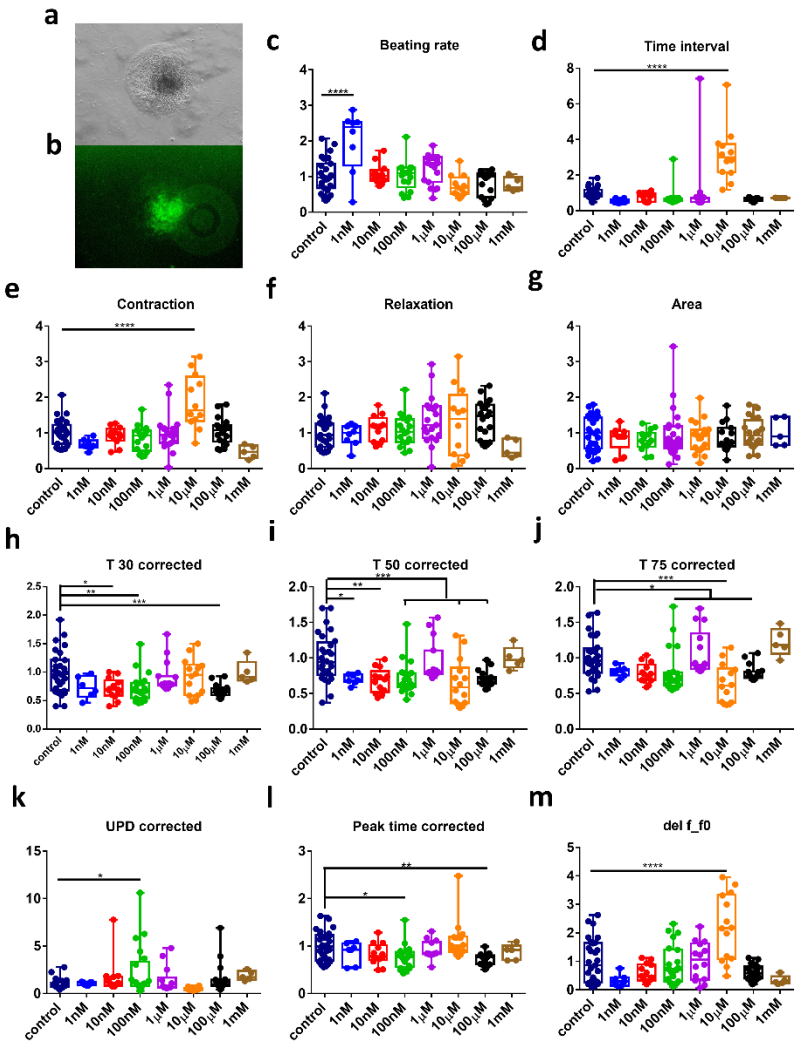

Figure 17. Cardiac organoids' function with amoxicillin treatment. (a, b) brightfield and GFP image of cardiac organoids at the end of differentiation. (c-f) Contraction motion result of cardiac organoids, the control group showed lower beating rate, shorter time interval, and lower contraction. (g) The area of functional tissue among different groups, there is no significant difference. (h-m) Calcium transient result of different groups. The control group showed higher T30, T50 and T75 but lower calcium transient signal change.

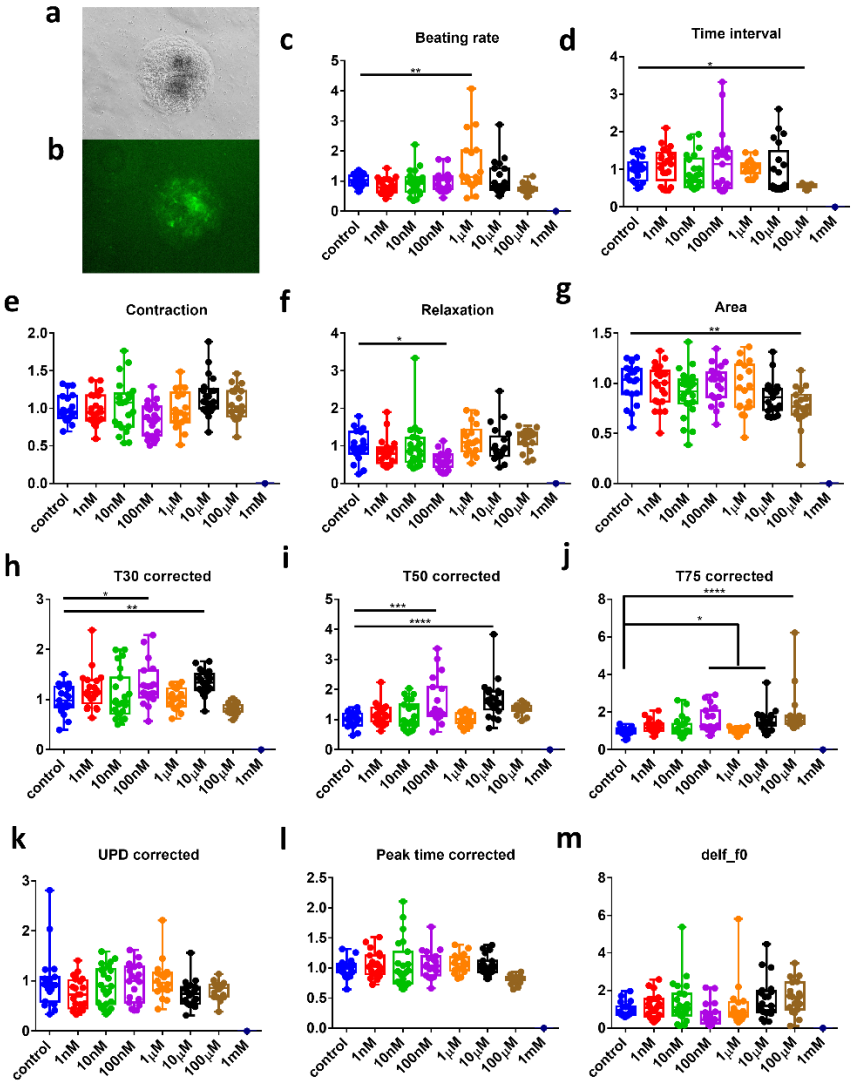

Figure 18. Cardiac organoids' function with buspirone treatment. (a, b) brightfield and GFP image of cardiac organoids at the end of differentiation. (c-f) Contraction motion result of cardiac organoids. (g) The area of functional tissue among different groups, the control group is much larger than the 100μM group. (h-m) Calcium transient result of different groups. The control group showed shorter T30, T50, and T75, but no significant difference in UPD, peak time, and calcium transient signal change result.

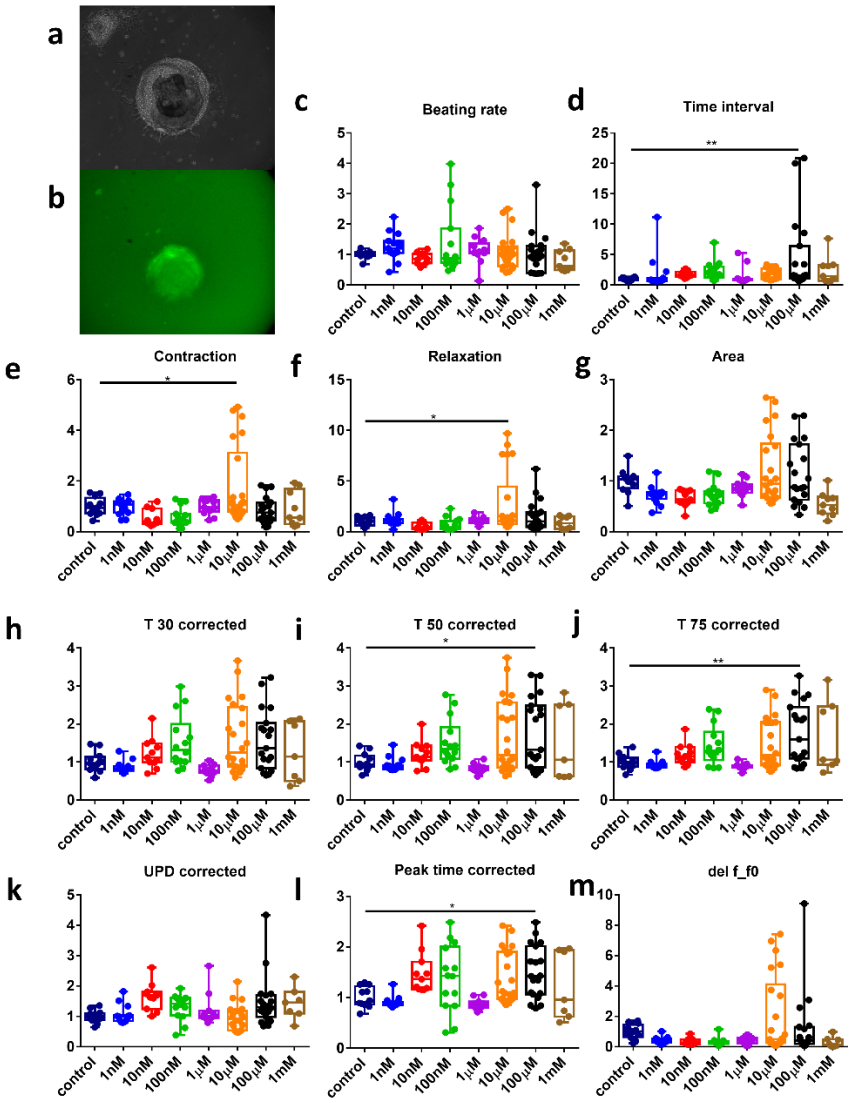

Figure 19. Cardiac organoids' function with aspirin treatment. (a, b) brightfield and GFP image of cardiac organoids at the end of differentiation. (c-f) Contraction motion result of cardiac organoids, there is no significant difference in group, except for the 100μM group showed a longer time interval and the 10μM group showed higher contraction and relaxation velocity. (g) Area of functional tissue among different groups, there is no significant difference. (h-m) Calcium transient result of different groups.

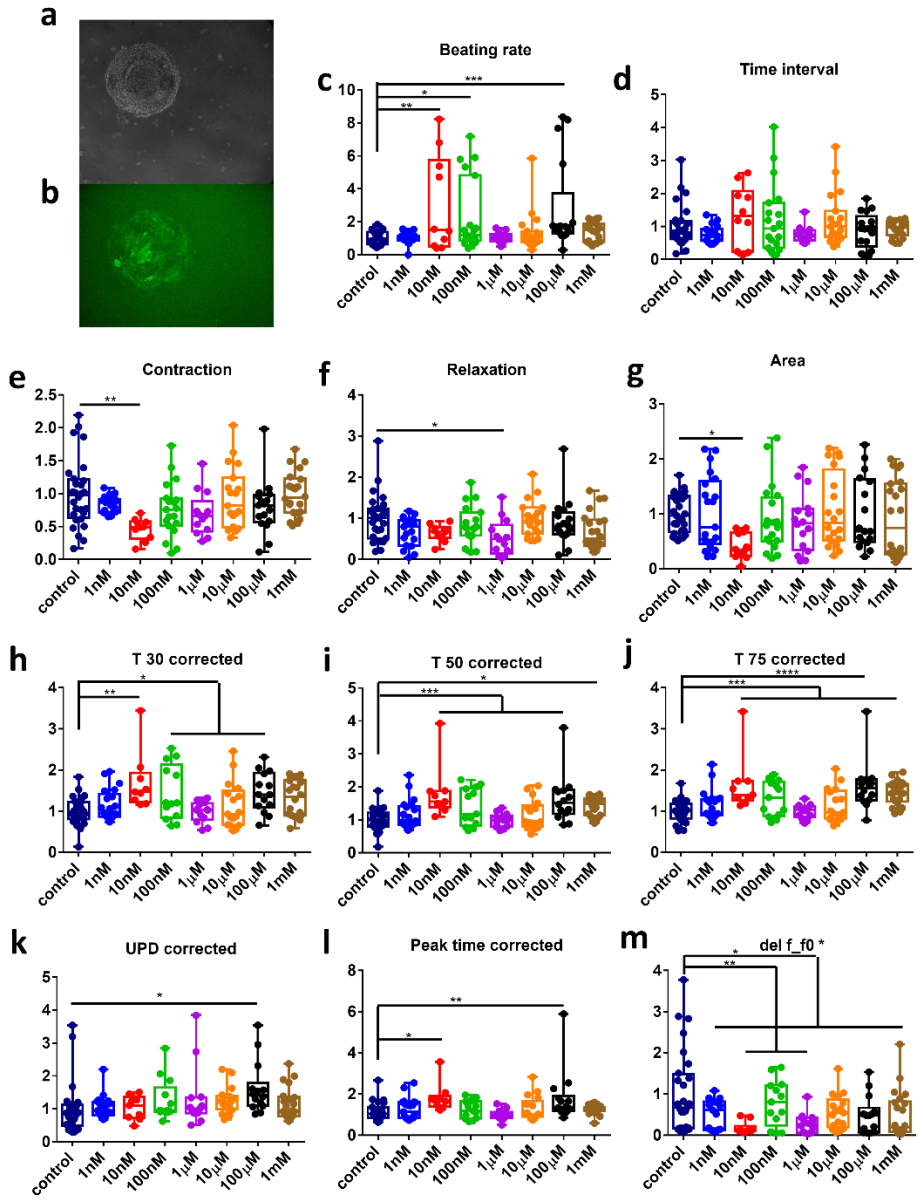

Figure 20. Cardiac organoids' function with caffeine treatment. (a, b) brightfield and GFP image of cardiac organoids at the end of differentiation. (c-f) Contraction motion result of cardiac organoids, the control group has a lower beating rate, and higher contraction and relaxation velocity (g) Area of functional tissue among different groups, 10nM group has the smallest function area. (h-m) Calcium transient result of different groups. The control group showed lower T30, T50, T75, UPD, and peak time, but higher calcium transient signal change.

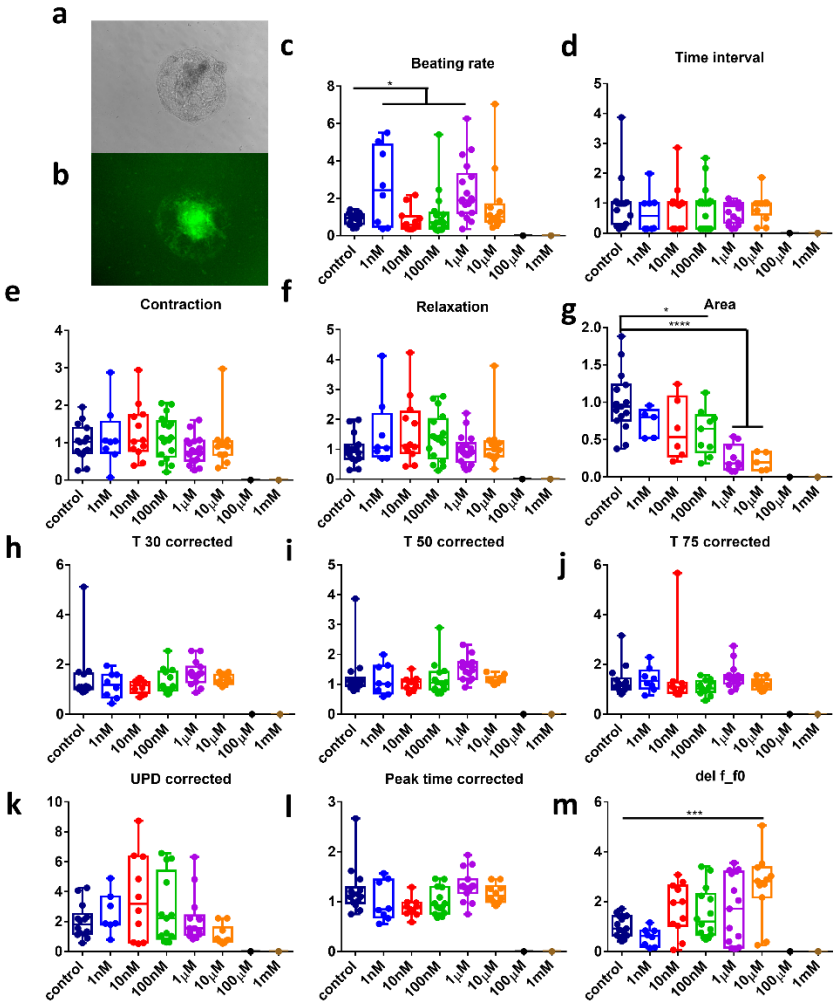

Figure 21. Cardiac organoids' function with caffeine treatment. (a, b) brightfield and GFP image of cardiac organoids at the end of differentiation. (c-f) Contraction motion result of cardiac organoids, the control group had a lower beating rate. (g) Area of functional tissue among different groups, the control group had the largest functional tissue, and the area significantly decreased as the concentration of rifampicin increased. (h-m) Calcium transient result of different groups. There is no difference in T30, T50, T75, UPD, and peak time, but the 10μM group showed higher calcium transient signal change.

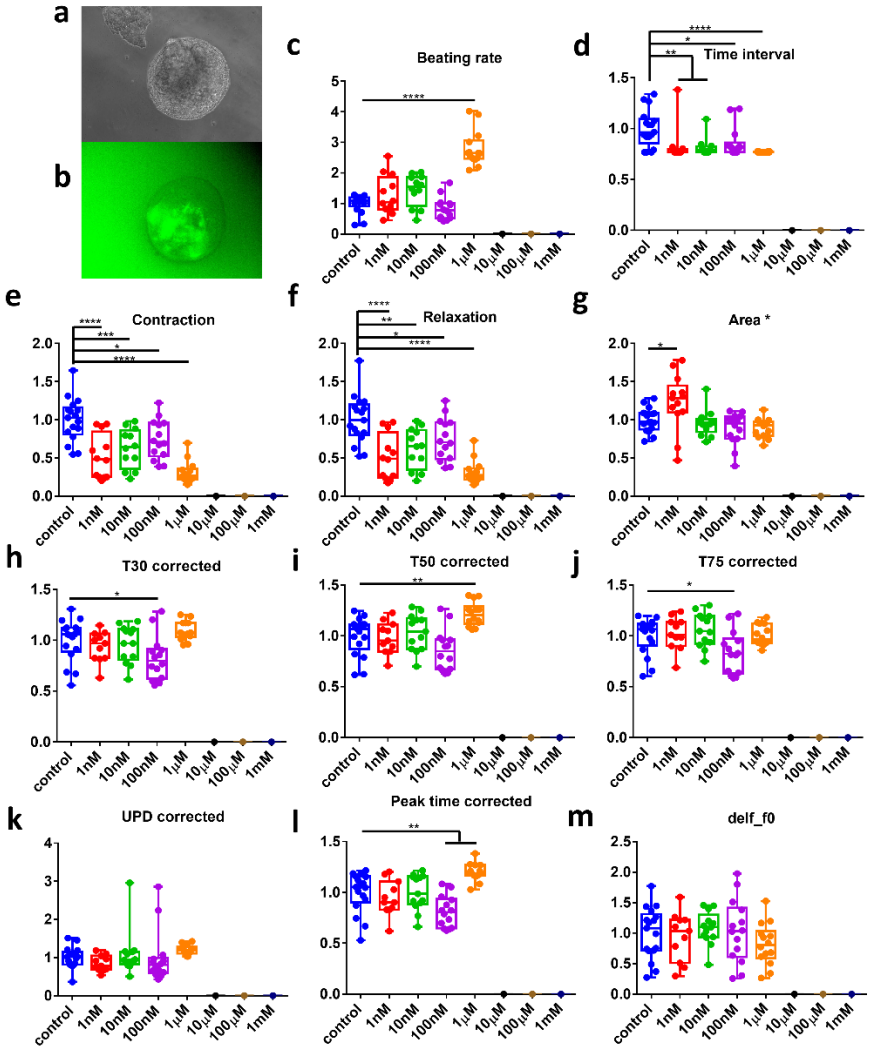

Figure 22. Cardiac organoids' function with retinoic acid treatment. (a, b) brightfield and GFP image of cardiac organoids at the end of differentiation. (c-f) Contraction motion result of cardiac organoids, the control group showed a lower beating rate but higher time interval, contraction velocity, and relaxation velocity. (g) Area of functional tissue among different groups, only the 1nM group showed a larger area than the control group. (h-m) Calcium transient result of different groups. 100nM group showed higher T30 and T75, and 1μM group had higher T50.

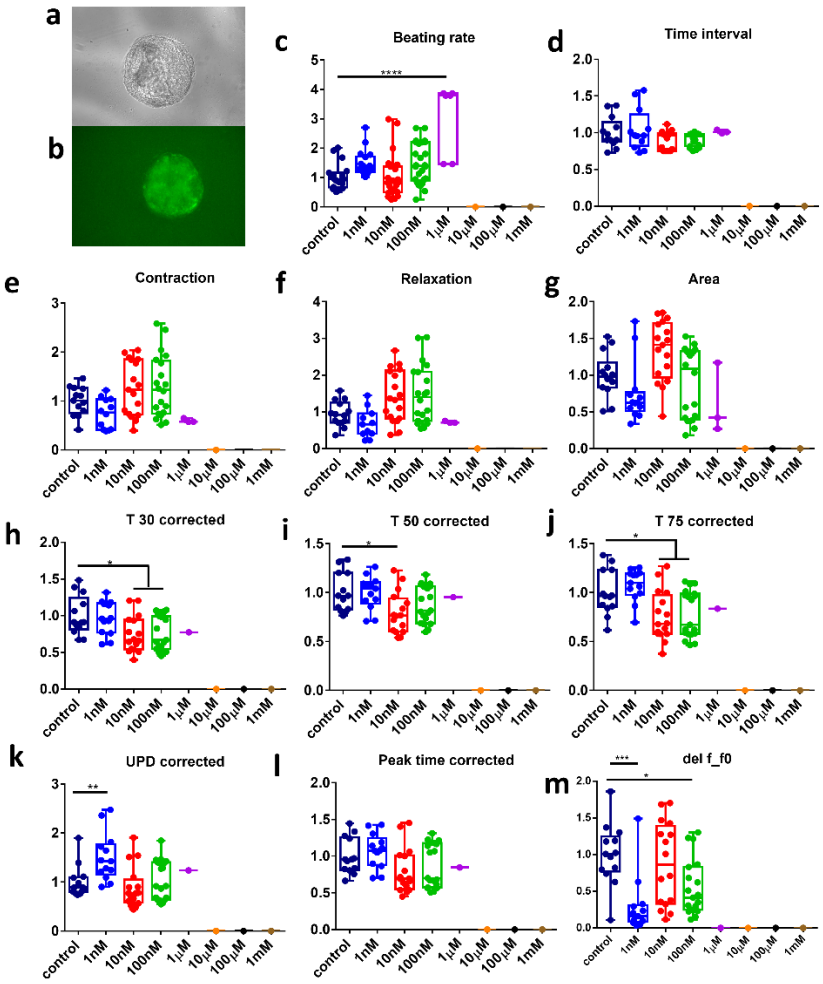

Figure 23. Cardiac organoids' function with 5-fluorouracil treatment. (a, b) brightfield and GFP image of cardiac organoids at the end of differentiation. (c-f) Contraction motion result of cardiac organoids, the control group only showed a lower beating rate. (g) Area of functional tissue among different groups, there is no significant difference. (h-m) Calcium transient result of different groups. The control group showed larger T30, T50, T75, UPD, and calcium transient signal change.

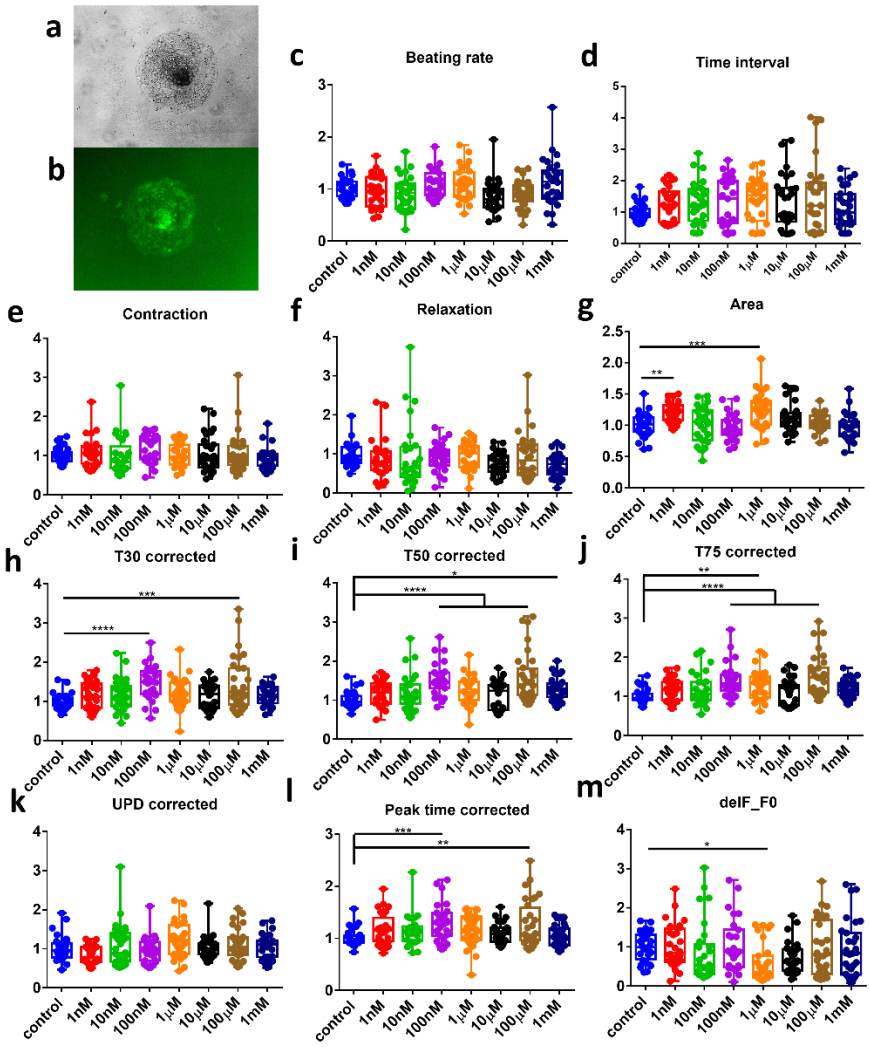

Figure 24. Cardiac organoids' function with lithium chloride treatment. (a, b) brightfield and GFP image of cardiac organoids at the end of differentiation. (c-f) Contraction motion result of cardiac organoids, there is no difference between different concentration groups. (g) Area of functional tissue among different groups, the control group is much smaller than the 1nM and 1μM groups. (h-m) Calcium transient result of different groups. The control group showed shorter T30, T50, T75, and peak time to 100nM and100μM groups, and the control group has a larger calcium transient signal change than 1μM groups.

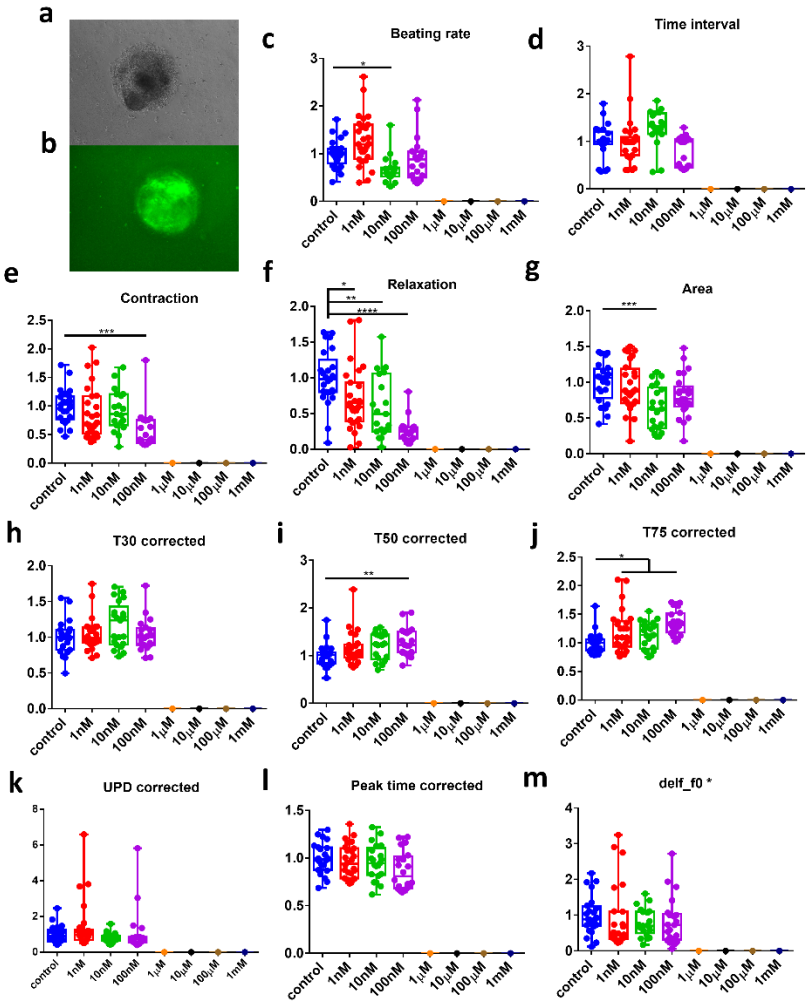

Figure 25. Cardiac organoids' function with amiodarone chloride treatment. (a, b) brightfield and GFP image of cardiac organoids at the end of differentiation. (c-f) Contraction motion result of cardiac organoids, there is no difference in time interval between different concentration groups, but control group showed higher contraction and relaxation velocity. (g) Area of functional tissue among different groups, the control group is much larger than 10nM. (h-m) Calcium transient result of different groups. The control group only showed shorter T50, T75 to 100nM and100μM groups, and shorter T75 to 1nM groups.

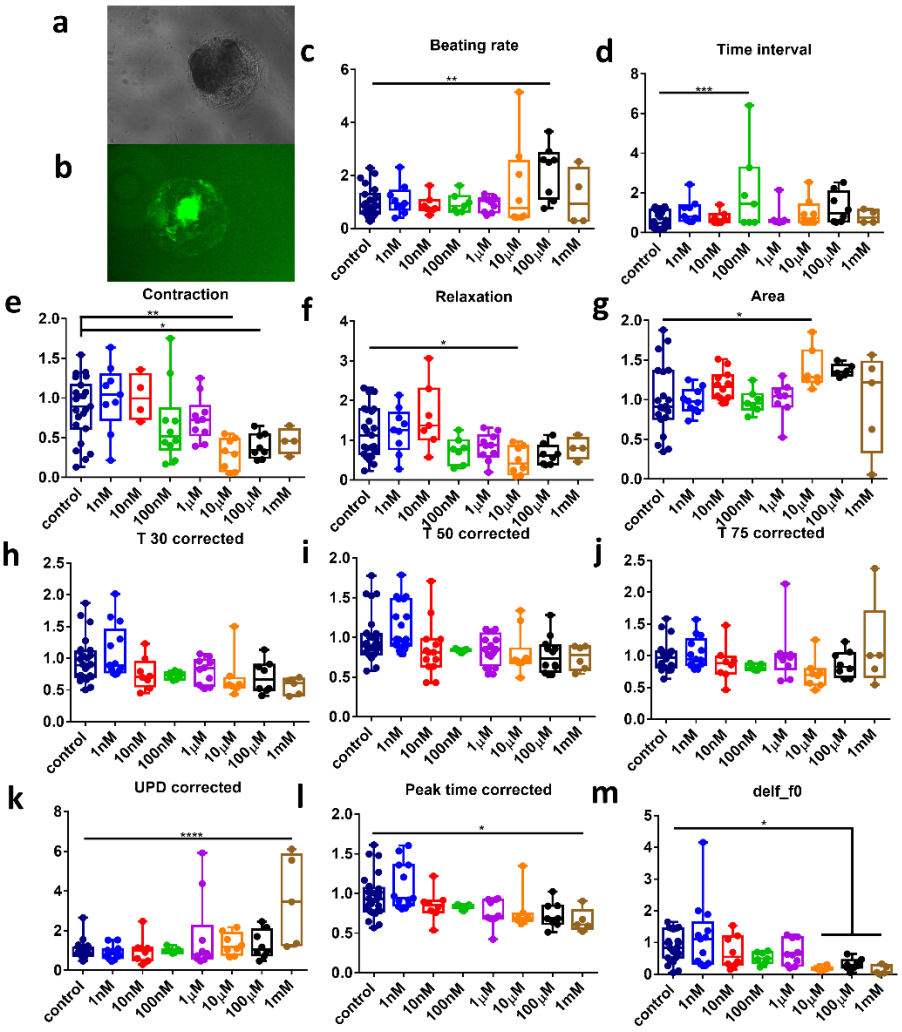

Figure 26. Cardiac organoids' function with thalidomide treatment. (a, b) brightfield and GFP image of cardiac organoids at the end of differentiation. (c-f) Contraction motion result of cardiac organoids, the control group only showed lower beating rate and time interval but contraction and relaxation velocity. (g) Area of functional tissue among different groups, the 10μM group was larger than the control group. (h-m) Calcium transient result of different groups. There is no significant difference in T30, T50, and T75, but the high concentration group showed larger UPD but lower peak time and calcium transient signal change.

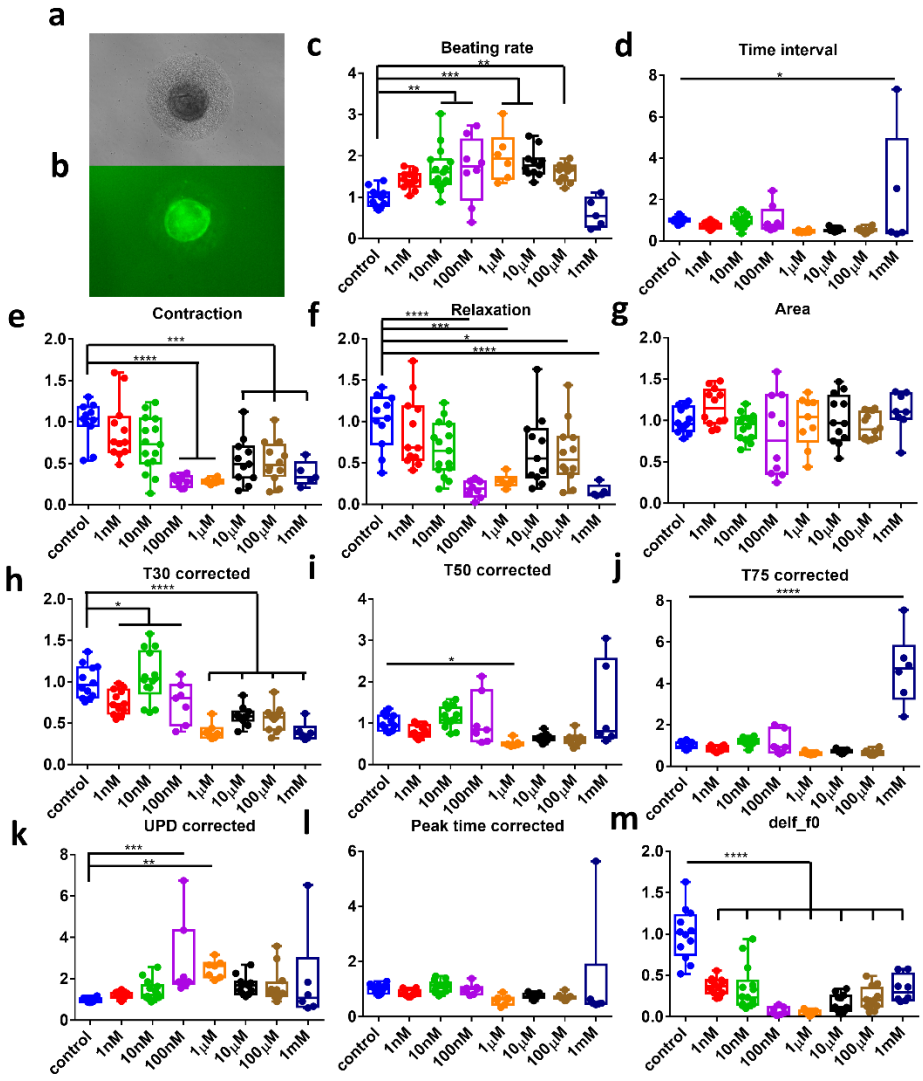

Figure 27. Cardiac organoids' function with acrylamide treatment. (a, b) brightfield and GFP image of cardiac organoids at the end of differentiation. (c-f) Contraction motion result of cardiac organoids, the peak value of beating was observed in the middle concentration, and the control group showed higher contraction and relaxation velocity. (g) Area of functional tissue among different groups, there is no significant difference. (h-m) Calcium transient result of different groups. The control group showed higher T30 and calcium transient signal change, but the UPD of the control group was much shorter.

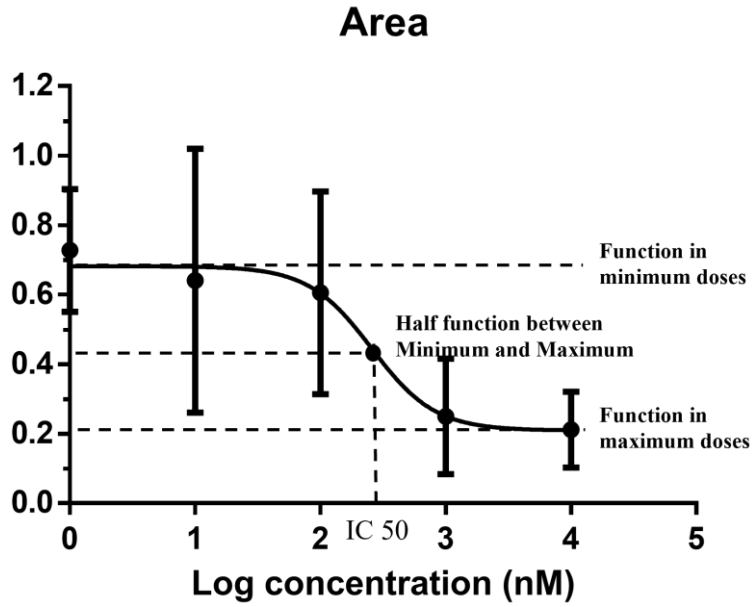

Figure 28. Dose-response curve of cardiac organoids' area with rifampicin treatment. The curve was set up by fitting the four-parameter logistic function formula to show the relationship between the inhibition on cardiomyocyte area and drug concentrations. The x axis is the logarithm-transformed drug concentrations. Y axis is area data normalized to the control group.

Table 4. IC50 (nM) of each function data of all drugs.

Drug	Beating rate	Time interval	Contraction velocity	Relaxation velocity	delf_f	T30	T50	T75	UPD	Peak time	Area ratio	Average	Cmax
Folic acid	283179	801142	827455	1.52E+06	205043	7.27E+08	1.27E-06	9.27E+12	148529	8.577	1.77E+06	8.43E+11	5.51E+05
Ascorbic acid	111.9	33.98	101.6	104.5	96.89	76.76	77	84.21	NA	3.85E+10	125.3	3.85E+09	50000
Doxylamine	NA	NA	NA	11.06	2.67E-14	6.418	0.5432	NA	NA	5.877	NA	4.780	3.66E+05
Amoxicillin	6.56E-05	NA	66250	642349	1.516	142	4.28E+06	1.57E+06	891.8	NA	1.07E+19	1.19E+18	1.12E+06
Buspirone	14.13	65152	1130	169.5	3641	29796	31.41	10235	2369	15231	11140	12628	6485
Aspirin	2.94E+07	61550	952.5	NA	NA	8.783	0	9268	NA	0.3748	NA	4.21E+06	3.01E+05
Caffeine	NA	NA	1430	3142	27.54	455.3	NA	NA	29.82	NA	32.68	852.89	9501
Rifampicin	NA	NA	109.6	110.9	0	104.3	112.7	NA	1599	115.9	252.3	300.5875	99640
Retinoic acid	803.9	0.01211	0.003927	0.00482	1442	NA	1748	NA	2.86E+08	1632	0.00482	3.18E+07	3428
Lithium chloride	NA	1.78E+06	4.88E+15	1550	NA	NA	NA	NA	0.5762	NA	171627	9.75E+14	1.47E+06
5-fluorouracil	154	3.798	NA	3.08	NA	1.274	NA	3.109	NA	3.964	113.7	40.42	1.68E+05
Amiodarone	NA	NA	NA	NA	NA	NA	NA	NA	NA	NA	NA	NA	774.8
Thalidomide	7515	NA	206.7	70.33	0	2.13E-05	1.28E-12	719245	2.89E+07	1.37E-13	NA	3.29E+06	3.23E+06
Acrylamide	159233	NA	10.73	481852	NA	106.3	416.2	786015	16.57	NA	263109	2.11E+05	8.68E+11

5. CHAPTER 5 SUMMARY AND FUTURE WORK

5.1 Conclusion

This dissertation discusses the engineering and development of new technology to model heart development and estimate cardiac physiology for advanced diagnostic capabilities, especially for drug-induced cardiac developmental toxicity. This dissertation primarily focused on engineering cardiac organoids using micropatterning to govern organoid cell assembly and tissue differentiation. In Chapter 2, we focus on the methodology of cardiac organoid engineering and introduce the whole experimental process of cardiac organoid development from iPSC seeding to cardiac tissue development and data analysis. We use the brightfield motion tracking and GCaMP signal to analyze cardiac function with Matlab software. In Chapter 3, we utilized different pattern designs to respectively investigate how the different geometrical confinement, including shape (square and rectangle), size (circle), and position (pentagram), influence 3D cardiac tissue formation and cardiac contractile functions to optimize organoid engineering. In Chapter 4, we applied the cardiac organoid as a testing platform to evaluate the embryotoxicity of the daily common drugs. This study demonstrates the engineering, application, and analysis of cardiac organoids utilizing micropatterning technology, and innovative techniques for cardiotoxicity medication testing. We anticipate that this effort will offer chances to progress in cardiovascular studies by using unique applications of tissue engineering and computational strategies.

Chapter 3 exploited how pattern geometry influences cardiac organoid tissue differentiation,

structure, and contractile function. In this part, the three categories of designs were utilized to investigate mechanical factors generated by patterns with different sizes and shapes. The result showed that the cardiac organoids were influenced by geometric confinements. Rectangular patterns with a larger aspect ratio improved the cardiac organoid function, showing as a larger function area and higher contraction activity properties but with lower tissue thickness. This might represent the cardiomyocytes had better spread and alignment in rectangle patterns with a larger aspect ratio. In addition, when organoid differentiation was performed in different pentagram patterns, the contracting cardiac tissues became larger with a smaller fraction of the central area relative to the entire pattern. Cardiac organoids with a smaller fraction of central area showed better function, and the area was located at the sharp corner, which proved the cardiomyocyte alignment better. The standard pentagram with central area ratio of 2 showed the best function in pentagram groups. This work demonstrates the adaptability of organoid engineering through micropatterning and how scientists can employ micropatterning to customize and precisely adjust stem cell organoids using biophysical restriction. This study can be broadened through further extensive functional assessments. For example, action potential is a prevalent method for investigating cardiac contraction since intracellular ion flow is directly linked to muscle contraction. We can investigate the potential change of organoids produced by different pattern geometries with action potential dye.

In Chapter 4, we utilized the cardiac organoids as an embryotoxicity platform to assess the drug developmental toxicity on cardiac development. Since the organoids are formed from the self-organization of differentiating hiPSCs, we believe this procedure might mimic in vivo heart development. Upon developing the cardiac organoids with a variety of drugs ranging in different

safety classifications, from A to X, we found our cardiac organoids are sensitive to different drugs with different concentrations, which shows that cardiac organoid function was interfered with by most of the drugs with high concentrations in different functional properties. In addition, the toxicity of different drugs was manifested as impairments in their unique functional properties. Some drugs reduce the motion activities, whereas other drugs showed that the calcium transient signal was disturbed. Through this research, we have determined that cardiac organoid development is sensitive to drug exposure, evident as structural and/or functional deficits. By incorporating time-lapse imaging, we can pinpoint occurrences in organoid growth influenced by pharmaceutical compounds and associate these occurrences with human organ development. Additionally, the analysis of genetic profiling through RNA sequencing can provide a chance to understand the cellular and molecular mechanisms that specific drugs might act on.

5.2 Future Work

5.2.1 Optimization of cardiac organoid generation

Although cardiac organoids with circles were proven to respond to drug treatment, organoid formation still has space to improve. Based on our computational model analysis, cardiac organoids with a 1 to 4 ratio rectangle pattern showed better cardiac organoid formation and cardiac function compared to 600 um circle pattern, possibly because the mechanical stress produced by these patterns improves the cardiac organoid development. In the future, we might use these or even more complex designs as the platform for drug developmental toxicity testing.

In addition, our results showed a positive effect of ascorbic acid on cardiac organoid development. Previous work also showed that ascorbic acid supplement in cardiac differentiation media could

improve function and differentiation. Therefore, we will attempt to optimize ascorbic acid concentration in the differentiation media for better cardiac organoid formation. Although hiPSCs were successfully developed into functional cardiac organoids with our current protocol, the flat bottom produces a different mechanical stimulation to hiPSCs compared to the natural environment. Hydrogels have been used more often to fabricate 3D scaffolds for cardiac organoid development. In the future, we will combine our cardiac organoid platform with synthetic hydrogels to increase the quality of cardiac organoids. Last, different batches of hiPSCs have considerable differences in cell viability and differentiation capability, which causes vast variance of the results. Thus, we believe that more replicates in a single batch of hiPSCs can reduce experimental variations and improve the reliability of the results.

5.2.2 Data-driven approaches to reduce batch variability

Despite efforts to normalize the results of different batches to their respective control group data, the batch variations in hiPSC differentiation and cardiac responses lead to high variability within the dataset. Filtering out low-quality data will help reduce the data variability and increase the dataset's quality. The standard methods to trim the low-quality data involve three popular ways. The first method was known as the median absolute deviation (MAD) algorithm, which takes the median of the dataset as standard and removes the data point that has a larger difference than double or triple the MAD value from a median of data. MAD value is the median of all difference values between each elementary of data and the median of data. Another popular method is the standard deviation algorithm, in which the data points with a larger difference than the triple

standard deviation from the mean of the dataset will be removed. Moreover, researchers can remove the biased data using the percentile algorithm. In the percentile algorithm, the maximum and minimum 5 to 10 percent data was treated as biased data and will be removed. To increase the dataset's quality, we will utilize single or multiple algorithms to reduce the variability of data and improve the quality of entire dataset.

During the experiment, we also observed that increasing drug concentration often caused a reduction in the total number of functional organoids. Part of organoids with high drug concentrations developed tissues without any beatings, or in some extreme cases, only single-layered cells were left in culture without tissue formation. This indicates that high concentrations of some drugs will lead to cardiac asystole, no cardiac differentiation, or even high cell apoptosis. Since all cell-covered patterns were considered to have the potential to develop functional and mature cardiac organoids, the proportion of functional organoids in all cell-confluent patterns can be considered as another crucial metric to illustrate developmental toxicity effects on cardiac organoid development. The larger proportion of functional organoids in higher concentration represents the lower risk of developmental toxicity on cardiac organoid formation.

5.2.3 High-throughput drug screening platform

A high-throughput organoid screening platform is an advanced and innovative setup designed to test various biological or pharmaceutical agents efficiently and rapidly on organoids. High-

throughput platforms enable the simultaneous testing of thousands of compounds or genetic conditions. This rapid screening capability accelerates the drug discovery process, reducing the time and cost associated with identifying promising drug candidates, which makes a large scale of drug developmental toxicity testing possible. Next, we aim to upgrade our cardiac organoids into a high-throughput drug screening platform. We can adopt 96 well plate format for high-throughput organoid development. First, we will induce the differentiation of iPSCs to cardiomyocytes in a 12-well plate, and differentiated cells will be centrifuged and resuspended in the hydrogel. The liquid mixture of cells and hydrogel will be dispensed into 96-well plates. Cells will reorganize themselves and spontaneously form the cardiac organoids in a few days. Alternatively, we can set up a microfluidic system with automatic control. Thus, we will combine and utilize more bioengineering technologies to develop our high-throughput organoid screening platform in the future.

5.2.4 Computational models for predicting drug developmental toxicity.

The current calculation of IC50 values for different drugs averages the IC50 values of all the function metrics, which is overly simple. It does not show the importance of each parameter in the whole functional performance. In a more sophisticated analytical approach, a weighted mean of all parameter-specific IC50 values can be calculated. Herein, parameters with higher importance will be ascribed to a greater weight in calculating the weighted mean of IC50. Computational models may be utilized to assign different importance and weights to each parameter. The new method involves identifying optimally developed and functioning cardiac organoids in the control

group as ideal samples. All functional parameters of these samples are then inputted into a machine learning model, and the algorithm autonomously determines the importance of parameters in cardiac function and shows the importance index of each parameter that can be used as their corresponding weights. We will calculate the weighted average of all functional parameters' IC50 based on their index to estimate the IC50 values across different drugs.

In addition, we could utilize the machine learning models to establish a scoring system, which will allow us to estimate the functional performance of cardiac organoids with specific drug concentrations and the toxicity on cardiac development. A possible commonly used computational model is the multi-layer neural network model, which involves a data input layer, a result output layer, and multiple hidden layers. For training this model, first, we will score the average value of each control group's functional parameter data as 100 scores, and the worst performance of each parameter as 0 score. For example, the lowest contraction and relaxation velocity will be scored 0, whereas the largest T30, T50, and T75 will be scored 0. Next, the qualified control group organoids will be marked as 100 score-sample, if their functional parameters are triple deviation within the average value, while the samples in the highest drug concentration groups with at least one parameter of 0 score will be marked as 0 score samples. We will input 80 percent of the 100-scored control group samples and 0-score samples data into the multi-layer perception learning model to train the model without any supervision, and the remaining 20 percent of the 100-score and 0-score samples as testing data to validate the model. In this model, we will input the functional

result of all cardiac organoids, and the model will evaluate all cardiac organoids' function and calculate a score. We will then plot the function-concentration curve of all organoids' functional scores with the drug concentrations. In the curve, we can locate the corresponding functional score at Cmax concentration for each drug and assess its toxicity on cardiac development. Ff the functional score at Cmax concentration is lower than 50, the drug is considered as high developmental toxicity. If the score is higher than 90, the drug is considered as low developmental toxicity. If the functional score is between 50 and 90, the drug is considered as moderate developmental toxicity. In addition, drug concentration with a functional score higher than 100 is considered to have a positive effect on cardiac organoid development, which could possibly provide a new differentiated approach in future.

Reference

1. Kolios G, Moodley Y. Introduction to Stem Cells and Regenerative Medicine. *Respiration*. 2012;85(1):3-10.
2. Dekoninck S, Blanpain C. Stem cell dynamics, migration and plasticity during wound healing. *Nat Cell Biol*. 2019;21(1):18-24.
3. Takahashi K, Yamanaka S. Induction of Pluripotent Stem Cells from Mouse Embryonic and Adult Fibroblast Cultures by Defined Factors. *Cell*. 2006;126(4):663-676.
4. Takahashi K, Tanabe K, Ohnuki M, et al. Induction of Pluripotent Stem Cells Dfrom Adult Human Fibroblasts by Defined Factors. *Cell*. 2007;131(5):861-872.
5. Yu J, Vodyanik MA, Smuga-Otto K, et al. Induced Pluripotent Stem Cell Lines Derived from Human Somatic Cells. *Science (1979)*. 2007;318(5858):1917-1920.
6. Shanks N, Greek R, Greek J. Are animal models predictive for humans? *Philosophy, Ethics, and Humanities in Medicine*. 2009;4(1):2.
7. Silva T, Bekman E, Carmo-Fonseca, Joaquim and Fernandes. Design principles for pluripotent stem cell-derived organoid engineering. *Stem Cells Int*. 2019;2019(Hindaw).
8. Przyborski SA. Differentiation of human embryonic stem cells after transplantation in immune-deficient mice. *Stem Cells*. 2005;23:1242-1250.
9. de Jongh D, Massey EK, Berishvili E, et al. Organoids: a systematic review of ethical issues. *Stem Cell Res Ther*. 2022;13(1):337.

10. Thomson JA, Itskovitz-Eldor J, Shapiro SS, et al. Embryonic Stem Cell Lines Derived from Human Blastocysts. *Science (1979)*. 1998;282(5391):1145-1147.

11. Spence JR, Mayhew CN, Rankin SA, et al. Directed differentiation of human pluripotent stem cells into intestinal tissue in vitro. *Nature*. 2011;470(7332):105-109.

12. Wilkinson DC, Alva-Ornelas JA, Sucre JMS, et al. Development of a Three-Dimensional Bioengineering Technology to Generate Lung Tissue for Personalized Disease Modeling. *Stem Cells Transl Med*. 2017;6(2):622-633.

13. Antonica F, Kasprzyk DF, Opitz R, et al. Generation of functional thyroid from embryonic stem cells. *Nature*. 2012;491(7422):66-71.

14. McCracken KW, Catá EM, Crawford CM, et al. Modelling human development and disease in pluripotent stem-cell-derived gastric organoids. *Nature*. 2014;516(7531):400-404.

15. Voges HK, Mills RJ, Elliott DA, Parton RG, Porrello ER, Hudson JE. Development of a human cardiac organoid injury model reveals innate regenerative potential. *Development*. 2017;144(6):1118-1127.

16. Xia Y, Nivet E, Sancho-Martinez I, et al. Directed differentiation of human pluripotent cells to ureteric bud kidney progenitor-like cells. *Nat Cell Biol*. 2013;15(12):1507-1515.

17. Huch M, Dorrell C, Boj SF, et al. In vitro expansion of single Lgr5+ liver stem cells induced by Wnt-driven regeneration. *Nature*. 2013;494(7436):247-250.

18. Paşca AM, Sloan SA, Clarke LE, et al. Functional cortical neurons and astrocytes from human pluripotent stem cells in 3D culture. *Nat Methods*. 2015;12(7):671-678.

19. Sina B, Tülay B, Marc van de W, Peter JP, Hans C. In Vitro Expansion of Human Gastric Epithelial Stem Cells and Their Responses to Bacterial Infection, Gastroenterology,. *Gastroenterology*. 2015;148(1):126-136.

20. McCracken KW, Catá EM, Crawford CM, et al. Modelling human development and disease in pluripotent stem-cell-derived gastric organoids. *Nature*. 2014;516(7531):400-404.

21. Xuyu Q, Ha NN, Mingxi MS, Hongjun S, Guo-li M. Brain-Region-Specific Organoids Using Mini-bioreactors for Modeling ZIKV Exposure,. *Cell*. 2016;165(5):1238-1254.

22. Amy LF, Tushar M, Gregory SP, et al. Functional Gene Correction for Cystic Fibrosis in Lung Epithelial Cells Generated from Patient iPSCs. *Cell Rep*. 2015;12(9):1385-1390.

23. Sylvia FB, Chang-Il H, Lindsey AB, Hans C, David AT. Organoid Models of Human and Mouse Ductal Pancreatic Cancer. *Cell*. 2015;160(1–2):324-338.

24. Dong G, Ian V, Andrea S, Charles LS, Yu C. Organoid Cultures Derived from Patients with Advanced Prostate Cancer. *Cell*. 2014;159(1):176-187.

25. Toshiro S, Daniel ES, Marc F, Peter DS, Hans C. Long-term Expansion of Epithelial Organoids From Human Colon, Adenoma, Adenocarcinoma, and Barrett's Epithelium,. *Gastroenterology*. 2011;141(5):1762-1772.

26. Huang L, Holtzinger A, Jagan I, et al. Ductal pancreatic cancer modeling and drug screening using human pluripotent stem cell– and patient-derived tumor organoids. *Nat Med*. 2015;21(11):1364-1371.

27. Hans C. Modeling Development and Disease with Organoids,. *Cell*. 2016;165(7):1586-

1597.

28. Jalan-Sakrikar N, Brevini T, Huebert RC, Sampaziotis F. Organoids and regenerative hepatology. *Hepatology*. 2022;n/a(n/a).

29. Yui S, Nakamura T, Sato T, et al. Functional engraftment of colon epithelium expanded in vitro from a single adult Lgr5+ stem cell. *Nat Med*. 2012;18(4):618-623.

30. Meritxell H, Helmuth G, Ruben van B, Edwin C, Hans C. Long-Term Culture of Genome-Stable Bipotent Stem Cells from Adult Human Liver. *Cell*. 2015;160(1–2):299-312.

31. Huch M, Dorrell C, Boj SF, et al. In vitro expansion of single Lgr5+ liver stem cells induced by Wnt-driven regeneration. *Nature*. 2013;494(7436):247-250.

32. Daniel ES, Bon-Kyoung K, Meritxell H, Jason CM, Hans C. Differentiated Troy+ Chief Cells Act as Reserve Stem Cells to Generate All Lineages of the Stomach Epithelium,. *Cell*. 2013;155(2):357-368.

33. Kessler M, Hoffmann K, Brinkmann V, et al. The Notch and Wnt pathways regulate stemness and differentiation in human fallopian tube organoids. *Nat Commun*. 2015;6(1):8989.

34. Corrò C, Novellasdemunt L, Li VSW. A brief history of organoids. *American Journal of Physiology-Cell Physiology*. 2020;319(1):C151-C165.

35. Jonathan AB, Matthias PL. Engineering Stem Cell Self-organization to Build Better Organoids. *Cell Stem Cell*. 2019;24(6):860-876.

36. Peerani R, Zandstra PW. Enabling stem cell therapies through synthetic stem cell--niche

engineering. *J Clin Invest*. 2010;120(Am Soc Clin Investig):60-70.

37. Kristine CR, Victor WW, Michael S, Michael TL, Geoffrey CG. Enhancement of mesenchymal stem cell angiogenic capacity and stemness by a biomimetic hydrogel scaffold. *Biomaterials*. 2012;33(1):80-90.

38. Perl A, Reinhoudt DN, Huskens J. Microcontact Printing: Limitations and Achievements. *Advanced Materials*. 2009;21(22):2257-2268.

39. Gjorevski N, Ranga A, Lutolf MP. Bioengineering approaches to guide stem cell-based organogenesis. *Development*. 2014;141(9):1794-1804.

40. North TE, Goessling W, Peeters M, et al. Hematopoietic Stem Cell Development Is Dependent on Blood Flow. *Cell*. 2009;137(4):736-748.

41. Lee HN, Choi YY, Kim JW, et al. Effect of biochemical and biomechanical factors on vascularization of kidney organoid-on-a-chip. *Nano Converg*. 2021;8(1):35.

42. Sorrentino G, Rezakhani S, Yildiz E, et al. Mechano-modulatory synthetic niches for liver organoid derivation. *Nat Commun*. 2020;11(1):3416.

43. Shkumatov A, Baek K, Kong H. Matrix rigidity-modulated cardiovascular organoid formation from embryoid bodies. *PLoS One*. 2014;9(Public Library of Science San Francisco, USA):e94764.

44. de Camps C, Aslani S, Stylianesis N, et al. Hydrogel Mechanics Influence the Growth and Development of Embedded Brain Organoids. *ACS Appl Bio Mater*. 2022;5(1):214-224.

45. Guvendiren M, Burdick JA. Stiffening hydrogels to probe short- and long-term cellular

responses to dynamic mechanics. *Nat Commun*. 2012;3(1):792.

46. Vincent LG, Choi YS, Alonso-Latorre B, del Álamo JC, Engler AJ. Mesenchymal stem cell durotaxis depends on substrate stiffness gradient strength. *Biotechnol J*. 2013;8(4):472-484.

47. Gjorevski N, Nikolaev M, Brown TE, et al. Tissue geometry drives deterministic organoid patterning. *Science (1979)*. 2023;375(6576):eaaw9021.

48. Nikolaev M, Mitrofanova O, Broguiere N, et al. Homeostatic mini-intestines through scaffold-guided organoid morphogenesis. *Nature*. 2020;585(7826):574-578.

49. Chen C, Rengarajan V, Kjar A, Huang Y. A matrigel-free method to generate matured human cerebral organoids using 3D-Printed microwell arrays. *Bioact Mater*. 2021;6(4):1130-1139.

50. Murphy S V, Atala A. 3D bioprinting of tissues and organs. *Nat Biotechnol*. 2014;32(8):773-785.

51. Tao X, Joyce J, Cassie G, James JH, Thomas B. Inkjet printing of viable mammalian cells. *Biomaterials*. 2005;26(1):93-99.

52. Park SE, Georgescu A, Huh D. Organoids-on-a-chip. *Science (1979)*. 2019;364(6444):960-965.

53. Kim S, Lee H, Chung M, Jeon NL. Engineering of functional, perfusable 3D microvascular networks on a chip. *Lab Chip*. 2013;13(8):1489-1500.

54. Kenneth MC, Daniel RP, Joe T. Formation of perfused, functional microvascular tubes in vitro,. *Microvasc Res*. 2006;71(3):185-196.

55. Yin F, Zhang X, Wang L, et al. HiPSC-derived multi-organoids-on-chip system for safety

assessment of antidepressant drugs. *Lab Chip*. 2021;21(3):571-581.

56. Zwi-Dantsis L, Gepstein L. Induced pluripotent stem cells for cardiac repair. *Cellular and Molecular Life Sciences*. 2012;69(19):3285-3299.

57. Wang Z, Wang SN, Xu TY, Miao ZW, Su DF, Miao CY. Organoid technology for brain and therapeutics research. *CNS Neurosci Ther*. 2017;23(10):771-778.

58. Soares CP, Midlej V, Oliveira MEW de, Benchimol M, Costa ML, Mermelstein C. 2D and 3D-organized cardiac cells shows differences in cellular morphology, adhesion junctions, presence of myofibrils and protein expression. *PLoS One*. 2012;7(Public Library of Science San Francisco, USA):e38147.

59. Cho J, Lee H, Rah W, Chang HJ, Yoon Y sup. From engineered heart tissue to cardiac organoid. *Theranostics*. 2022;12:2758.

60. Lancaster MA, Knoblich JA. Organogenesis in a dish: modeling development and disease using organoid technologies. *Science (1979)*. 2014;345:1247125.

61. LaBarge W, Mattappally S, Kannappan R, Fast VG, Berry JL, Zhang J. Maturation of three-dimensional, hiPSC-derived cardiomyocyte spheroids utilizing cyclic, uniaxial stretch and electrical stimulation. *PLoS One*. 2019;14(Public Library of Science San Francisco, CA USA):e0219442.

62. Hyeonyu K, Roger DK, Gordana VN, Joseph CW. Progress in multicellular human cardiac organoids for clinical applications. *Cell Stem Cell*. 2022;29(4):503-514.

63. Paşca AM, Sloan SA, Clarke LE, et al. Functional cortical neurons and astrocytes from

human pluripotent stem cells in 3D culture. *Nat Methods*. 2015;12(7):671-678.

64. Khademhosseini A, Eng G, Yeh J, et al. Microfluidic patterning for fabrication of contractile cardiac organoids. *Biomed Microdevices*. 2007;9(2):149-157.

65. Filippo Buono M, von Boehmer L, Strang J, P. Hoerstrup S, Y. Emmert M, Nugraha B. Human Cardiac Organoids for Modeling Genetic Cardiomyopathy. *Cells*. 2020;9(7).

66. Forsythe SD, Devarasetty M, Shupe T, Soker S, Skardal A. Environmental toxin screening using human-derived 3D bioengineered liver and cardiac organoid. *Front Public Health*. 2018;6:103.

67. Noor N, Shapira A, Edri R, Gal I, Wertheim L, Dvir T. 3D Printing of Personalized Thick and Perfusable Cardiac Patches and Hearts. *Advanced Science*. 2019;6(11):1900344.

68. Pablo Hofbauer, tefan M. Jahnel, Nora Papai, Maria Novatchkova, Sasha Mendjan. Cardioids reveal self-organizing principles of human cardiogenesis. *Cell*. 2021;184(12):3299-3317.

69. Lewis-Israeli YR, Wasserman AH, Gabalski MA, et al. Self-assembling human heart organoids for the modeling of cardiac development and congenital heart disease. *Nat Commun*. 2021;12(1):5142.

70. Kim M, Hwang JC, Min S, et al. Multimodal Characterization of Cardiac Organoids Using Integrations of Pressure-Sensitive Transistor Arrays with Three-Dimensional Liquid Metal Electrodes. *Nano Lett*. 2022;22(19):7892-7901.

71. Zhao D, Lei W, Hu S. Cardiac organoid — a promising perspective of preclinical model.

Stem Cell Res Ther. 2021;12(1):272.

72. Hofbauer P, Jahnel SM, Mendjan S. In vitro models of the human heart. *Development*. 2021;148(16):dev199672.

73. Martin M, Gähwiler EKN, Generali M, Hoerstrup SP, Emmert MY. Advances in 3D Organoid Models for Stem Cell-Based Cardiac Regeneration. *Int J Mol Sci*. 2023;24(6).

74. Zhang Y, Aleman J, Shin SR, Chae S, Hu N. Multisensor-integrated organs-on-chips platform for automated and continual in situ monitoring of organoid behaviors. *Proceedings of the National Academy of Sciences*. 2017;114:E2293-E2302.

75. Tai CK, Douglas S. DETECTION OF DRUG USE DURING PREGNANCY. *Obstet Gynecol Clin North Am*. 1998;25(1):43-64.

76. Bantle JA, Fort DJ, James BL. Identification of developmental toxicants using the frog embryo teratogenesis assay-Xenopus (FETAX). *Environmental Bioassay Techniques and their Application: Proceedings of the 1st International Conference held in Lancaster, England, 11--14 July 1988*. 1989;(Springer):577-585.

77. Anna B van W, Cor Snel, Eke R, Aswin M, André W. Zebrafish embryotoxicity test for developmental (neuro)toxicity: Demo case of an integrated screening approach system using anti-epileptic drugs,. *Reproductive Toxicology*. 2014;49:101-116.

78. Modarresi Chahardehi A, Arsad H, Lim V. Zebrafish as a Successful Animal Model for Screening Toxicity of Medicinal Plants. *Plants*. 2020;9(10).

79. Ali S, Mil HG van, Richardson MK. Large-scale assessment of the zebrafish embryo as a

possible predictive model in toxicity testing. *PLoS One*. 2011;6(Public Library of Science San Francisco, USA):e21076.

80. Te-Hao C, Yen-Hsin W, Yu-Hwan W. Developmental exposures to ethanol or dimethylsulfoxide at low concentrations alter locomotor activity in larval zebrafish: Implications for behavioral toxicity bioassays. *Aquatic Toxicology*. 2011;102(3–4):162-166.

81. Arnold H, Kerstin N, Heinz-R. Köhler, Rita T. Comparative embryotoxicity and proteotoxicity of three carrier solvents to zebrafish (Danio rerio) embryos. *Ecotoxicol Environ Saf*. 2006;63(3):378-388.

82. Esther de J, Marta B, Sanne ABH, Jos GMB, Aldert HP. Comparison of the mouse Embryonic Stem cell Test, the rat Whole Embryo Culture and the Zebrafish Embryotoxicity Test as alternative methods for developmental toxicity testing of six 1,2,4-triazoles. *Toxicol Appl Pharmacol*. 2011;253(2):103-111.

83. Bowen SE, Hannigan JH. Developmental toxicity of prenatal exposure to toluene. *AAPS J*. 2006;8(2):49.

84. Chan LY, Chiu PY, Siu SSN, Lau TK. A study of diclofenac-induced teratogenicity during organogenesis using a whole rat embryo culture model. *Human Reproduction*. 2001;16(11):2390-2393.

85. Klaus D. Embryotoxic effects of environmental chemicals: Tests with the South African clawed toad (Xenopus laevis), Ecotoxicology and Environmental Safety. *Ecotoxicol Environ Saf*. 1987;13(3):324-338.

86. Knudsen TB, Fitzpatrick SC, De Abrew KN, et al. FutureTox IV Workshop Summary: Predictive Toxicology for Healthy Children. *Toxicological Sciences*. 2021;180(2):198-211.

87. Andrea S, Anke V, Roland B, Elke G, Horst S. Improvement of an in vitro stem cell assay for developmental toxicity: the use of molecular endpoints in the embryonic stem cell test. *Reproductive Toxicology*. 2004;18(2):231-240.

88. Paul RW, April MW, Alan MS, Elizabeth LRD, Gabriela GC. Predicting human developmental toxicity of pharmaceuticals using human embryonic stem cells and metabolomics. *Toxicol Appl Pharmacol*. 2010;247(1):18-27.

89. Rodney N, Malini K, Andrew J, Marie C. Human embryonic stem cell model of ethanol-mediated early developmental toxicity. *Exp Neurol*. 2012;234(1):127-135.

90. Aikawa N. A novel screening test to predict the developmental toxicity of drugs using human induced pluripotent stem cells. *J Toxicol Sci*. 2020;45(4):187-199.

91. Adler S, Pellizzer C, Paparella M, Hartung T, Bremer S. The effects of solvents on embryonic stem cell differentiation. *Toxicology in Vitro*. 2006;20(3):265-271.

92. Kirkwood-Johnson L, Katayama N, Marikawa Y. Dolutegravir Impairs Stem Cell-Based 3D Morphogenesis Models in a Manner Dependent on Dose and Timing of Exposure: An Implication for Its Developmental Toxicity. *Toxicological Sciences*. 2021;184(2):191-203.

93. Kirkwood-Johnson L, Marikawa Y. Developmental toxicity of remdesivir, an anti-COVID-19 drug, is implicated by in vitro assays using morphogenetic embryoid bodies of mouse and human pluripotent stem cells. *Birth Defects Res*. 2023;115(2):224-239.

94. Ying H, Yuanyuan M, Bo C, Jingpu Z, Changqin H. Hazard assessment of beta-lactams: Integrating in silico and QSTR approaches with in vivo zebrafish embryo toxicity testing. *Ecotoxicol Environ Saf*. 2022;229.

95. Brown NA, Spielmann H, Bechter R, et al. Screening Chemicals for Reproductive Toxicity: The Current Alternatives: The Report and Recommendations of an ECVAM/ETS Workshop (ECVAM Workshop 12)1,2. *Alternatives to Laboratory Animals*. 1995;23(6):868-882.

96. Minghui L, Jing G, Lixiong G, Jiahui K, Haiwei X. Advanced human developmental toxicity and teratogenicity assessment using human organoid models. *Ecotoxicol Environ Saf*. 2022;235.

97. David P, Katharina B, Pierre L, Thomas H, Helena TH. Rotenone exerts developmental neurotoxicity in a human brain spheroid model. *Toxicol Appl Pharmacol*. 2018;354(114):101.

98. Schwartz MP, Hou Z, Propson NE, et al. Human pluripotent stem cell-derived neural constructs for predicting neural toxicity. *Proceedings of the National Academy of Sciences*. 2015;112(40):12516-12521.

99. Nzou G, Wicks RT, Wicks EE, et al. Human Cortex Spheroid with a Functional Blood Brain Barrier for High-Throughput Neurotoxicity Screening and Disease Modeling. *Sci Rep*. 2018;8(1):7413.

100. Landgren M, Svensson L, Strömland K, Andersson Grönlund M. Prenatal Alcohol Exposure and Neurodevelopmental Disorders in Children Adopted From Eastern Europe. *Pediatrics*.

2010;125(5):e1178-e1185.

101. Arzua T, Yan Y, Jiang C, et al. Modeling alcohol-induced neurotoxicity using human induced pluripotent stem cell-derived three-dimensional cerebral organoids. *Transl Psychiatry*. 2020;10(1):347.

102. Ao Z, Cai H, Havert DJ, et al. One-Stop Microfluidic Assembly of Human Brain Organoids To Model Prenatal Cannabis Exposure. *Anal Chem*. 2020;92(6):4630-4638.

103. Wang Y, Wang L, Zhu Y, Qin J. Human brain organoid-on-a-chip to model prenatal nicotine exposure. *Lab Chip*. 2018;18(6):851-860.

104. Yin F, Zhu Y, Wang Y, Qin J. Engineering Brain Organoids to Probe Impaired Neurogenesis Induced by Cadmium. *ACS Biomater Sci Eng*. 2018;4(5):1908-1915.

105. Landgren M, Svensson L, Andersson Gronlund M. Prenatal alcohol exposure and neurodevelopmental disorders in children adopted from eastern Europe. *Pediatrics*. 2010;125:e1178-e1185.

106. Seiler AEM, Spielmann H. The validated embryonic stem cell test to predict embryotoxicity in vitro. *Nat Protoc*. 2011;6(7):961-978.

107. Esther de J, Lianne van B, Aldert HP. Comparison of osteoblast and cardiomyocyte differentiation in the embryonic stem cell test for predicting embryotoxicity in vivo. *Reproductive Toxicology*. 2014;48:62-71.

108. Maillet A, Tan K, Chai X, et al. Modeling Doxorubicin-Induced Cardiotoxicity in Human Pluripotent Stem Cell Derived-Cardiomyocytes. *Sci Rep*. 2016;6(1):25333.

109. Acimovic I, Vilotic A, Pesl M, et al. Human pluripotent stem cell-derived cardiomyocytes as research and therapeutic tools. *Biomed Res Int*. 2014;2014(Hindawi).

110. Aikawa N, Kunisato A, Nagao K, Kusaka H, Takaba K, Ohgami K. Detection of Thalidomide Embryotoxicity by In Vitro Embryotoxicity Testing Based on Human iPS Cells. *J Pharmacol Sci*. 2014;124(2):201-207.

111. Zhao L, Zhang B. Doxorubicin induces cardiotoxicity through upregulation of death receptors mediated apoptosis in cardiomyocytes. *Sci Rep*. 2017;7(1):44735.

112. Richard JM, Benjamin LP, Gregory AQR, Enzo RP, James EH. Drug Screening in Human PSC-Cardiac Organoids Identifies Pro-proliferative Compounds Acting via the Mevalonate Pathway. *Cell Stem Cell*. 2019;24(6):895-907.

113. Amabile G, Meissner A. Induced pluripotent stem cells: current progress and potential for regenerative medicine. *Trends Mol Med*. 2009;15(2):59-68.

114. Antonica F, Kasprzyk DF, Opitz R, et al. Generation of functional thyroid from embryonic stem cells. *Nature*. 2012;491(7422):66-71.

115. Mills RJ, Titmarsh DM, Koenig X, et al. Functional screening in human cardiac organoids reveals a metabolic mechanism for cardiomyocyte cell cycle arrest. *Proceedings of the National Academy of Sciences*. 2017;114(40):E8372-E8381.

116. Pal R, Mamidi MK, Kumar Das A, Bhonde R. Human embryonic stem cell proliferation and differentiation as parameters to evaluate developmental toxicity. *J Cell Physiol*. 2011;226(6):1583-1595.

117. Han SB, Kim JK, Lee G, Kim DH. Mechanical Properties of Materials for Stem Cell Differentiation. *Adv Biosyst*. 2020;4(11):2000247.

118. Xu X, Jiang S, Gu L, et al. High-throughput bioengineering of homogenous and functional human-induced pluripotent stem cells-derived liver organoids via micropatterning technique. *Front Bioeng Biotechnol*. 2022;10.

119. Seo K, Cho S, Lee JH, et al. Symmetry breaking of hPSCs in micropattern generates a polarized spinal cord-like organoid (pSCO) with dorsoventral organization. *bioRxiv*. Published online January 1, 2021:2021.09.18.460734.

120. Abilez OJ, Yang H, Tian L, et al. Micropatterned Organoids Enable Modeling of the Earliest Stages of Human Cardiac Vascularization. *bioRxiv*. Published online January 1, 2022:2022.07.08.499233.

121. Deglincerti A, Etoc F, Guerra MC, et al. Self-organization of human embryonic stem cells on micropatterns. *Nat Protoc*. 2016;11(11):2223-2232.

122. Jakob， J. Metzger, Carlota P, Arjun A, et al. Deep-learning analysis of micropattern-based organoids enables high-throughput drug screening of Huntington's disease models. *Cell Reports Methods*. 2022;2(9).

123. Hoang P, Wang J, Conklin BR, Healy KE, Ma Z. Generation of spatial-patterned early-developing cardiac organoids using human pluripotent stem cells. *Nat Protoc*. 2018;13(4):723-737.

124. Yin F, Zhang X, Wang L, Qin J, Yu H. HiPSC-derived multi-organoids-on-chip system for

safety assessment of antidepressant drugs. *Lab Chip*. 2021;21:571-581.

125. Menke A, Weimann HJ, Achtert G, Schuster O, Menke G. Absolute bioavailability of folic acid after oral administration of a folic acid tablet formulation in healthy volunteers. *Arzneimittelforschung*. 1994;44(9):1063-1067.

126. Kavuri M. The utilization of embryonic stem cells to discern embryotoxicity in vitro. Published online 2022.

127. Adler S, Pellizzer C, Hareng L, Hartung T, Bremer S. First steps in establishing a developmental toxicity test method based on human embryonic stem cells. *Toxicology in Vitro*. 2008;22(1):200-211.

128. Lykkesfeldt J, Tveden-Nyborg P. The pharmacokinetics of vitamin C. *Nutrients*. 2019;11:2412.

129. Duchesnay USA I. DICLEGIS- doxylamine succinate and pyridoxine hydrochloride tablet, delayed release. Duchesnay USA, Inc.

130. Lee JH, Park SY, Ahn C, et al. Pre-validation study of alternative developmental toxicity test using mouse embryonic stem cell-derived embryoid bodies. *Food and Chemical Toxicology*. 2019;123:50-56.

131. de Velde F, de Winter BCM, Koch BCP, van Gelder T, Mouton JW, consortium on behalf of the CN. Non-linear absorption pharmacokinetics of amoxicillin: consequences for dosing regimens and clinical breakpoints. *Journal of Antimicrobial Chemotherapy*. 2016;71(10):2909-2917.

132. Pezzanite L, Chow L, Piquini G, et al. Use of in vitro assays to identify antibiotics that are cytotoxic to normal equine chondrocytes and synovial cells. *Equine Vet J*. 2021;53(3):579-589.

133. Mahmood I, Sahajwalla C. Clinical Pharmacokinetics and Pharmacodynamics of Buspirone, an Anxiolytic Drug. *Clin Pharmacokinet*. 1999;36(4):277-287. 3

134. Wu Y, Geng X chao, Wang J feng, Miao Y fa, Lu Y li, Li B. The HepaRG cell line, a superior in vitro model to L-02, HepG2 and hiHeps cell lines for assessing drug-induced liver injury. *Cell Biol Toxicol*. 2016;32(1):37-59.

135. Nagelschmitz J, Blunck M, Kraetzschmar J, Ludwig M, Wensing G, Hohlfeld T. Pharmacokinetics and pharmacodynamics of acetylsalicylic acid after intravenous and oral administration to healthy volunteers. *Clin Pharmacol*. 2014;6(null):51-59.

136. White JR, Padowski JM, Zhong Y, et al. Pharmacokinetic analysis and comparison of caffeine administered rapidly or slowly in coffee chilled or hot versus chilled energy drink in healthy young adults. *Clin Toxicol*. 2016;54(4):308-312.

137. Witt G, Keminer O, Leu J, et al. An automated and high-throughput-screening compatible pluripotent stem cell-based test platform for developmental and reproductive toxicity assessment of small molecule compounds. *Cell Biol Toxicol*. 2021;37(2):229-243.

138. Abulfathi AA, Decloedt EH, Svensson EM, Diacon AH, Donald P, Reuter H. Clinical Pharmacokinetics and Pharmacodynamics of Rifampicin in Human Tuberculosis. *Clin Pharmacokinet*. 2019;58(9):1103-1129.

139. Clewell HJ, Andersen ME, Wills RJ, Latriano L. A physiologically based pharmacokinetic model for retinoic acid and its metabolites. *J Am Acad Dermatol*. 1997;36(3, Supplement):S77-S85.

140. Inoue A, Nishimura Y, Matsumoto N, et al. Comparative study of the zebrafish embryonic toxicity test and mouse embryonic stem cell test to screen developmental toxicity of human pharmaceutical drugs. *Fundam Toxicol Sci*. 2016;3(2):79-87.

141. Shiga T, Tanaka T, Irie S, Hagiwara N, Kasanuki H. Pharmacokinetics of intravenous amiodarone and its electrocardiographic effects on healthy Japanese subjects. *Heart Vessels*. 2011;26(3):274-281.

142. Ahn C, Jeong S, Jeung EB. Mitochondrial dynamics when mitochondrial toxic chemicals exposed in 3D cultured mouse embryonic stem cell. *Toxicol Res*. 2023;39(2):239-249.

143. Sirenko O, Hancock MK, Hesley J, et al. Phenotypic Characterization of Toxic Compound Effects on Liver Spheroids Derived from iPSC Using Confocal Imaging and Three-Dimensional Image Analysis. *Assay Drug Dev Technol*. 2016;14(7):381-394.

144. Di Paolo A, Lencioni M, Amatori F, et al. 5-Fluorouracil Pharmacokinetics Predicts Disease-free Survival in Patients Administered Adjuvant Chemotherapy for Colorectal Cancer. *Clinical Cancer Research*. 2008;14(9):2749-2755.

145. Hunter R. Steady-state pharmacokinetics of lithium carbonate in healthy subjects. *Br J Clin Pharmacol*. 1988;25(3):375-380.

146. zur Nieden NI, Baumgartner L. Assessing developmental osteotoxicity of chlorides in the

embryonic stem cell test. *Reproductive Toxicology*. 2010;30(2):277-283.

147. Aras Y, Erguven M, Aktas E, Yazihan N, Bilir A. Antagonist activity of the antipsychotic drug lithium chloride and the antileukemic drug imatinib mesylate during glioblastoma treatment in vitro. *Neurol Res*. 2016;38(9):766-774.

148. Ghanayem BI, Bai R, Burka LT. Effect of Dose Volume on the Toxicokinetics of Acrylamide and Its Metabolites and 2-Deoxy-d-glucose. *Drug Metabolism and Disposition*. 2009;37(2):259.

149. Zang R, Xin X, Zhang F, Li D, Yang ST. An engineered mouse embryonic stem cell model with survivin as a molecular marker and EGFP as the reporter for high throughput screening of embryotoxic chemicals in vitro. *Biotechnol Bioeng*. 2019;116(7):1656-1668.

150. Lindeman B, Johansson Y, Andreassen M, et al. Does the food processing contaminant acrylamide cause developmental neurotoxicity? A review and identification of knowledge gaps. *Reproductive Toxicology*. 2021;101:93-114.

Shiyang Sun

Email: ssun08@syr.edu Cell Phone: (858)231-5753
60 Presidential Plaza Apt 1203, Syracuse, NY, US 13202

EDUCATION

Ph.D. Bioengineering | Syracuse University, USA | 2018 – Present
M.S. Bioengineering | Syracuse University, USA | 2016 – 2019
University Credit Program | University of California San Diego Extension, USA | 2014 – 2016
B.S. Biological Pharmacy | Jilin University, China | 2009 – 2013

RESEARCH EXPERIENCE

PhD Graduate Research Assistant (2018 – Present) *Research Advisor: Dr. Zhen Ma*
Department of Biomedical and Chemical Engineering, Syracuse University
Dissertation: Engineering human cardiac organoids for developmental drug screening

- Utilize PEG-based micropatterning technique to develop cardiac organoids under geometric confinement.
- Create cardiac organoids with different geometries to investigate the effect of mechanical stresses on organoid structure and cardiac functions.
- Test 14 drugs and each with 8 concentrations to determine the drug toxicity on embryonic heart development.

Independent Study (2020 – 2021) *Research Advisor: Dr. James Henderson*
Department of Biomedical and Chemical Engineering, Syracuse University
Project: Triple-phase shape memory polymer

- Fabricate shape memory polymer (SMP) using TBA, PCL and graphene oxide composite.
- Achieve multiple recovery of programmed SMP via dual triggering of light and heat.
- Test cytocompatibility of SMP to biological cells

Master Graduate Research Assistant (2017 – 2019) *Research Advisor: Dr. Zhen Ma*
Department of Biomedical and Chemical Engineering, Syracuse University
Thesis: Dynamic change of cardiomyocytes on shape memory polymer (SMP)

- Fabricate SMP with dynamic topographic changes with temperature triggering.
- Grow human induced pluripotent stem cell-derived cardiomyocytes (iCMs) on SMP for cell alignment.
- Study progressive myofibril reorganization of iCMs due to dynamic change of surface topography.

PUBLICATIONS

1. Chen, Junjiang, **Shiyang Sun,** Mark M Macios, Elizabeth Oguntade, Ameya R Narkar, Patrick T Mather, James H Henderon. "Thermally and Photothermally Triggered Cytocompatible Triple-Shape-Memory Polymer Based on a Graphene Oxide-Containing Poly (ε-caprolactone) and Acrylate Composite." *ACS Applied Materials & Interfaces* 15(44): 50962–50972 (2023).
2. Hoang, Plansky, **Shiyang Sun (equal contribution),** Bearett A. Tarris, and Zhen Ma. "Controlling Morphology and Functions of Cardiac Organoids by Two-Dimensional Geometrical Templates." *Cells Tissues Organs* 212(1) 61-70 (2023).
3. Shi, Huaiyu, Xiangjun Wu, **Shiyang Sun,** Chenyan Wang, Zacharias Vangelatos, Ariel Ash-Shakoor, Costas P. Grigoropoulos, Patrick T. Mather, James H. Henderson, and Zhen Ma. "Profiling the responsiveness of focal adhesions of human cardiomyocytes to extracellular dynamic nano-topography." *Bioactive Materials* 10, 367- 377 (2022).
4. Winston, Tackla S., Chao Chen, Kantaphon Suddhapas, Bearett A. Tarris, Saif Elattar, **Shiyang Sun,** Teng Zhang, and Zhen Ma. "Controlling Mesenchyme Tissue Remodeling via Spatial Arrangement of

Mechanical Constraints." *Frontiers in Bioengineering and Biotechnology* 10: 833595 (2022).
5. **Sun, Shiyang,** Huaiyu Shi, Sarah Moore, Chenyan Wang, Ariel Ash-Shakoor, Patrick T. Mather, James H. Henderson, and Zhen Ma. "Progressive myofibril reorganization of human cardiomyocytes on a dynamic nanotopographic substrate." *ACS Applied Materials & Interfaces* 12(19): 21450-21462 (2020).

PRESENTATIONS

1. Kowalczewski A., **Sun S.,** Hoang P., Ma Z. "*Functional Physiomics of Engineered Cardiac Organoids Enabled by Explored Data Analytics*" BMES, San Antonio 2022. *Poster*
2. **Sun S.,** Ma Z. *"The influence of mechanical stress on cardiac organoid development"* ECS Research Day, Syracuse, NY 2021, *Oral*
3. **Sun S.,** Hoang P., Tarris B., Ma Z. *"Controlling Morphology and Functions of Cardiac Organoids by Two- Dimensional Geometrical Templates"* ECS Research Day, Syracuse, NY 2021, *Poster*
4. **Sun S.,** Shi H., Moore S., Wang C., Ash-Shakoor A., Mather P.T., Henderson J.H., **Ma Z.** "*Probing developmental mechanobiology of human cardiomyocytes using a dynamic nano-topographic substrate*" BMES, Virtual 2020. *Poster*
5. **Sun S.,** Moore S., Wang C., Ash-Shakoor A., Henderson J., Ma Z. "*Dynamic Change of Human Stem Cell- Derived Cardiomyocytes on the Programmable Biomaterial Substrate"* Stevenson Biomaterials Lecture Series, Syracuse, NY 2019, *Poster*
6. **Sun S.,** Moore S., Wang C., Ash-Shakoor A., Henderson J., Ma Z. "*Dynamic Change of Human Stem Cell- Derived Cardiomyocytes on the Programmable Biomaterial Substrate"* ECS Research Day, Syracuse, NY 2019, *Poster*
7. **Sun S.,** Moore S., Wang C., Ash-Shakoor A., Henderson J., Ma Z. "*Dynamic Change of Human Stem Cell- Derived Cardiomyocytes on the Programmable Biomaterial Substrate"* CNY Cytoskeleton, Syracuse, NY 2019, *Poster*
8. Moore S., **Sun S.,** Wang C., Hoang P., Henderson J.H., Ma Z. "*Alignment of human cardiomyocytes through nano-wrinkles on shape memory polymers*" NEBEC, Rutgers, NJ 2019 *Oral*
9. **Sun S.,** Moore S., Wang C., Ash-Shakoor A., Henderson J., Ma Z. "*Myofibril remodeling of human stem cell-derived cardiomyocytes responding to dynamic surface topography*" SFB, Seattle, WA 2019, *Rapid Fire*
10. **Sun S.,** Moore S., Wang C., Ash-Shakoor A., Henderson J., Ma Z. *"Dynamic Change of Human Stem Cell- Drived Cardiomyocytes on the Programmable Biomaterial Substrate"* BMES, Philadelphia, PA 2019, *poster*
11. Moore S., **Sun S.,** Wang C., Hoang P., Henderson J., Ma Z. "*Topographic alignment of human cardiac myocytes using shape memory polymers*" Summer UG Research Symposium, Syracuse, NY 2018 *Poster*